

**Abstract**

Determining Seasonal Corrosion Rates in Ferrous-Hulled Shipwrecks:  
A Case Study of the USS *Huron*

by

Thomas Wilde Horn

October, 2014

Director of Thesis (Nathan Richards, Ph.D.)

Major Department: (Maritime Studies, History)

This is a study designed to examine if there are seasonal environmental factors that affect the corrosion rates of ferrous-hulled shipwrecks in an archaeological setting. The remains of USS *Huron*, a warship that sank off the coast of Nags Head, North Carolina in 1877 is used as a case study.

This study correlates rates of corrosion to seasonal variables such as changes in temperature, salinity, dissolved oxygen, and sediment coverage. Understanding the complex relationship between ferrous-hulled shipwrecks and the environment is critical for the creation of adequate management plans to protect cultural resources. In addition to corrosion monitoring, this study utilizes three-dimensional modeling to enhance understanding of *Huron's* site formation processes.



DETERMINING SEASONAL CORROSION RATES IN FERROUS-HULLED  
SHIPWRECKS: A CASE STUDY OF THE USS *HURON*

A Thesis

Presented To the Faculty of the Department of History

East Carolina University

In Partial Fulfillment of the Requirements for the Degree

Master of Arts in Maritime Studies

by

Thomas Wilde Horn

October, 2014

© Thomas Wilde Horn, 2014

DETERMINING SEASONAL CORROSION RATES IN FERROUS-HULLED  
SHIPWRECKS: A CASE STUDY OF THE USS *HURON*

by

Thomas Wilde Horn

APPROVED BY:

DIRECTOR OF  
THESIS: \_\_\_\_\_

(Nathan Richards, Ph.D.)

COMMITTEE MEMBER: \_\_\_\_\_

(Bradley A. Rodgers, Ph.D.)

COMMITTEE MEMBER: \_\_\_\_\_

(David Stewart, Ph.D.)

COMMITTEE MEMBER: \_\_\_\_\_

(David Conlin, Ph.D.)

CHAIR OF THE DEPARTMENT  
OF HISTORY: \_\_\_\_\_

(Gerald Prokopowicz, Ph.D.)

DEAN OF THE  
GRADUATE SCHOOL: \_\_\_\_\_

(Paul Gemperline, Ph.D.)

Dedicated to Kevin Flanagan (1970 – 2012). Your contributions to underwater science are immeasurable and everlasting.

## ACKNOWLEDGEMENTS

I would like to thank my father for his contagious love of research. In addition, this project could not have happened without the patience and professionalism of my advisor Dr. Nathan Richards and the University of North Carolina Coastal Studies Institute. I would like to express my gratitude to the North Carolina Sea Grant Maritime Heritage Fellowship (2012) for their generous financial support. I am grateful to Mark Keusenkothen and Jason Nunn from East Carolina University Diving and Water Safety for their training and sharing their equipment, boats, and personnel. Additionally, to the divers who braved the cold murky water: Greg Stratton, David Sybert, Ryan Bradley, and the students from the 2012 fall field school, thank you for diving in the often challenging conditions. Lastly, thank you Jessica Bingham for the generous topside support throughout this project.

## TABLE OF CONTENTS

Abstract .....	i
LIST OF FIGURES .....	xi
LIST OF TABLES .....	xiv
CHAPTER ONE: INTRODUCTION.....	1
Research Question and Hypothesis.....	3
Iron Corrosion in a Marine Environment.....	3
Conclusion .....	8
CHAPTER 2: LITERATURE REVIEW OF CORROSION STUDIES AND THEIR APPLICATION TO MANAGEMENT OF SHIPWRECK SITES .....	9
Introduction.....	9
History of the Application of Electrochemistry to the Study of Shipwrecks .....	10
Conclusion .....	20
CHAPTER 3: HISTORY AND CONSTRUCTION OF USS <i>HURON</i> .....	21
Introduction.....	21
American Transition from Wood to Iron Ships in the Nineteenth-Century .....	21
USS <i>Huron</i> 's Construction .....	26
USS <i>Huron</i> 's Working Life .....	32
Wrecking Event .....	34
Public Outrage and Lasting Consequence of the Loss of the USS <i>Huron</i> .....	40
Conclusion .....	41
CHAPTER 4: METHODOLOGY .....	43

Introduction.....	43
Digital Three-Dimensional Model of the USS <i>Huron</i> as Built in 1875 .....	43
Survey and Mapping.....	47
Three-Dimensional Model of the <i>Huron</i> Wreck site .....	49
Side Scan Sonar Imaging of <i>Huron</i> .....	51
Corrosion Rate .....	52
Water Parameters .....	58
Analysis.....	58
Sedimentation Survey From Yearly Site Reports.....	61
Conclusion .....	62
<b>CHAPTER 5: RESULTS OF DATA COLLECTION.....</b>	<b>64</b>
Introduction.....	64
Mapping .....	64
Summer 2012.....	67
Winter 2012-2013 .....	68
Spring 2013.....	68
Summer 2013 .....	69
Winter 2013-2014.....	70
Cumulative Water Parameter Data and Corrosion Potential Data.....	72
Collection of Sediment Data.....	74
Conclusion .....	77
<b>CHAPTER 6: ANALYSIS AND DISCUSSION OF SEASONAL WATER PARAMETERS AND CORROSION RATES AT THE USS <i>HURON</i>.....</b>	<b>78</b>

Introduction.....	78
Analyses of Average Ecorr Across Seasons .....	79
Average Seasonal Ecorr Compared to Dissolved Oxygen .....	79
Average Ecorr in Relation to Sedimentation of the Wreck Site .....	81
Discussion .....	82
Site Specific Analyses of the Wreck.....	83
Port versus Starboard Corrosion Potential Comparison .....	84
Bow, Midships, Stern Corrosion Comparison .....	89
Inboard versus Outboard Ecorr.....	94
Features versus Hull Plates Ecorr .....	98
Discussion .....	100
CHAPTER 7: CONCLUSION .....	106
Future Work .....	108
Corrosion Remediation .....	111
Conclusion .....	112
REFERENCES CITED.....	113

## LIST OF FIGURES

Figure 1. Location of the wreck of the USS <i>Huron</i> (Google Earth 2014; Accessed from North Carolina Department of Cultural Resources Underwater Archaeology Branch ( <a href="http://www.archaeology.ncdcr.gov/ncarch/underwater/huron.htm">http://www.archaeology.ncdcr.gov/ncarch/underwater/huron.htm</a> ). 1 April 2011. ....	2
Figure 2. “Schematic diagram showing the micro-environment that develops for an iron artifact covered by concretion after many years in the sea” (MacLeod 1989:1). ....	6
Figure 3. The Tafel equation and a description of variables (Gamry Instruments 2010). ....	13
Figure 4. “Diagram showing the relationship between the corrosion rate ( $I_{corr}$ ), the voltage, the individual components of the oxidation and reduction reactions and the observed value of the corrosion potential, $E_{corr}$ ” (MacLeod 1989:8). ....	13
Figure 5. Pourbaix diagram of iron and its species demonstrating the relationship between cathodic voltage, pH and corrosion ( <a href="http://www.wou.edu/las/physci/ch412/pourbaix.htm">http://www.wou.edu/las/physci/ch412/pourbaix.htm</a> ) Accessed May 29, 2011. ....	14
Figure 6. Using an ultrasonic thickness gauge on the USS <i>Arizona</i> to determine remaining plate thickness (Past Foundation 2004) ....	17
Figure 7. The construction of an iron ship in America during this time period closely resembled that of a wooden ship (Barnard 1878:641, taken from Thiesen 2006:102). ....	23
Figure 8. Illustration of a bar keel, the most common keel type used by American shipbuilders in <i>Huron</i> ’s era (Thearle 1886:26). ....	27
Figure 9. Example of <i>Huron</i> ’s side bar keel taken from the builder’s cross section (U.S. Naval Inquiry 1877:52). ....	28
Figure 10. Example of transverse framing (Thearle 1886:34). ....	29

Figure 11. Transverse frames from the USS <i>Huron</i> 's builder's plans (U.S. Naval Inquiry 1877:52).	29
Figure 12. Sail and Spar plan of the USS <i>Huron</i> (Friday 1988:21).	32
Figure 13. USS <i>Huron</i> fully rigged and ready to sail (courtesy of The Mariners Museum, Newport News, Virginia).	33
Figure 14. Mathematical modeling of the USS <i>Huron</i> demonstrating its strength of construction (U.S. Naval Inquiry 1877:49)	38
Figure 15. USS <i>Huron</i> 's Construction specifics compared to those required by Liverpool underwriters (U.S. Naval Inquiry 1877:52).	39
Figure 16. "Death on Economy," a cartoon published in Harper's Weekly, 29 December 1877 with a caption that reads, "I suppose I must spend a little on Lifesaving Service, Life-boat Stations, Life-Boats, Surf-Boats, etc; but it is too bad to be obliged to waste so much money" (Friday 1988:79).	40
Figure 17. Site plan of USS <i>Huron</i> , by Joe Friday 1988. Accessed from North Carolina Department of Cultural Resources Underwater Archaeology Branch ( <a href="http://www.archaeology.ncdcr.gov/images/ncarch/huron.gif">http://www.archaeology.ncdcr.gov/images/ncarch/huron.gif</a> ). 1 April 2011.	41
Figure 18. Sign posted off of Highway 12 and the adjoining gazebo dedicated to the loss of the USS <i>Huron</i> . (Photo by author, 2013.)	42
Figure 19. Builder's plan for the USS <i>Huron</i> (Friday 1988:22).	44
Figure 20. Lines taken from the USS <i>Huron</i> 's builder's plans and then digitally traced in <i>Rhinoceros</i> . (Image by author, 2013.)	44
Figure 21. Hull lines extrapolated onto the keel at the indicated stations. (Image by author, 2013.)	45

Figure 22. The loose loft function in <i>Rhinoceros</i> created the hull surface. (Image by author, 2013.) .....	46
Figure 23. Complete three-dimensional model of the USS <i>Huron</i> as it was built and fitted in 1875. (Image by author, 2013.).....	46
Figure 24. Map showing the location of USS <i>Huron</i> . Accessed from North Carolina Department of Cultural Resources Underwater Archaeology Branch <a href="http://www.archaeology.ncdcr.gov/ncarch/underwater/huron.htm">(<a href="http://www.archaeology.ncdcr.gov/ncarch/underwater/huron.htm">http://www.archaeology.ncdcr.gov/ncarch/underwater/huron.htm</a>)</a> . 1 April 2011. ....	48
Figure 25. Digitally traced port side profile view of the USS <i>Huron</i> wreck site with the planar curves extruded into solids. (Image by author, 2013.).....	50
Figure 26. Plan view of the USS <i>Huron</i> Site. The solids are then bent into shape using the bend function on <i>Rhinoceros</i> . (Image by author, 2013.) .....	50
Figure 27. Complete three-dimensional model of the wreck USS <i>Huron</i> . (Image courtesy of Nathan Richards and University of North Carolina Coastal Studies Institute, 2013.) .....	51
Figure 28. Map of the original sampling sites on the USS <i>Huron</i> site (Friday 1988:114). (Amendments by author, 2013.) .....	52
Figure 29. The pneumatic drill powered by a SCUBA tank. (Photo by author, 2013.).....	53
Figure 30. Multimeter in waterproof housing with silver/silver chloride reference electrode (wrapped in plastic to protect it) and platinum tipped electrode. This instrument was replaced with a Polartrak CP bathycorrometer. (Photo by author, 2013.) .....	55
Figure 31. Internals of the Polatrak CP Bathy Corrometer (Deep Water Corrosion Services, Inc 2010:6). .....	57
Figure 32. Town of Nags Head yearly <i>Huron</i> survey checklist showing sedimentation of specific features (Lawrence 2008:4). .....	61

Figure 33. Joe Friday’s 1988 site plan used to aid the Town of Nags Head’s yearly site surveys (Lawrence 2008:5). Note that the stern portion of the wreck has been erased. ....	62
Figure 34. <i>Huron</i> site plan (left) and three-dimensional rendering (right) from ECU’s Program in Maritime Studies 2012 fall field school. (Right image by author, 2013.) .....	65
Figure 35. Three-dimensional representation of the USS <i>Huron</i> showing the location of the study’s sampling sites. (Image by author, 2014.) .....	66
Figure 36. Summer 2013 side scan sonar image of the <i>Huron</i> wreck site. (Image courtesy of Nathan Richards and University of North Carolina Coastal Studies Institute, 2013.) .....	66
Figure 37. An aerial photo from 2007 and 1949 of Nags Head, NC. The <i>Huron</i> site is represented and the two shorelines are transposed atop each other showing a stable shoreline (red border). (Time series by Ian Conery of East Carolina University Department of Geological Sciences, 2013.) .....	75
Figure 38. Sedimentation time series taken from the <i>Huron</i> wreck preserve yearly reports (Lawrence 2004, 2005, 2006, 2007, 2008, 2009; Zorc 2010). (Image by author, 2013.).....	76
Figure 39. Relative amounts of dissolved oxygen to average corrosion potential. Lower Ecorr readings (red) indicate higher corrosion environments. (Image by author, 2014.).....	80
Figure 40. Seasonal sediment model of the wreck site and resulting <i>Rhinoceros</i> area analysis. (Image by author, 2014.).....	82
Figure 41. <i>Huron</i> sampling sites with areas of site specific analysis indicated. (Image by author, 2014.) .....	84
Figure 42. Corrosion potential readings partitioned into port and starboard sides of the wreck. (Image by author, 2014.).....	85

Figure 43. Graph of port and starboard corrosion potentials (Ecorr) for summer 2013. (Image by author, 2014.) .....	86
Figure 44. Corrosion potential readings partitioned into port and starboard sides of the wreck for winter 2013-2014. (Image by author, 2014.) .....	87
Figure 45. Graph of port and starboard side corrosion potentials (Ecorr) for winter 2013-2014. Invalid readings are not included. (Image by author, 2014.) .....	87
Figure 46. Port versus starboard Ecorr for Summer 2013 and Winter 2013-2014. (Image by author, 2014.) .....	88
Figure 47. Summer 2013 bow, midships, and stern section corrosion potential results. (Image by author, 2014.) .....	90
Figure 48. Graph of the bow, midships, and stern corrosion potentials (Ecorr) from the summer 2013 sampling season. (Image by author, 2014.) .....	90
Figure 49. Winter 2013-2014 bow, midships, and stern section corrosion potential results. (Image by author, 2014.) .....	91
Figure 50. Graph of the bow, midships, and stern corrosion potentials (Ecorr) from the summer 2013 sampling season. Invalid readings are not included. (Image by author, 2014.) .....	92
Figure 51. Bow, midships, and stern Ecorr for summer 2013 and winter 2013-2014. (Image by author, 2014.) .....	93
Figure 52. Summer 2013 inboard versus outboard Ecorr comparison. (Image by author, 2014.)	94
Figure 53. Graph of the summer 2013 inboard versus outboard Ecorr. (Image by author, 2014.)	95
Figure 54. Winter 2013-2014 inboard versus outboard Ecorr comparison. (Image by author, 2014.) .....	96

Figure 55. Graph of the winter 2013-2014 inboard versus outboard Ecorr. Invalid readings are not included. (Image by author, 2014.)..... 96

Figure 56. Inboard versus outboard Ecorr for summer 2013 and winter 2013-2014. (Image by author, 2014.)..... 97

Figure 57. Summer 2013 hull plate versus feature Ecorr comparison. (Image by author, 2014.) 99

Figure 58. Graph of the summer 2013 hull plates versus features Ecorr. (Image by author, 2014.) ..... 99

## LIST OF TABLES

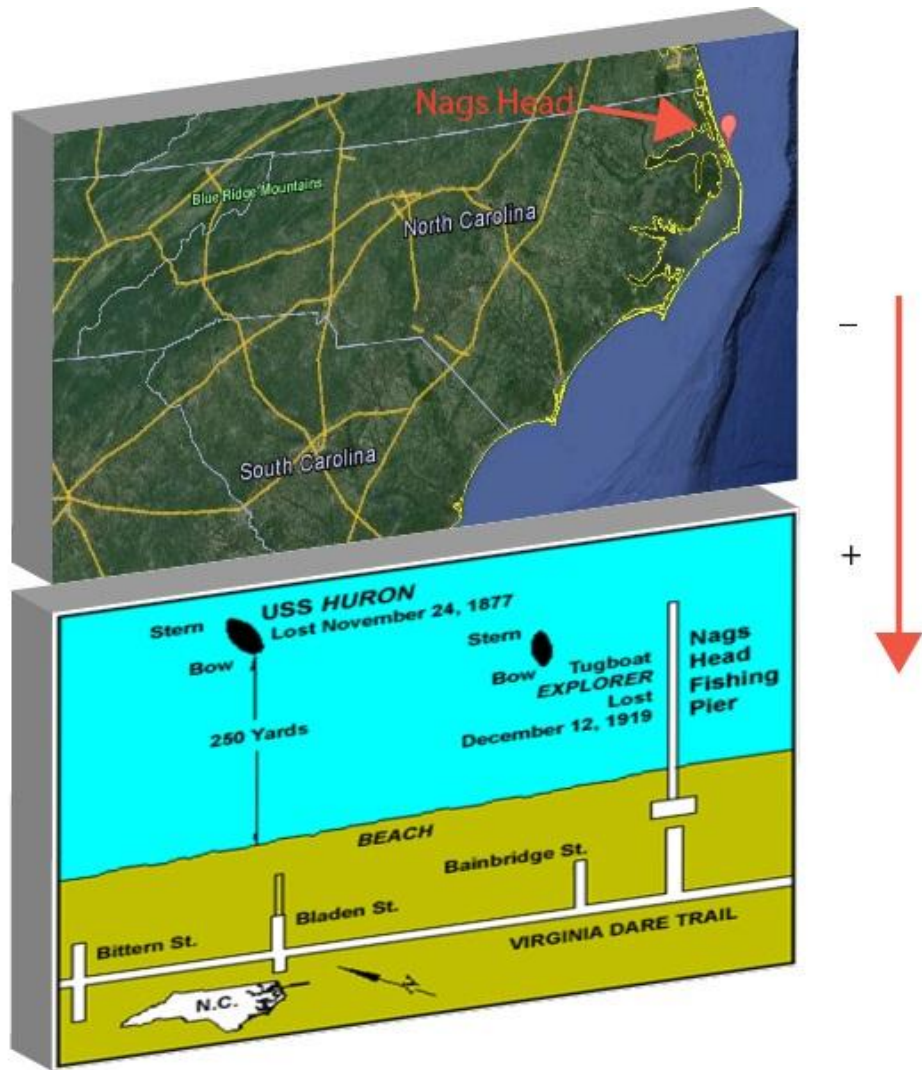
Table 1. Wreck sites mentioned in the literature review (and methods section) in chronological order and the in-situ corrosion measurement method used. ....	11
Table 2. Plate thickness of the USS <i>Huron</i> compared to Liverpool Insurance specifications (U.S. Naval Inquiry 1877:52).....	30
Table 3. Measurements of water parameters taken from the CTD sensor.....	67
Table 4. Measurements from the multimeter and concretion thickness. The Ecorr has been temperature corrected.....	67
Table 5. Winter 2012-2013 environmental data. ....	68
Table 6. Spring 2013 environmental data.....	69
Table 7. Summer 2013 water parameters. ....	70
Table 8. Repeat sampling sites (did not need to be temperature corrected). ....	70
Table 9. New sampling sites (did not need to be temperature corrected).....	70
Table 10. Winter 2013-2014 temperature corrected Ecorr readings (0.008 V).....	72
Table 11. Winter 2013-2014 water parameters.....	72
Table 12. Cumulative water parameter data from all the seasons. ....	72
Table 13. Cumulative seasonal temperature corrected Ecorr readings from the “ <i>Huron</i> Project.” .....	73
Table 14. Ecorr sampling sites with location descriptions. ....	73
Table 15. Average seasonal Ecorr and dissolved oxygen (mg/L) for each season.....	80
Table 16. Average Ecorr from summer 2013 compared to the Ecorr of Winter 2013-2014 with percent change in corrosion rate. ....	89

Table 17. Average Ecorr of summer 2013 and winter 2013-2014 with percent change in corrosion rate. ....	93
Table 18. Comparison between the Ecorr of inboard and outboard portions of the wreck for summer 2013 and winter 2013-2014. ....	97

## CHAPTER ONE: INTRODUCTION

The primary goal of this research project was to complete a yearlong study of the corrosion rate of a ferrous-hulled shipwreck and to determine whether seasonal variables affect this important archaeological resource. The seasonal variables sampled were sedimentation, water temperature, salinity, and dissolved oxygen. These variables influence metal's exposure to oxygen, a principal driver of cathodic ferrous corrosion (MacLeod 1981:292).

The wreck of USS *Huron*, which sank off the coast of Nags Head, North Carolina in 1877 serves as a case study (Figure 1). This seasonal corrosion research will be the first study of its kind in near-shore North Carolina waters, a region rich in submerged cultural resources. The “*Huron* Project” includes both an in-situ corrosion monitoring component and three-dimensional modeling in order to illustrate the site's interaction with its environment. The data collected may be used to evaluate the management of the *Huron* site and will be available for inclusion in local and international datasets related to ferrous corrosion in a marine environment such as NOAA's Resources and UnderSea Threats program (RUST) (Overfield 2004). It is hoped that data sets like these, composed of numerous and quality data, will provide site managers with accurate predictive or explanatory models of site corrosion. The near shore environment of North Carolina's Outer Banks is a dynamic environment with large changes in multiple variables from season to season (Dolan 1966:705). The cultural significance of the wreck site and the substantial fluctuation of environmental parameters make the USS *Huron* wreck ideal for this project.



**Figure 1. Location of the wreck of the USS *Huron* (Google Earth 2014; Accessed from North Carolina Department of Cultural Resources Underwater Archaeology Branch (<http://www.archaeology.ncdcr.gov/ncarch/underwater/huron.htm>). 1 April 2011.**

Corrosion studies are an integral part of managing submerged sites which contain an abundance of metallic objects. In 1989, Ian MacLeod published “The Application of Corrosion Science to the Management of Maritime Archaeological Sites.” This article states that routine measurement of corrosion potential can be immensely valuable to understanding site formation processes and contribute to cultural resource management decisions. Corrosion is potentially a major destructive post-depositional process, and understanding how different variables affect corrosion rate is important in understanding the site as a whole. The goal is to quantify a

destructive post-depositional transform (corrosion) and how it affects the wreck site. Corrosion products can also be deduced using Pourbaix diagrams. The *Huron* corrosion study also informs on the need and practicality of options for in-situ conservation such as cathodic protection via sacrificial anodes on the *Huron* wreck site.

### *Research Question and Hypothesis*

The overall primary research question outlined in the present study asks, *is there a relationship between seasonal water parameters (temperature, salinity, dissolved oxygen, and sedimentation cover), and the corrosion rates of ferrous metal shipwrecks in a near shore environment?* In order to adequately assess this question, a series of multiple-working hypotheses are offered:

*Null hypothesis:* There is no relationship between seasonal water parameters and sedimentation to corrosion rates of ferrous metal in a near shore environment.

*Ia:* There is an increase in corrosion rate observed during periods of less sedimentation cover and increased exposure to cold water with high dissolved oxygen content.

*Ib:* There is a decrease in corrosion rate observed during periods of less sedimentation cover and increased exposure to cold water with high dissolved oxygen content.

*Ic:* There is no observed corrosion during the study period, indicating the wreck is in a state of equilibrium.

*Id.* Mixed corrosion rates are observed with no correlation to the studies variables.

### *Iron Corrosion in a Marine Environment*

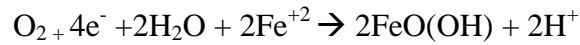
Other than iron from meteorites found and worked by people, wrought iron is the oldest form of iron produced by humans and is composed of pure iron uniformly mixed with a very small amount of slag (Rodgers 2004:71). The slight silicate impurities present in wrought iron

mean that it is actually an iron aggregate and slag intrusions in the material lead to a wood grain like appearance when corroded (Rodgers 2004:73). Large-scale production of wrought iron became possible when Henry Cort patented the process of using grooved rollers and puddling iron in 1784 (Rodgers 2004:72). Puddling iron is the process of heating pig iron in a furnace and agitating the resulting molten puddle with a rabble. This action is used to remove impurities from the iron such as carbon, silicon, and phosphorous. The resulting iron in the furnace assumes a paste like consistency which is then rolled into balls. These balls are then run between grooved rollers and treated to eventually become plates (Moore 2011:21-22). This creates the familiar iron form with enhanced physical properties such as increased malleability and strength, but these products are not completely stable. Corrosion is the process of metallic compounds returning to their basic and stable elemental state. When an iron object is first immersed in seawater it immediately experiences a period of high corrosion activity evidenced by the formation of the familiar red rust corrosion products. For an iron object lying exposed on the seabed these products are typically iron oxyhydroxide and are formed through the interaction of iron, water, and oxygen to form these rust products (Moore 2011:160).

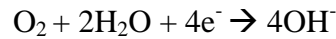


The reaction above is a combination of two reactions occurring on separate areas of the iron object which forms the corrosion product. The corroding metal needs to maintain a neutral charge and consists of both a cathodic and anodic portion. The first reaction is the anodic oxidation reaction (the iron loses electrons) that results in the production of ferrous ( $\text{Fe}^{+2}$ ) ions. The  $\text{Fe}^{+2}$  ions are then oxidized into  $\text{Fe}^{+3}$  ions as they move away from the iron's surface (North 1982:76). This is the anodic reaction which is described as,





Or in simpler terms, iron exposed to oxygen and water will eventually turn into rust, acid, and electrons (Rodgers 2004:75). The second part of the reaction is the cathodic reaction and it results in the formation of hydroxide ions ( $\text{OH}^-$ ) using the electrons from the oxidation of the iron interacting with water and oxygen.



The cathodic reaction is made possible by the flow of ions from the anodic portion of the metal to the cathodic portion. This flow needs a solution with high conductivity and in the case of iron objects in a marine environment, this is seawater. Chloride ions ( $\text{Cl}^-$ ) in the seawater are attracted to the anodic portion of the object and increase the corrosion rate. The positively charged iron ions produced in the corrosion process attract the negatively charged chloride ions and these ions penetrate the metal through “inward diffusion” (MacLeod 2002:698). The chloride ions then react with the iron ions to form  $\text{FeCl}_2$  (North 1982:80).

The cathodic reaction also needs oxygen to perpetuate the reaction, and the amount of oxygen available to the cathodic site will dictate the corrosion rate (Moore 2011:161-163). This is why salinity and dissolved oxygen are important variables that need to be sampled in any quantitative corrosion study of ferrous objects in a marine environment. It needs to be noted, that the reaction just mentioned is an oversimplification in that a shipwreck is not one giant circuit, but rather potentially thousands of galvanic cells. These cells will form in areas of stress, or differential pH, differential dissolved oxygen levels, and temperatures (Hamilton 1999:39-40).

A ferrous artifact will eventually become covered in a concretion consisting of calcium carbonate, corrosion products, and organisms. Coralline algae have a calcium carbonate ( $\text{CaCO}_3$ ) exoskeleton and will colonize any suitable surface in the marine environment. The coralline

algae will form layers of calcium carbonate on the iron object until it is completely covered. Additionally, iron ions from the object will migrate into the calcium carbonate concretion encountering a more alkaline environment, and precipitate into a hard concretion known as cementite (Rodgers 2004:79-80). The concretion on an iron object will have the external appearance of any natural concretion, but when disturbed will have a black to gray appearance. The dull hue will give way to a bright orange color, as the disturbed portion of the concretion is exposed to oxygen, resulting in flash rusting within the concretion (North 1976:253).

The concretion acts as a semi-permeable membrane and creates an acidic microenvironment resulting from the hydrolysis of iron ions as shown in Figure 2 (Welsh 2010:54). Hydrolysis is the breakdown of a material by reaction with water. In this case, the result releases hydrogen ions that further acidify the microenvironment. The pH of seawater is about 8.2 and pH measurements of as low as 4.2 have been measured in the iron/concretion interface (MacLeod 2002:698). This hydrogen is well documented, and often hydrogen and methane gas will bubble out of disturbed concreted submerged sites (Rodgers 2004:80). The concretion also determines how much oxygen is available for the cathodic reaction and thus, the overall corrosion rate as it acts as a passive electrical barrier (MacLeod 1989:1).

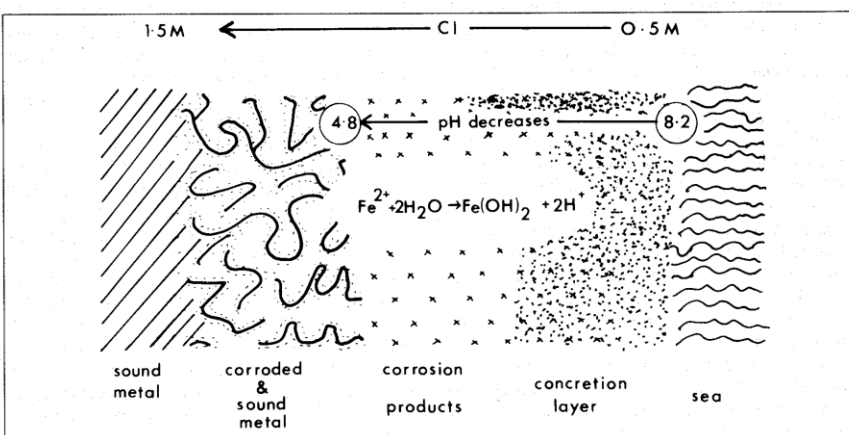


**Figure 2. “Schematic diagram showing the micro-environment that develops for an iron artifact covered by concretion after many years in the sea” (MacLeod 1989:1).**

Galvanic coupling is another form of corrosion prevalent on ferrous wrecks, and it occurs when dissimilar metals come into direct electrical contact. A less noble metal will corrode preferentially to a more noble metal. Cuprous metals, or copper alloys, are common on wreck sites and the result is that iron will corrode preferentially to the cuprous alloys, and guards the cuprous metals from corrosion in a form of cathodic protection. This phenomenon can also be used to protect ferrous objects by connecting them to a metal that is less noble than iron, such as aluminum or zinc.

Microorganisms also contribute to corrosion in both aerobic and anaerobic environments. This interplay between ferrous materials and microbes has been studied since the early twentieth century, but the exact mechanisms are still under investigation. Microbial induced corrosion occurs in aerobic conditions through the oxidation of iron. This corrosion is further intensified from bacterial waste products which create an acidic microenvironment. However, the role of microbial corrosion in an anaerobic environment is a much larger problem. In low or oxygen free environments, the principal driver of iron corrosion is attributed to Sulfate Reducing Bacteria (SRB), which are believed to corrode iron through a process known as depolarization. The SRB metabolize hydrogen that colonize the surface of the iron, and this causes a cathodic depolarization (resulting in a V drop in the anode's direction, or in other words, a higher corrosion potential), with the net result being an increase in material loss at the objects anode (Gu 2000:915,920,924). In addition to sulphate reducing bacteria, methanogenic bacteria also use hydrogen to metabolize iron and carbon dioxide with methane and water as waste products through methanogenesis, further contributing to the corrosion of iron objects (Rodgers 1989:338). The combined effect of sulphate reducing bacteria and methanogenic bacteria in an

anoxic environment can effectively consume ferrous objects from an archaeological site, despite the favorable conditions for the preservation of organic materials (Rodgers 1989:335).

### *Conclusion*

Determining Seasonal Corrosion Rates in Ferrous-Hulled Shipwrecks: A Case Study of the USS *Huron*, contains a literature review regarding the nature of iron shipwreck corrosion and the direct environmental influence on this electrochemical process. The literature review also appraises the sampling techniques that researchers use and have used in the past. This thesis continues with a brief outline of the history and construction of USS *Huron* in order to put the wreck in context with world history and the its subsequent site formation. Following this, the “*Huron* Project” methodology is explained in detail and the subsequent results displayed. The project’s results are subjected to in-depth analyses and discussion. In the conclusion, the project’s many parts are surmised and future work suggested.

## **CHAPTER 2: LITERATURE REVIEW OF CORROSION STUDIES AND THEIR APPLICATION TO MANAGEMENT OF SHIPWRECK SITES**

### *Introduction*

Tying together the most current methods of determining corrosion rates with a detailed knowledge of the construction of the USS *Huron* is paramount in order to test if there is a relationship between seasonal environmental parameters and corrosion. It is important to review the published literature of electrochemical applications to shipwreck preservation in order to refine the theory and methods used on the USS *Huron* project. This literature review focuses on applications that pertain to submerged sites with an abundance of ferrous materials although many of the techniques used in these studies are also used in the oil and gas industry.

There are a few ways to measure corrosion of ferrous metal in a marine environment; cutting edge techniques include concretion equivalent corrosion rate (CECR), while more mainstream techniques include using a multimeter and silver/silver chloride reference electrode to measure the corrosion potential ( $E_{corr}$ ) of the metal. Each method has both pros and cons and merely understanding the electrochemistry of a ferrous wreck site is not enough to understand the site formation processes. The importance of the specific ship construction techniques, materials, and history cannot be understated in terms of their importance in determining the effects of corrosion on site formation processes. What follows is a review of in-situ shipwreck corrosion studies and the methods used.

Admittedly, there is an alternative approach to the quantitative methodology utilized in this study as it pertains to the management of ferrous hulled shipwrecks. Jaqueline Piero in her 2004 Master's thesis titled, "Deterioration of Ferrous Hulled Shipwrecks" presents a qualitative site formation classification scheme for ferrous hulled shipwrecks. This classification system

focuses on ship construction and the environment of deposition to ascertain the future of shipwreck sites from a multitude of different ocean environments. While it does take corrosion into consideration, corrosion measurement and water parameters such as dissolved oxygen content are not considered. In fact, water parameters were specifically shown to not be dominant site formation variables (Piero 2004:95). However, based on the body of literature that will be discussed, a quantitative approach was chosen as a suitable theoretical and methodological framework for formulating hypotheses and analyzing corrosion during the “*Huron* Project.

#### *History of the Application of Electrochemistry to the Study of Shipwrecks*

In-situ studies of ferrous shipwreck corrosion date back to the early 1980s. Ian MacLeod pioneered the theory and methods used in quantitative shipwreck corrosion studies and Western Australia is the epicenter of in situ shipwreck corrosion studies because of him (MacLeod 1981). In Hawai’i, minimally invasive procedures have been further tested by the National Park Service Submerged Resources Center in conducting corrosion studies on USS *Arizona* (Russell et al. 2006).

Table 1 outlines studies pertinent to the in situ corrosion monitoring of *Huron* in chronological order. These studies are important to the *Huron* study because they focus on different corrosion sampling methodologies and approaches to novel research questions. The selected sites also have an abundance of ferrous material and are submerged in saltwater. These studies are the basis for the “*Huron* Project,” which hopes to build on the international body of literature concerning corrosion of shipwrecks in a marine environment.

Site	Study Start	Published	In-Situ Corrosion Analysis
<i>SS Xantho</i>	1983	1986	Multimeter and pH.
<i>HMVS Cerberus</i>	1993	1996	Multimeter, pH, and ultrasonic thickness gauge.
<i>City of Launceston</i>	1993	2011	Multimeter, pH, and ultrasonic thickness gauge.
Duart Point wreck	1994	1999	Multimeter and pH
<i>Clan Ranald</i>	1998	1998	Ultrasonic thickness gauge.
J-Class submarines	2004	2005	Multimeter and pH.
<i>USS Arizona</i>	2006	2006	Multimeter, pH, coupon, ultrasonic thickness gauge, and CECR.
Wrecks of the <i>Taifun</i> and Meyer's Slip Vessel	2008	2011	Multimeter, pH, potentiodynamic polarization scan.

**Table 1. Wreck sites mentioned in the literature review (and methods section) in chronological order and the in-situ corrosion measurement method used.**

Ian MacLeod published “Shipwrecks and Applied Electrochemistry” in the *Journal of Electroanalytical Chemistry* in 1981. This paper describes shipwrecks as a “series of long term corrosion experiments which cannot be simulated under laboratory conditions... [This] information has potential application in the design of offshore oil installations and in long term storage of radioactive wastes in a marine environment” (MacLeod 1981:291). Setting the stage for future research, this paper describes the complexity and potential wealth of knowledge that can be gleaned from wreck sites.

The practical application of corrosion science came into being in 1983 with the *Xantho* project. The iron-hulled steamer *Xantho*, built in 1848, was lost off Western Australia in 1872. The project required the expertise of maritime archaeologists, corrosion scientists, and marine

biologists and was the first to consider in-situ corrosion monitoring. One goal of the project was to determine the relationship between the site's formation processes and the environment, in order to monitor changes on the site to further establish an effective management plan (McCarthy 2000:70,186).

MacLeod used a hand drill to penetrate the concretion on the SS *Xantho* until sound metal was reached. A digital multimeter in a waterproof case was then used to measure the corrosion potential ( $E_{corr}$ ). The multimeter detects the difference in voltage between a platinum electrode placed on the sampling site and a silver chloride electrode in the seawater. As discussed in Chapter One, this voltage is a product of the oxidation of iron into ferrous ions ( $Fe \rightarrow Fe^{2+} + 2e^-$ ) and then ( $O_2 + 4e^- + 2H_2O + 2Fe^{+2} \rightarrow 2FeO(OH) + 2H^+$ ) and the opposing cathodic reaction is determined by the rate of oxygen diffusion through the concretion to form hydroxide ions ( $O_2 + 2H_2O + 4e^- \rightarrow 4OH^-$ ) (MacLeod 1989:7-8).

The rate at which the cathodic reaction and the anodic reaction occur is the  $E_{corr}$  (Moore 2011:218). Rate of corrosion cannot be determined directly using the multimeter, but it can be estimated from the  $E_{corr}$  measurement by using the Tafel Equation (Figure 3) on both the anodic and cathodic elements of the corrosion cell to estimate the corrosion rate (Figure 4) ( $I_{corr}$  in units of mm/year). This calculation does require multiple measurements of cast iron artifacts and resulting graphitization from corrosion, to determine a baseline of iron corrosion on a specific wreck site. Percentage change in corrosion rate, however, can be easily observed on a site through  $E_{corr}$  sampling (MacLeod 2002:700-701).

$$I = I_0 e^{(2.3(E-E_0)/\beta)}$$

$I$  = the current resulting from the reaction  
 $I_0$  = the reaction dependent constant called the Exchange Current  
 $E$  = the electrode potential  
 $E_0$  = the equilibrium potential (constant for a given reaction)  
 $\beta$  = the reaction's Tafel Constant (constant for a given reaction).  
 Beta has units of volts/decade.

**Figure 3. The Tafel equation and a description of variables (Gamry Instruments 2010).**

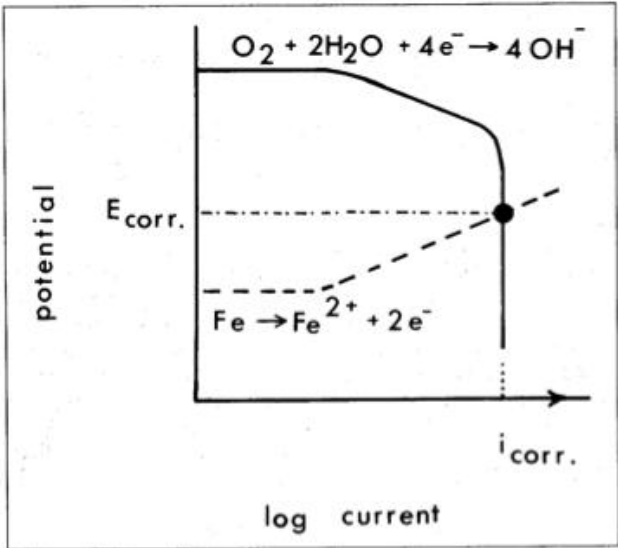


**Figure 4. “Diagram showing the relationship between the corrosion rate ( $I_{corr}$ ), the voltage, the individual components of the oxidation and reduction reactions and the observed value of the corrosion potential,  $E_{corr}$ ” (MacLeod 1989:8).**

Total corrosion rate can be determined through methods as simple as measuring concretion thickness (only with cast iron) or as detailed as a Concretion Equivalent Corrosion Rate (CECR) study which can determine a ferrous object’s corrosion rate based on the chemistry of its concretion. CECR will be discussed further in the following pages, as it pertains to the “USS *Arizona* Project” (Wilson et al. 2007; Welsh 2010:55).

To determine corrosion products, a portable pH meter is used to measure the pH at the iron/concretion interface. pH is a measure of hydrogen ion activity in a solution, and the results are used to create a Pourbaix diagram (Figure 5) to determine corrosion products (MacLeod 1981:8; Buck 2002:2172). These diagrams not only reveal if a metal is in an active, passive, or immune state of corrosion, but also the specific corrosion product. It is important to note that they do not represent corrosion rate (Silverman 2000:1180-1182). Iron in an underwater archaeological setting is usually actively corroding (strongly reducing state) with the microenvironment having a pH of 4.8 on average (MacLeod 2002:700).

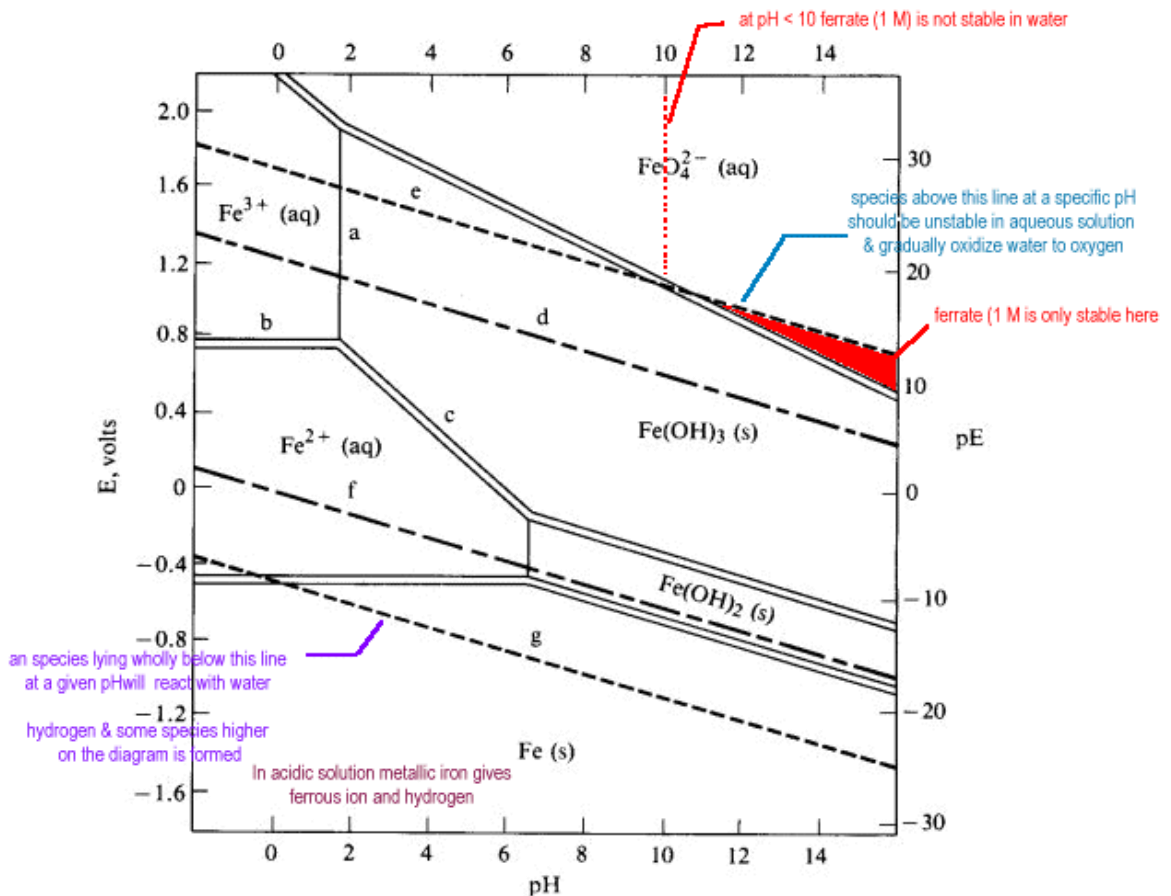


**Figure 5. Pourbaix diagram of iron and its species demonstrating the relationship between cathodic voltage, pH and corrosion (<http://www.wou.edu/las/physci/ch412/pourbaix.htm>) Accessed May 29, 2011.**

The *Xantho* study also used sacrificial anodes to provide cathodic protection (the process of a less noble metal corroding preferentially to a more noble metal when they are electrically connected) to the SS *Xantho*'s engine. The sacrificial anode was an old aluminum engine block and the system worked until the block was buried in the sediment and its protective electrical flow slowed (McCarthy 2000). This project pioneered the use of in-situ sacrificial anodes which is now an established methodology in mitigating corrosion of metallic features on shipwrecks (Moore 2011:182). The results of the corrosion potential survey clearly showed that features lying proud of the seabed and exposed to the prevailing currents had a higher corrosion rate than features in the lee of the currents (McCarthy 2000:77). The *Xantho* Project was a milestone in the use of electrochemistry in maritime archaeology for monitoring and conserving submerged archaeological sites.

Today, a less invasive means of determining corrosion rate is being pursued and involves the use of an ultrasonic thickness gauge in lieu of using the drill and multimeter. Theoretically, drilling has a higher potential to prompt corrosion by increasing the exposure of iron to dissolved oxygen. It has been proposed that sealing the drill hole with a pH neutral marine epoxy or hydraulic cement will prevent this (Foecke et al. 2010:316). This issue is further discussed in the methods chapter of this thesis.

MacLeod tested the feasibility of using an ultrasonic thickness gauge to measure residual metal thickness in 1996 on the wreck of HMVS *Cerberus* (this study also included corrosion potential and pH measurements as previously mentioned). The goal of this study was to test whether the ultrasonic thickness gauge could be used in determining residual thickness of the iron scantlings and then utilize this data to deduce the original thickness of an iron object after years of corrosion. Prior to this, residual thickness measurements required removing portions of

the wreck and concretion in order to obtain a measurement. The results showed the extent of corrosion along different portions of the *Cerberus* wreck and the original dimensions of the scantlings were deduced by using this data in conjunction with data collected from cast iron graphitization (MacLeod 2006).

This method was further refined on a study of the wreck *Clan Ranald*, when the use of an ultrasonic thickness gauge and associated data from the graphitization of cast iron off the wreck were used to determine the original dimensions of the boilers. These studies validated the use of the ultrasonic thickness gauge in shipwreck archaeology (MacLeod 2002:708-710). However, the USS *Huron* project would require a measurement resolution not available from the ultrasonic thickness gauge when measuring minute seasonal changes in iron thickness.

In 2006, a team from the National Park Service and the University of Nebraska-Lincoln published, “A Minimum-Impact Method for Measuring Corrosion Rate of Steel-Hulled Shipwrecks in Seawater” (Russell 2006:310-318). This study was to quantify corrosion rates on USS *Arizona* for inclusion in a computer modeled finite element analysis, which is a detailed digital multivariate model that is used to predict the ship’s degradation over time (Russell 2006:312). The project used two direct measuring techniques (coupon hull sampling and ultrasonic thickness measurements) and one indirect technique (concretion equivalent corrosion rate or CECR). CECR takes into account concretion density, thickness, and uses direct wet chemical analysis of iron in the concretion sample to determine corrosion rate (Wilson 2007; Donald Johnson 2011, elec. comm.).

Hull coupon sampling is an invasive technique that involves removing small portions of the wreck for analysis, the results of which corrosion analysts may then utilize as a control for other minimally invasive techniques. Ultrasonic thickness measurements were taken with an

ultrasonic thickness gauge (Figure 6) and would be completely non-invasive if not for the requisite polishing of the encrustation to give a uniform measurement surface. This project did have problems obtaining measurements with the ultrasonic thickness gauge because of pitting that inhibited reliable thickness measurements (Russell 2010). Although the ultrasonic method proved problematic, the study shows the merit of using less invasive means of corrosion analysis.



**Figure 6. Using an ultrasonic thickness gauge on the USS *Arizona* to determine remaining plate thickness (Past Foundation 2004)**

In 2011, Ian MacLeod published a chapter titled “Assessment of the impact of scallop dredging, site clearance and cathodic protection on *City of Launceston* (1865) through *in-situ* corrosion monitoring.” This study correlated variation in sedimentation rates from a moratorium on scallop dredging to variable corrosion rates on the iron shipwreck *City of Launceston* using corrosion measurements taken over 18 years (MacLeod 2011). Corrosion potential (using a multimeter), pH, residual metal thickness studies, and the depth of graphitization were used to quantify corrosion of different parts of the wreck in terms of mm/year rates of corrosion.

This study is useful to the “*Huron* Project” because it includes an aspect of periodic burial and its influence on corrosion rates. It should be noted however, that graphitization

analysis was not used on the USS *Huron* project (the wreck is largely wrought iron).

Importantly, this study also validates year-to-year corrosion measurements to quantify the annual corrosion rate. In addition to monitoring environmental influences on corrosion, the data from this study was used to assess the impact of archaeological work on the site, divers, and a scallop-dredging moratorium (MacLeod 2011).

The Duart Point wreck is a 17<sup>th</sup> century ship lost in the cold waters of Scotland. The wreck has five cannon and a large iron anchor. In 1994 MacLeod took corrosion potential readings of these artifacts and recommended the attachment of sacrificial anodes to two cannons and the anchor to mitigate the artifacts rapid deterioration. In 1996, scrap aluminum ingots were electrically connected to the artifacts using copper wire. The efficacy of these sacrificial anodes was tested in 1997 using a multimeter and silver/silver chloride electrode and pH sampling probe. The result of this study showed that the anodes were extremely effective in lowering the corrosion rate of the chosen artifacts. Additionally, it was found that the pH increased at the concretion iron interface aiding in the removal of chlorides from the iron (Gregory 1999). This study highlights the value of cost effective sacrificial anodes to *in situ* conservation of iron artifacts in a marine environment.

In 2008 PhD candidate, James Daniel Moore III of University of Rhode Island, led a study on two ferrous-hulled ships in Bermuda. Two ships were selected, *Taifun* (originally *Ancon*) a Scottish built steel vessel launched in 1894, and the Meyer's Slip Vessel, a wrought iron British gunboat of the *Medina*-class launched in 1876. The latter ship mentioned is either the HMS *Medina* or the HMS *Medway*, sister ships that served together. One of these ships sank in the early twentieth century, but currently neither the historical record nor the archaeological record states which one is the Meyer's Slip Vessel (Moore 2011).

The project used a Buckleys Bathycorrometer complete with a silver/silver chloride reference electrode to measure the Ecorr at different locations along both wrecks. The results showed once again that sampling sites exposed to prevailing currents, in this case from a shipping channel, had higher rates of corrosion. In addition to the corrosion monitoring study, Moore performed a laboratory-based study comparing the in-situ corrosion behavior of iron and steel to previously corroded iron and steel in simulated marine environments. The results were quantified using potentiodynamic polarization scans to establish corrosion rates. The non-corroded iron behaved as expected in the simulated marine environments, but the previously corroded samples had a corrosion rate 15 times higher than that seen on actual wrecks (Moore 2011:275-276). The lab based work tried to correlate corrosion potential with actual corrosion rate, but failed to mimic an actual shipwreck.

The methodology used in 1983 on the SS *Xantho* is not only a valid and proven method, but also economical. The cutting edge of corrosion rate determination, such as CECR modeling combined with finite elemental analysis, is coming into its own as a powerful management tool although not as economically accessible as using a multimeter to determine corrosion potential. Management plans of any submerged wreck site with metallic objects can benefit from in-situ monitoring, and these prior studies demonstrate the value and potential of in-situ monitoring to conserve maritime heritage. Any variable that might alter the environment (macro and micro) of the wreck site can potentially affect the corrosion rate resulting in a bounty of novel research questions such as shown by the “*City of Launceston Project*” that considered the effect of archaeological field work and scallop dredging on corrosion rates. Of course, environment of deposition is not the only factor that determines how corrosion affects a wreck site. The materials and construction of the ship dictate how it will be affected by the post-depositional transforms

## *Conclusion*

The body of literature concerning corrosion studies on submerged archaeological sites is extensive, and this review of the evolution of this field is vital in preparing the methodology of the “*Huron* Project.” The literature review spanning from Ian MacLeod’s “Shipwrecks and Applied Electrochemistry” in 1981, to the “*Arizona* Project” in 2006 were used to fine tune this thesis project’s methodology. In order to understand and better protect submerged heritage resources, both the natural and cultural variables of wreck site formation need to be thoroughly investigated as shown by the “*Xantho* Project” and the “*City of Launceston* Project.” The natural and cultural variables acting on the USS *Huron*’s site formation are explored in the following chapters.

## CHAPTER 3: HISTORY AND CONSTRUCTION OF USS *HURON*

### *Introduction*

In order to understand the site formation of the USS *Huron* archaeological site, it is necessary to put the ship's construction in context within American shipbuilding of the time (McCarthy 2002:7). While *Huron* lagged behind the technological curve with its iron hull (as opposed to steel), auxiliary sails, and smooth bore ordnance, it served admirably in a role as a peacetime warship until its untimely end in 1877. This chapter outlines *Huron's* construction, working life, wrecking event, and salvage.

Samuel Thearle, a nineteenth-century marine architect, wrote a shipbuilding treatise titled *The Modern Practice of Shipbuilding in Iron and Steel*, published in 1888. This work details ferrous ship construction from the keel up and is used as a comparative study with *Huron's* original builders plans to demonstrate the inherent seaworthiness of this vessel. Joe Friday Jr. wrote "A History of the Wreck of the USS *Huron*" in 1988 as his graduate thesis for the Program in Maritime Studies at East Carolina University. Friday's thesis included an extensive history of USS *Huron* and performed an archaeological survey of the wreck site. A transcription from a U.S. Navy Court of Inquiry surrounding the loss of *Huron* also provides a firsthand account of the wrecking event and subsequent salvage (U.S. Naval Inquiry 1877).

### *American Transition from Wood to Iron Ships in the Nineteenth-Century*

From 1820 until the end of the American Civil War (1861-1865), the United States was a leader in producing high quality wooden vessels at a low price. American shipbuilders embraced an egalitarian craftwork based view of ship labor which valued simple hand tools and practical experience. This perspective was in direct contrast to what they considered the "elitist" British

ideal of technical mathematics-based engineering. American ship designers whittled wooden half models instead of inking technical drawings. These models were consulted and then scaled to manufacture the ships scantlings.

The emphasis on wooden ship construction was not just born of American shipbuilding culture, but was also a matter of economics. America's timberlands were a source of cheap materials that fueled the wooden ship economy. This growth was further emphasized by high start-up costs for iron shipyards and quality British iron was cost prohibitive because of high import tariffs (Thiesen 2006:57-58). Even in 1875 when the USS *Huron* was built, iron ships were constructed in a manner almost identical to those of wood ships, except for the material used and the employee of riveting. In fact, wood workers still oversaw the building of the iron vessels (Figure 7).

American shipbuilder's fostered familial networks in the shipyards and this form of nepotism became the U.S. Navy policy in 1868 with preference given to hiring shipyard employee's children as apprentices. It was through family and practical hands-on experience that the American shipbuilding tradition was transmitted, not through technical handbooks as in the British fashion (Thiesen 2006:44-46).

Iron shipbuilding was met with skepticism in America. The first iron-hulled vessel built in the United States was *Cordorus*, built in 1825 by John Elgar. This vessel was made of wrought iron sheets, readily available to Elgar who was a manufacturer of nails (Rodgers 1996:8). In 1834, people gathered along the shore and watched in disbelief as the iron-hulled *John Randolph* was launched, expecting the metal ship to founder.

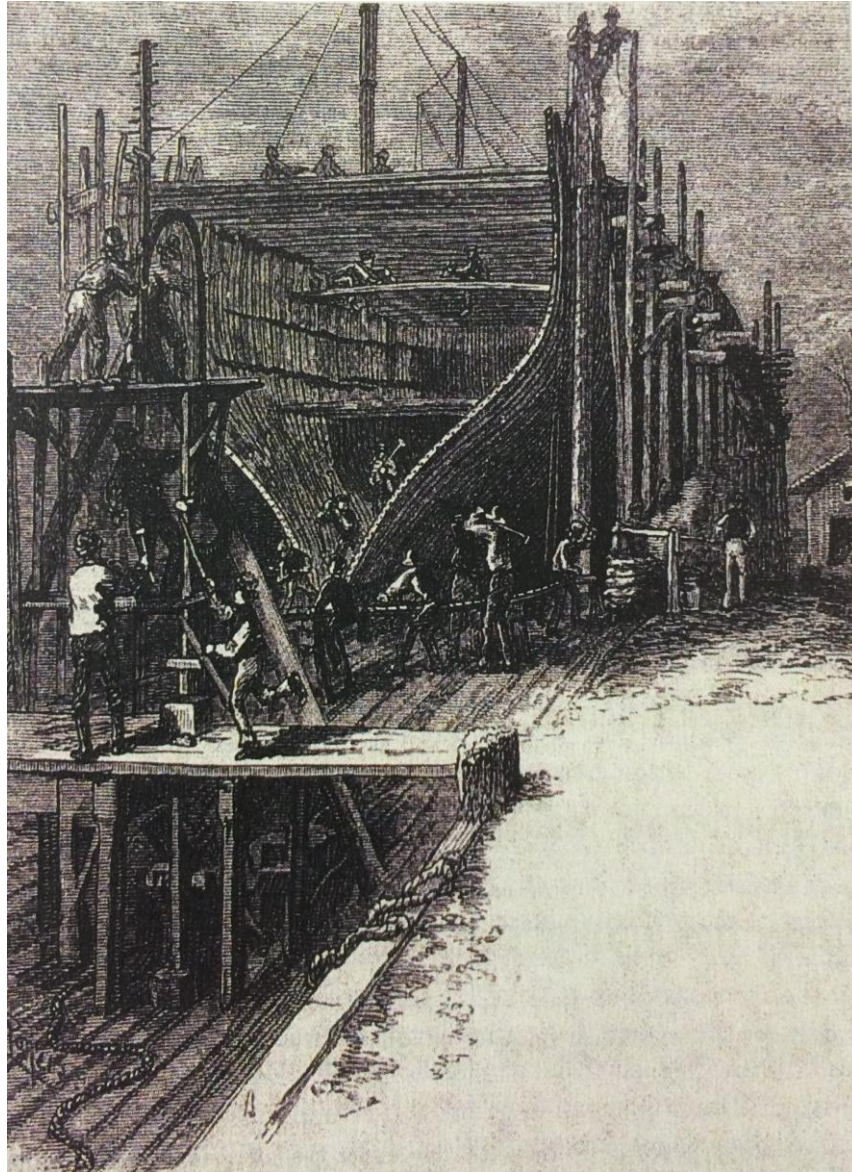


**Figure 7. The construction of an iron ship in America during this time period closely resembled that of a wooden ship (Barnard 1878:641, taken from Thiesen 2006:102).**

Iron shipbuilding was gradually accepted as questions of iron's buoyancy and durability were addressed. Wooden ships are highly susceptible to fires, a danger exacerbated by the introduction of fire burning boilers. Iron minimizes this risk. Collisions and groundings were events that often destroyed wooden vessels. Iron vessels, especially when engineered with a double hull and watertight compartments, had a much higher survivability rate during what were previously catastrophic events (Thiesen 2006:82-83).

An iron vessel has much more longitudinal strength than a wood vessel. This strength helps prevent hogging, which is the sagging of the bow and stern of a vessel resulting from the buoyancy discrepancy between the center of a vessel and its less voluminous ends. This allows longer ships with narrower beams to be built. This rigidity also reduced drive shaft misalignment reducing stress on the drive train and allowing the ship to run with adequate power during heavy seas. Wooden steam powered vessels are also susceptible to damage from steam power plants as the vibration works seams and fastenings loose (Thiesen 2006:82).

There are problems inherent in ferrous hulls, the first being biofouling, which has always been a concern for any vessel left in the water, as barnacles and other organisms colonize a ship's hull increasing drag and slowing a ship. Wooden ships are vulnerable to teredo worms, which are mollusks that burrow into wood and ravage hulls. Iron ships are not vulnerable to teredo worms. Wooden ships can be sheathed in copper, a material with natural biocide properties that helps limit the extent of biofouling. Iron ships cannot be sheathed in the same way because of the effects of corrosion from galvanic coupling between the dissimilar metals. The iron would rapidly corrode as it rusted preferentially to the less noble copper alloy.

By the middle of the nineteenth century hundreds of biofouling paints had been tested and none were found comparable to copper sheathing. Marine architects resorted to sheathing the iron hull with an intermediary layer of wood and then placing a copper layer outboard to shield the dissimilar metals from galvanic corrosion. This added expense to ships and the simplest solution was to haul the ships out every few months and clean the hull (Rodgers 1996:36).

The second issue with iron-hulled ships is compass correction. Magnetic distortion causes the compass to deviate as the mass of iron from the ship's hull interferes with the ship's compass. Royal Astronomer George Airy developed a method to calibrate an iron ship's

compass in 1839. He developed a technique that came to be known as “swing ship,” a process where the ship is turned in a complete circle on a single axis and the compass deviation is noted. Magnets are then strategically placed on the binnacle to counteract the ferrous hull’s distortion of the compass (Rodgers 1996:35). This process needs to be repeated periodically, otherwise compass deviation will become a problem.

The first iron-hulled ship produced for the US Navy was the USS *Michigan* launched in 1843 bound for duty on the Great Lakes. This first-class paddle steamer had a fourteen-knot cruising speed, meaning that no ship powerful enough to destroy *Michigan* could even catch it during this time period. It was faster, lighter, and better-armed with pivoting shell guns, had watertight compartments to absorb battle damage, and was, more importantly, cheaper than a comparable wooden ship. The USS *Michigan* demonstrated the superiority of iron-hulled ships, but nonetheless, iron shipbuilding remained secondary in the US shipbuilding industry (Rodgers 1996:7-9).

Boston and New York were the centers of wooden shipbuilding up to the Civil War period, but high prices for labor and lack of proximity to raw materials prevented these areas from competing with the Delaware Valley as the center of iron ship building in America. The Delaware Valley was in a prime location to receive rolled iron from eastern Pennsylvania and Jesse W. Starr built the second iron vessel in America there in 1829. By the 1840s the Starr family was manufacturing iron tugboats. Experimentation with propeller technology flourished in New York and the Delaware Valley, but the wooden ship builders of New York preferred the less efficient, but less damaging paddle wheel (in terms of canal erosion from the ship’s wake). The Delaware Valley was technologically progressive and the world’s first screw-propeller warship, USS *Princeton*, was built there in 1843 (Thiesen 2006:84). Access to finished materials

and technological expertise coalesced in the Delaware Valley making it the epicenter of American iron shipbuilding. It was there that the USS *Huron* was designed and then constructed in 1875.

### *USS Huron's Construction*

The United States Navy was one of the largest navies in the world during the American Civil War (1861-1865). The USS *Huron* was built only a decade after the war, but by this time the United States Navy had dwindled from over seven hundred ships to a paltry forty-eight outmoded vessels. Congress and the American public were preoccupied with the post-Civil War Reconstruction of the South and additionally were focused on settling the American West and finishing the transcontinental railroad. The US Navy was an afterthought to a war weary nation and funding slowed to a trickle (Friday 1988:3). USS *Huron* was commissioned in 1875 and was one of the last iron ships built for the United States Navy (two other ships were built on the same plans: *Alert* and *Ranger*). Notably, *Huron* was also the last to use a combination of both steam and sail propulsion and to be armed with smooth bore ordinance.

*Huron* measured 175 feet long (length between perpendiculars) with a beam of 32 feet (a length to beam ratio nearing 5.5 to 1), a dry displacement of 541 tons, and a fully loaded displacement of 1,020 tons. The ship was classified as a third rate gunboat and equipped with a two cylinder, back acting compound engine producing 605 horsepower, and a 12 foot four bladed propeller in addition to its schooner rig, making the ship capable of a healthy 10 knot speed. USS *Huron* was a robustly built ship, complete with 4 inch iron frames spaced 21 inches apart, complemented by a wide side-bar iron keel, keelsons, and 5/8 inch thick side plates (U.S. Naval Inquiry 1877:49-52).

The keel provides the longitudinal strength necessary to avoid hogging. It acts as the ship's backbone, and the USS *Huron* had a keel of significant quality. The most common form of keel from *Huron's* era, whether it be iron or steel, is the bar keel (Figure 8) seen atop the blocks used as the foundation for building the ship. It consists of lengths of iron or steel split into lengths of approximately 40 feet and then joined using a vertical scarph to the length necessary for the ship's size. The keel is then further bolstered by the attachment of the garboard strake (Thearle 1886:26). The bar keel served admirably as a cost effective and reliable keel design for most vessels.

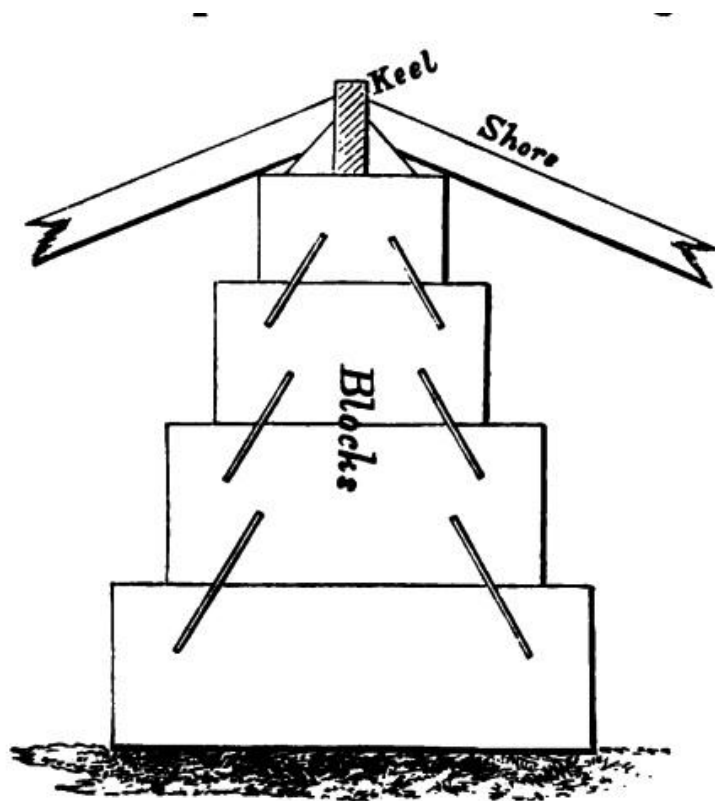


**Figure 8. Illustration of a bar keel, the most common keel type used by American shipbuilders in *Huron's* era (Thearle 1886:26).**

The USS *Huron* did not use the bar keel, but rather had a side bar keel. This design has a much higher cost, but it is a superior design known for its strength. The defining characteristic of the side bar keel is the “continuous vertical plate extending from the underside of the keel to the

top of the floors” (Thearle 1886:27). The USS *Huron*’s side bar keel is shown in Figure 9, and the keel centerplate bar goes beyond the ship’s floors and tops off at the ceiling planks. It is then sandwiched between two keelsons (shown between the ceiling and garboard strake) that run the length of the keel and are made of stout 3/8-inch iron plate.

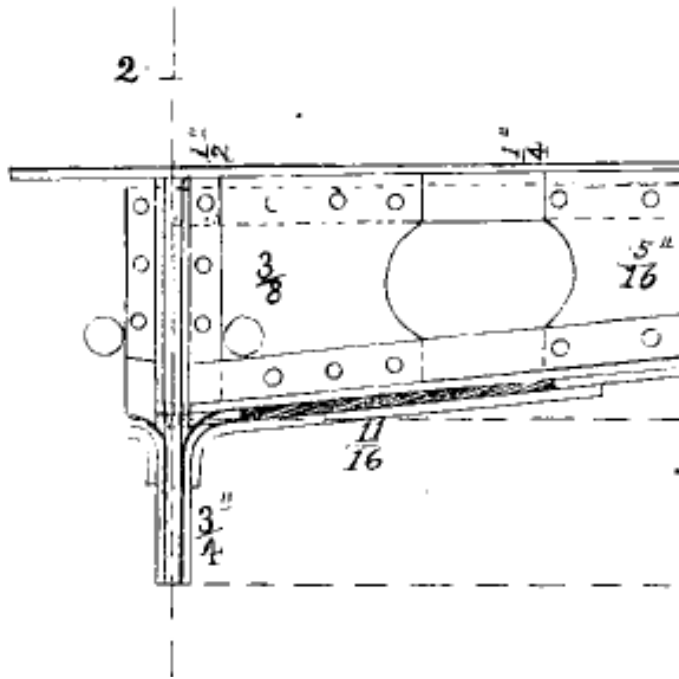


**Figure 9. Example of *Huron*’s side bar keel taken from the builder’s cross section (U.S. Naval Inquiry 1877:52).**

The keel is then laid and longitudinal strength established. The next step was to create lateral strength through framing. The transverse system of framing was the most common system found in iron ship’s, including the USS *Huron*. This system requires transverse frames to be fastened to the ship’s keel to create the ribs of the ship. The frames consist of three different components. The first being a frame angle bar, fastened along the hull plates from the keel to the gunwale. Second, a floor plate was then riveted on its bottom edge to the frame angle bar and then riveted on its top edge to the third piece being the reverse angle bar. This bar extends opposite to the frame angle bar and was attached to the ship’s ceiling plates (Figure 10). To further strengthen the frame, a reverse frame is fastened to each frame set (Thearle 1886:36).

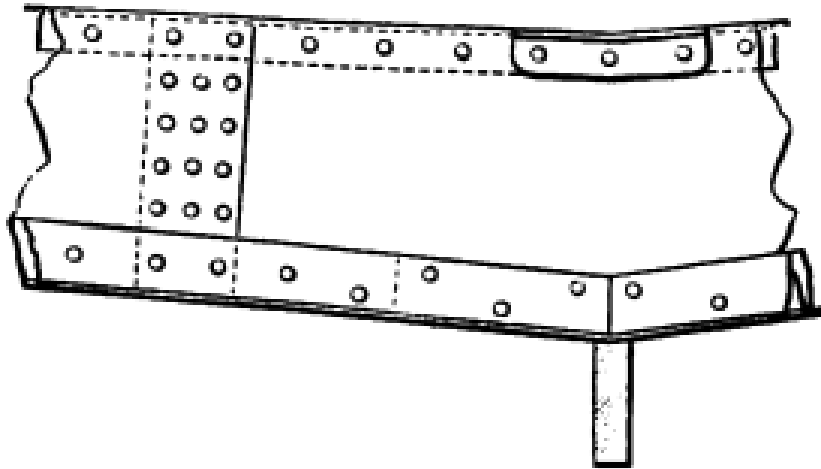


**Figure 10. Example of transverse framing (Thearle 1886:34)**

The USS *Huron*'s frames were built to a size of 4" by 3.5" by 6/16" while Liverpool insurance underwriters only required a ship comparable to *Huron* to have frames measuring 3.5" by 3" by 6/16". Additionally, the USS *Huron*'s frames were each 21 inches apart, while a comparable ship would have required its frames to be 23 inches apart. This means *Huron* not only had more frames than a comparable ship, but its frames are significantly thicker (Figure 11) (U.S. Naval Inquiry 1877:52).

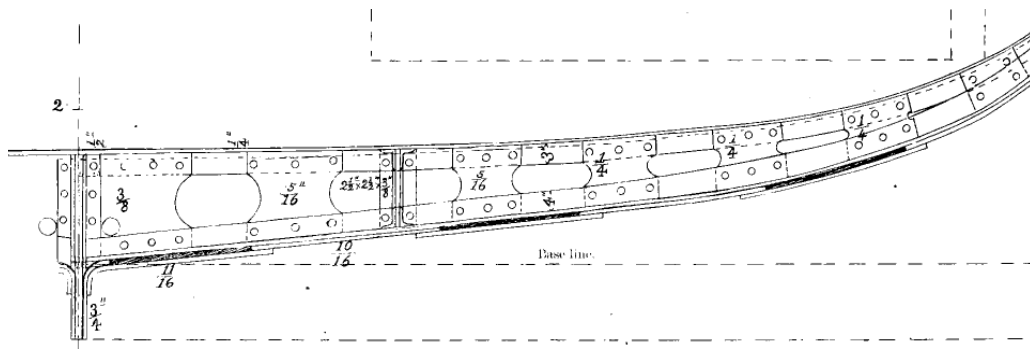


**Figure 11. Transverse frames from the USS *Huron*'s builder's plans (U.S. Naval Inquiry 1877:52).**

*Huron* would then have its 8-inch thick beams laid atop 29-inch knees (9 inches deeper than insurance underwriters prescribed) on its lower deck. Instead of deck stringers, *Huron* had a complete iron deck (topped by wood), interrupted only by two hatches (U.S. Naval Inquiry

1877:52). This created a watertight main deck and added some additional longitudinal strength to the ship (Thearle 1886:100). The ship had thick iron hull plating consisting of sheer, side, bilge, bottom, garboard, and bulwark plates. These plates were fitted using the clencher system (overlapping plates). The plates were all thicker than required, resulting in not only a stronger ship, but also one that lasts longer in the face of oxidation. The thickest plates were the sheer and garboard, as they formed the top and bottom plates and acts as a girder (Thearle 1886:130-133) (Table 2).

<b>Plate</b>	<b>Liverpool specifications</b>	<b><i>Huron</i>'s specifications</b>
Sheer	10/16"	11/16"
Side, Bilge, Bottom	8/16" or 9/16"	10/16"
Garboard	9/16"	11/16"
Bulwark	5/16"	6/16"

**Table 2. Plate thickness of the USS *Huron* compared to Liverpool Insurance specifications (U.S. Naval Inquiry 1877:52).**

John Roach's Chester, Pennsylvania rolling mill manufactured *Huron*'s plates. The plates were painstakingly fitted, and outlines of both the shape and rivet placement were made using wooden templates. The iron plates were then bent into the correct shape using steam driven rollers. Plates that needed extreme curvature were hammered into shape by hand and when that was not enough, canines were used to pull a block and tackle system to bend the plate into shape. Workers would then mark the location with chalk where the rivets would be driven on the plate. A steam powered punching machine could punch out the rivet holes with a top speed of twenty holes a minute. After the plates were shaped and punched, workers laboriously hoisted the plates into place on the ship and bolted every other rivet hole holding the plate until they could be riveted in place (Thiesen 2006:104-106).

Each plate was then riveted to the ship's transverse framing with the rivets fastened in a zig-zag fashion, while the butt straps (metal bands that run vertically on the clenched plates) were treble riveted in a line (Thearle 1886:37,139). While a wooden ship would have its seams filled with oakum to seal the ship, iron ships were already watertight from the riveting, but to keep water from entering between the plates and contributing to undue corrosion, the edges were hammered tight (Thiesen 2006:107).

While *Huron* was a well-built, seaworthy vessel, it was also a victim of conservative Naval command that refused to acknowledge the vast potential of steam propulsion. In 1869, a general order required that all naval vessels be fitted with a full complement of sails (Figure 12) (Friday 1988:3). This resistance to the commiserate technological evolution of naval vessels, led to the USS *Huron* being a sturdy built ship, but it lacked key technology found in ships built immediately after *Huron*, such as rifled ordinance.

The ship was armed with a smoothbore 11-inch Dahlgren cannon, sixty-pounder Parrott rifle, two nine-inch Dahlgrens and a twelve-pound Howitzer. The Howitzer could also be mounted on a field carriage for shore duty. *Huron* also had a fifty-caliber Gatling gun and an assortment of small arms including: sixty-three Remington rifles, thirty-seven Remington pistols, twelve Colt revolvers, and fifty-one cutlasses. These weapons were standard US Navy equipment of the time, but the larger smoothbore ordnance would be replaced by superior rifled ordnance after *Huron* was built (Friday 1988:15-16).

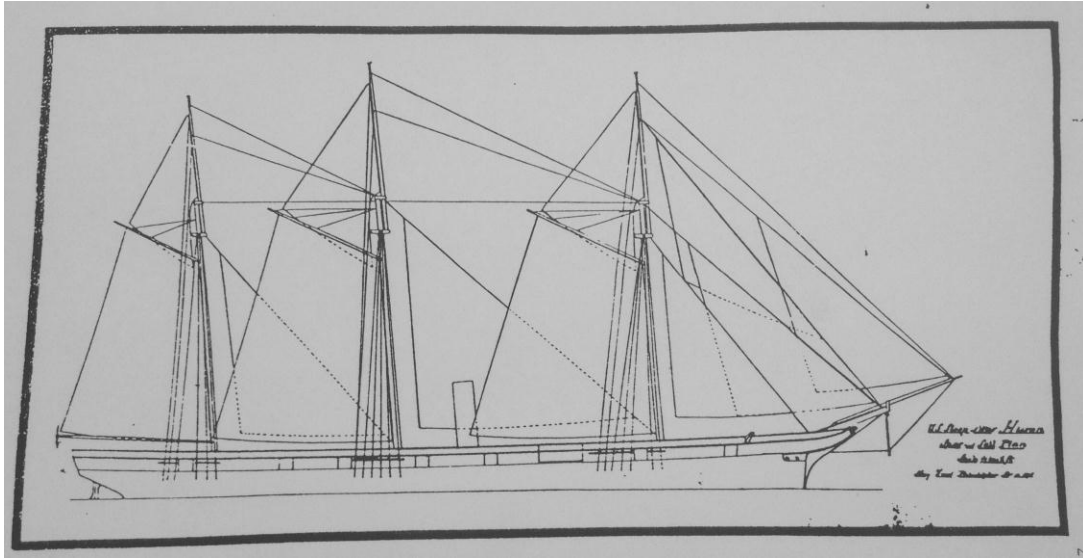


**Figure 12. Sail and Spar plan of the USS *Huron* (Friday 1988:21).**

The USS *Huron* and the *Alert*-class ships represented the end of an era for iron shipbuilding. The next ships to be built for the U.S. Navy would not be seen until 1884. U.S. Congress authorized \$1,300,000 to construct the United States' first modern warships in 1883. The "ABCD fleet," as the vessels came to be known were comprised of the USS *Atlanta*, *Boston*, *Chicago*, and *Dolphin*. These ships were constructed entirely out of American steel and were armed with breech loading, rifled ordnance. Like *Huron*, these ships were also outfitted with both sails and steam power (Thiesen 2006:153-154).

#### *USS Huron's Working Life*

Charles C. Carpenter took command of the newly commissioned USS *Huron* 15 November 1875. Immediately after the commissioning ceremony, *Huron* was loaded with supplies and final outfitting completed (Figure 13). Commander Carpenter reported *Huron* ready for sea on 1 December 1875, and steamed south from the Philadelphia Shipyard to Norfolk,

Virginia, headquarters of the North Atlantic Squadron to report for duty.

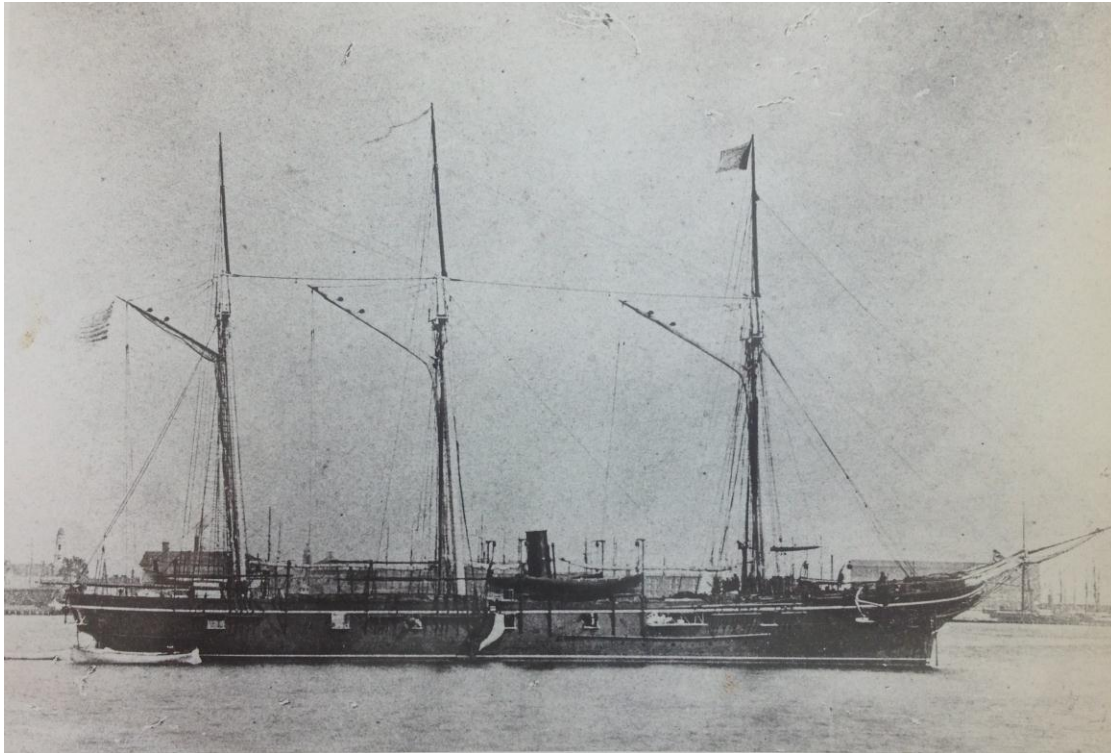


**Figure 13. USS *Huron* fully rigged and ready to sail (courtesy of The Mariners Museum, Newport News, Virginia)**

The crew of the USS *Huron* idled away quietly, towing Navy monitors in and around Port Royal, South Carolina until 9 April 1876 when they were called to Vera Cruz, Mexico for a three-month deployment. Border disputes along the Mexico/Texas border were creating a diplomatic nightmare, and the Mexican government was in political turmoil as Porfirio Diaz, a former leader in the Mexican military, attempted a violent coup. His revolutionaries struck the ever-weakening Mexican government with ferocious attacks on communication and transportation networks. *Huron* was ordered to project US power in Vera Cruz and to report on any developments on both the status of the Mexican government and the state of U.S. citizen's welfare and property in the country. *Huron* completed its assignment in Mexico 25 July 1876 and returned to Port Royal, South Carolina (Friday 1988:25-33).

Commander Carpenter relinquished his command of the USS *Huron* to attend torpedo instruction school. Commander George Ryan was his successor and took command 8 September 1876. Commander Ryan's previous post was on Kerguelen Island off South Africa, where he set up an astronomical observation station whose mission was to record the transit of Venus across the sun in December 1874 (Friday 1988:34-35).

The Navy, probably citing Commander Ryan's scientific experience off South Africa, ordered *Huron* to sail to South America to run trials on a new chronometer to establish accurate longitude readings. Before the USS *Huron* set sail from Charleston, South Carolina in January 1877, the ship's executive officer Lieutenant Fletcher went on a drinking bender and deserted. Fletcher was court martialed. In his hearing he cited his fear of the sea and knew *Huron* was an ill-fated ship. His prediction would become part of the lore of the wrecking of the USS *Huron* (Friday 1988:38).

The crew of the USS *Huron* performed admirably on their South American expedition and their next task was to survey the monitor *Tecumseh*, which wrecked off Mobile Bay, Alabama and report its precise location to the Navy. By this time, the ship's hull held so much biofouling, its cruising speed went from over ten knots to just barely over 5 knots. Command ordered the ship to Norfolk, Virginia for hull-scraping. En route, the USS *Huron* was redirected to Washington and Baltimore, where a railroad strike escalated into a riot. *Huron* landed Marines who were used to suppress the rioters. The USS *Huron* then sailed down the Chesapeake Bay and to Norfolk, Virginia where it was finally overhauled (Friday 1988:40-42).

### *Wrecking Event*

Surviving crewmember testimonies describe the events leading to the wrecking, and recount this terrifying ordeal in a United States Senate hearing held on 5 December 1877. The

U.S. sloop of war received orders to reconnoiter the coast of Cuba and amend any hazards not shown on standard charts. After a propeller refit and steam trials, the ship left Hampton Roads, Virginia on 22 November 1877. Upon leaving the harbor, the ship crew was met with calm conditions aboard the sturdy vessel. Inspections showed the ship to be in satisfactory condition, but the compass might have been affected by magnetic interference from the iron hull and the deviation incorrectly noted (U.S. Naval Inquiry 1877:28). It is not stated that this caused the wrecking, but might have been a contributing factor.

Surviving crewmember Ensign Lucien Young was in his berth when the USS *Huron* grounded. He gave his recollection of the wrecking event to the USS *Huron* Court of Inquiry formed shortly after the wrecking event. Young describes waking up to the sound of *Huron* grounding and Commander Ryan calling from his cabin, “hard down, hard astarboard!” Young rushed to get his pants and coat and arrived on the main deck. Commander Ryan was already there, having not changed out of his clothes during the night. Orders were given to throw the 9-inch Dahlgren guns overboard. The ship was pounded by an unrelenting swell and crewmembers began to be swept from the decks. Over 100 distress rockets were fired, but the Lifesaving Service station located only a few miles from the wreck site had closed a month prior. The ship listed to a forty-five degree angle on its port side, and the orders to abandon ship were given. A wave crashed over the deck sweeping Young into the gaff where his legs were badly hurt. The vessel was listing badly and coupled with his injuries, he struggled to stand (U.S. Naval Inquiry 1877:14-18).

He heard men calling for help and in the next instance, another swell washed the deck and swept those men into the sea. Young managed to make his way to the forecabin despite his injuries and huddled there with other survivors. They took refuge in downed sails and tried to

stay warm. He saw men struggling to get the ship's launch into the water only to be crushed and killed by it. He jury-rigged a belay pin and some line and reported a sounding of 8 feet. He described the ship as settling into the sand and the tide rising (U.S. Naval Inquiry 1877:15-17).

Young and another man grabbed pieces of rigging and made a raft they hoped would allow them to negotiate the pounding surf. They were desperately cold and weak. They jumped into the surf and upon hitting the water, were entangled. A wave capsized the raft. The men managed to right the makeshift vessel, cut the offending line with a penknife, and carry on towards shore. Exhausted and desperate, they struggled in the surf. Guided by telegraph poles they could barely make out in the fog, they made it to the beach.

Young was approached by fisherman on the beach, and he asked them if they saw the signal flares. The fisherman replied that they saw the first signal flare. Young asked them why they didn't go to the Lifesaving station and grab a lifeboat hours before. They replied that they were scared to break the lock and grab the necessary equipment that would have saved lives. Young was barefoot and injured, but managed to make it to the Lifesaving station himself and put together a mule team and a mortar and lines. He made it back to the *Huron* wreck around 9:30 AM, in time to see the last mast fall into the surf. There were no more men on the deck and Young had no need for the mortar that would have been used to fire a line to the ship in order to rescue. Locals were patrolling the beach and finding a few survivors scattered among a vast number of corpses. In all, ninety-eight crewmen died, and only thirty-four managed to survive the horrible disaster (U.S. Naval Inquiry 1877:17-18).

The horror of the *Huron* disaster was not finished. Two days after *Huron* wrecked, the US Navy ships *Swatara*, *Powhatan*, *Fortune*, and the wrecking ship *B&J Baker* arrived to assess and salvage what they could from *Huron*. The surf was still high, and the ships could not launch

their surfboats. Finally, that afternoon a surfboat from *B&J Baker* attempted to clear the pounding surf with a crew of nine, including Captain E.M. Stoddard of the wrecking ship *B&J Baker* and Captain John Guthrie, Superintendent of the Lifesaving Service's seventh district, and a reporter from the Norfolk-based newspaper *Virginian*. The surfboat managed to clear the first wave of the set, but the next wave caught the boat and instead of riding the wave straight down, the boat turned perpendicular to the breaking wave, pearled, and was tossed ten feet in the air and capsized in a violent manner. The reporter, Captain Stoddard, and one crewmember managed to cling onto the boat as it washed through the surf zone. The other six of the landing party including Captain Guthrie drowned in the surf bringing the casualties of that weekend to 104 dead (Friday 1988:61-62).

The grim task of body recovery fell to hired local fisherman, U.S. Marines, and surviving crewmembers from *Huron*. Many of the bodies were found in an advanced state of decomposition and free of personal artifacts. This made identifying the victims difficult, however, surviving crewmember Samuel Clark had tattooed many of his fellow sailors and through these marks he was able to successfully identify many of the deceased. The bodies were buried in Nags Head, and Lieutenant-Commander Jas. G. Green and Commodore J. Blakelely Creighton recorded the locations of the graves (U.S. Naval Inquiry 1877:44-45).

The Naval Court of Inquiry ruled that the USS *Huron* was a sound vessel in the most unfavorable conditions. It was found through mathematical modeling that the ship had a safety factor of 2.5 times the load bearing capabilities between perpendiculars built into the ship when it was fully loaded (Figure 14) (U.S. Naval Inquiry 1877:49-51).



	Scantlings re- quired by rules of Liverpool un- derwriters.	Scantlings of United States Steamer Hu- ron.
<b>Keel:</b> Thickness of center-plate .....	$\frac{8}{16}$ "	$\frac{12}{16}$ "
Depth below floors .....	8"	12"
Thickness of side-plates .....	$\frac{12}{16}$ "	$\frac{12}{16}$ "
Horizontal keelson-plate, width .....	28"	24"
Horizontal keelson-plate, thickness .....	$\frac{8}{16}$ "	$\frac{8}{16}$ "
<b>Frames:</b> Spacing of frames .....	23"	21"
Dimensions of frames .....	$3\frac{1}{2}$ " $\times$ 3" $\times$ $\frac{6}{16}$ "	4" $\times$ $3\frac{1}{2}$ " $\times$ $\frac{6}{16}$ "
Dimensions of reverse frames .....	$2\frac{1}{2}$ " $\times$ $2\frac{1}{2}$ " $\times$ $\frac{5}{16}$ "	3" $\times$ 3" $\times$ $\frac{5}{16}$ "
<b>Floors:</b> Depth at center .....	21"	18"
Thickness .....	$\frac{8}{16}$ "	$\frac{6}{16}$ "
<b>Intercostal keelson:</b> Thickness .....	$\frac{6}{16}$ "	$\frac{6}{16}$ "
<b>Plates, thickness:</b> Sheer .....	$\frac{10}{16}$ "	$\frac{11}{16}$ "
Side, bilge, and bottom .....	$\frac{8}{16}$ " or $\frac{9}{16}$ "	$\frac{10}{16}$ "
Garboard .....	$\frac{9}{16}$ "	$\frac{11}{16}$ "
Bulwark .....	$\frac{5}{16}$ "	$\frac{6}{16}$ "
<b>Beams:</b> Depth .....	8"	8"
Depth of knees .....	20"	29"
<b>Beam-stringers, lower deck:</b> Width .....	23"	15"
Thickness .....	$\frac{8}{16}$ "	$\frac{8}{16}$ "
<b>Beam-stringers, main deck, width</b> .....	35"	Iron deck.

**Figure 15. USS *Huron*'s Construction specifics compared to those required by Liverpool underwriters (U.S. Naval Inquiry 1877:52).**

The U.S. Naval Court of Inquiry ruled that the final cause of the wrecking of the USS *Huron* was a lack of seamanlike attention by Commander Ryan. It ruled that care was not taken when taking a bearing off the Currituck Lighthouse to reveal just how close the USS *Huron* was to shore. In addition, the soundings taken at the time the bearing was recorded were of little value, as the depths in this region are so irregular as to be unreliable indicators of how far a vessel is offshore.

Had Commander Ryan known that *Huron* was skirting the coastline he would have opted not to carry as much sail in a leeward wind, as this tends to push a vessel towards shore and encourages the quartermaster to simultaneously steer into the shore as they attempt to keep the sails full. Compass deviation may also have been a factor, as *Huron* was due for a calibration (U.S. Naval Inquiry 1877:35-36). The court also acknowledged that many seaworthy vessels

commanded by competent mariners have been lost in the same area as *Huron* (U.S. Naval Inquiry 1877:30).

*Public Outrage and Lasting Consequence of the Loss of the USS Huron*

Citizens of the United States were stunned at the immense loss of life and believed that this tragedy could have been avoided had adequate emergency assistance been available. The newspapers in America were awash with reports of the *Huron* disaster and were quick to levy criticism on the U.S government (Figure 16). Congress quickly and unanimously approved funding for compensating the crews' families. Newspapers called for the government to increase both funding and the active season that the Lifesaving Service stations operated (Friday 1988:79).

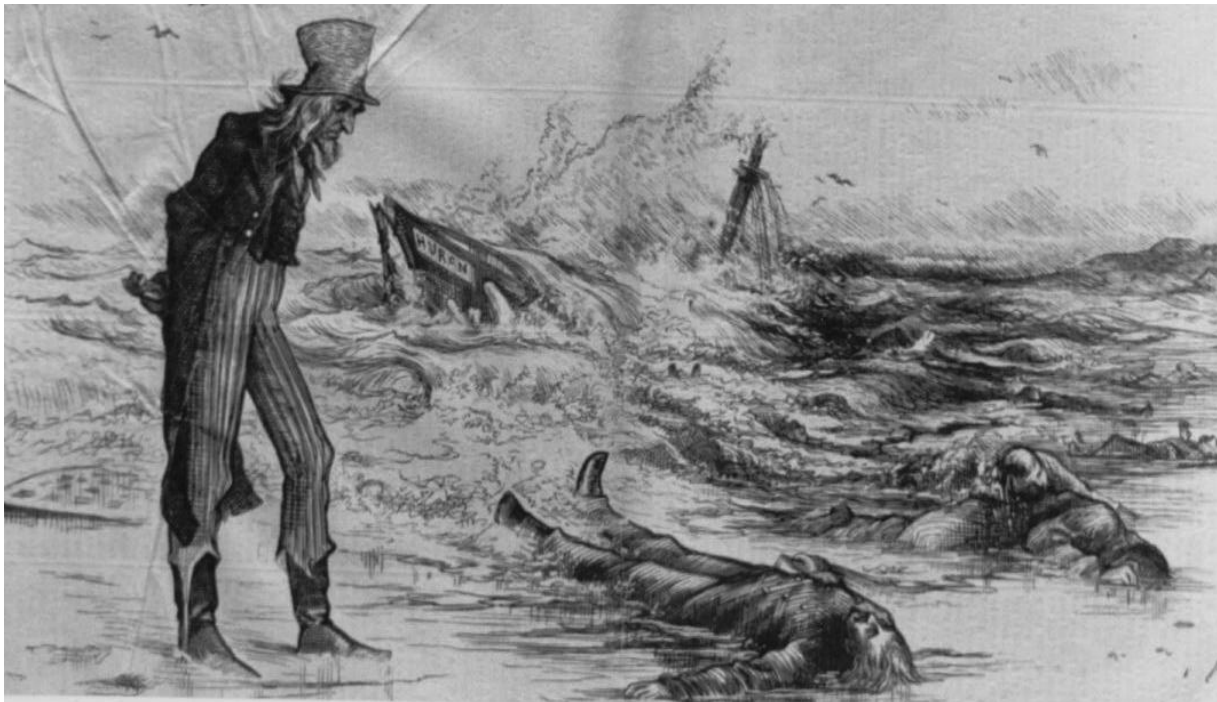


**Figure 16. “Death on Economy,” a cartoon published in Harper’s Weekly, 29 December 1877 with a caption that reads, “ I suppose I must spend a little on Lifesaving Service, Life-boat Stations, Life-Boats, Surf-Boats, etc; but it is too bad to be obliged to waste so much money” (Friday 1988:79).**

The *Huron* disaster was not impetus enough for Congress to make necessary improvements to the Lifesaving Service, to halt the continued and often needless loss of life on United States shores. It took another tragedy to finally motivate the United States government to make an effective change.

The next year, *Metropolis*, a merchant steamship, grounded twenty miles north of Nags Head, only 100 yards from shore. The Lifesaving Service arrived at the wreck site but failed to mitigate the disaster and eighty-five crew drowned. This disaster was the straw that broke the proverbial camel's back and combined with the loss of *Huron*, finally led to the expansion of the Lifesaving Service, the direct predecessor of the United States Coast Guard (Friday 1988:80-81).

### Conclusion

USS *Huron* was only active for two years before it met its tragic end. The ship served admirably in peacetime, but its lasting legacy is one of tragedy. The North Carolina Department of Cultural Resources and the Town of Nags Head manage the USS *Huron* site (Figure 17)(Zorc 2010:1).

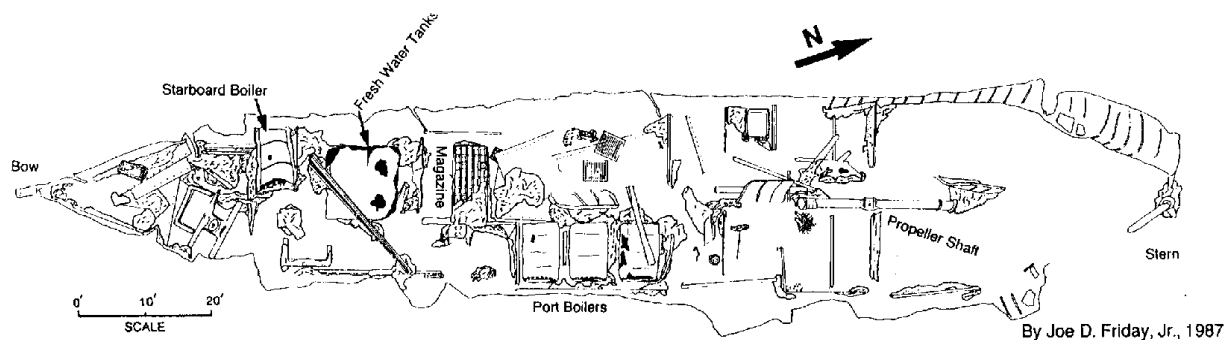


**Figure 17. Site plan of USS *Huron*, by Joe Friday 1988. Accessed from North Carolina Department of Cultural Resources Underwater Archaeology Branch (<http://www.archaeology.ncdcr.gov/images/ncarch/huron.gif>). 1 April 2011.**

The ship lies where it grounded and is an easily accessible cultural resource with a rich history. Local dive shops offer guided dives on the wreck site and it is a popular snorkeling spot in the summer when the water is warm and clear. There is a highway marker designating the

historic site and a gazebo off the Bladen Beach access dedicated to the USS *Huron*, complete with information on the history and wrecking of the infamous ship (Figure 18). The wreck site is now a designated U.S. National Register of Historic Places shipwreck preserve. The next chapter will outline the methodology used to put this historical ship in context with the wreck's site formation and seasonal influences.



**Figure 18. Sign posted off of Highway 12 and the adjoining gazebo dedicated to the loss of the USS *Huron*. (Photo by author, 2013.)**

## CHAPTER 4: METHODOLOGY

### *Introduction*

The primary goal of the “*Huron* Project was to periodically collect corrosion, salinity, temperature, dissolved oxygen and sediment data and to explore whether there exists seasonal factors that are influencing the corrosion of the shipwreck. A three-dimensional model of the USS *Huron*, as it was built in 1875, was created using McNeel’s *Rhinoceros Nurbs Modeling for Windows (Rhinoceros)* modeling software based on the original builder’s plans. Ship builder’s plans don’t necessarily represent the finished vessel and changes in construction can vary from the original specifications (David Stewart 2014, pers. comm.). Therefore, these plans serve as the theoretical baseline from which the archaeological site’s formation is modeled.

In 2012 East Carolina University’s Program in Maritime Studies fall field school mapped the wreck site in plan and profile view. A three-dimensional model of the wreck site was then created from this data using *Rhinoceros*. The step-by-step method of corrosion potential sampling is shown and data obtained for the 2012 summer, 2013 summer, and 2013 fall field seasons. Water parameters were sampled for the 2012 summer, 2013 winter, 2013 spring, 2013 summer, and 2013 fall field seasons as well. Analysis of the relationship between the corrosion potential data and the environmental parameters was then explored.

### *Digital Three-Dimensional Model of the USS Huron as Built in 1875*

A three-dimensional model was made representing USS *Huron* as it was built in 1875, using the original builder’s plans for the *Alert*-class ships and the *Rhinoceros*

computer program (Figure 19). The builder's plans were scanned and then uploaded into the program as a bitmap file and then digitally traced using the Polyline tool (Figure 20).

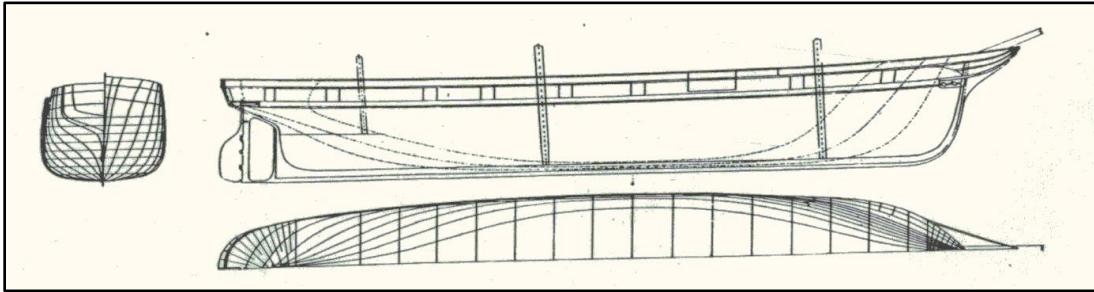


**Figure 19. Builder's plan for the USS *Huron* (Friday 1988:22).**

The portside hull lines were traced and were laid onto the ship's keel at the indicated stations. The hull lines were then snapped into the correct placement along the keel line. This provides the structure of the hull and is the skeleton from which the hull surface was created (Figure 21).

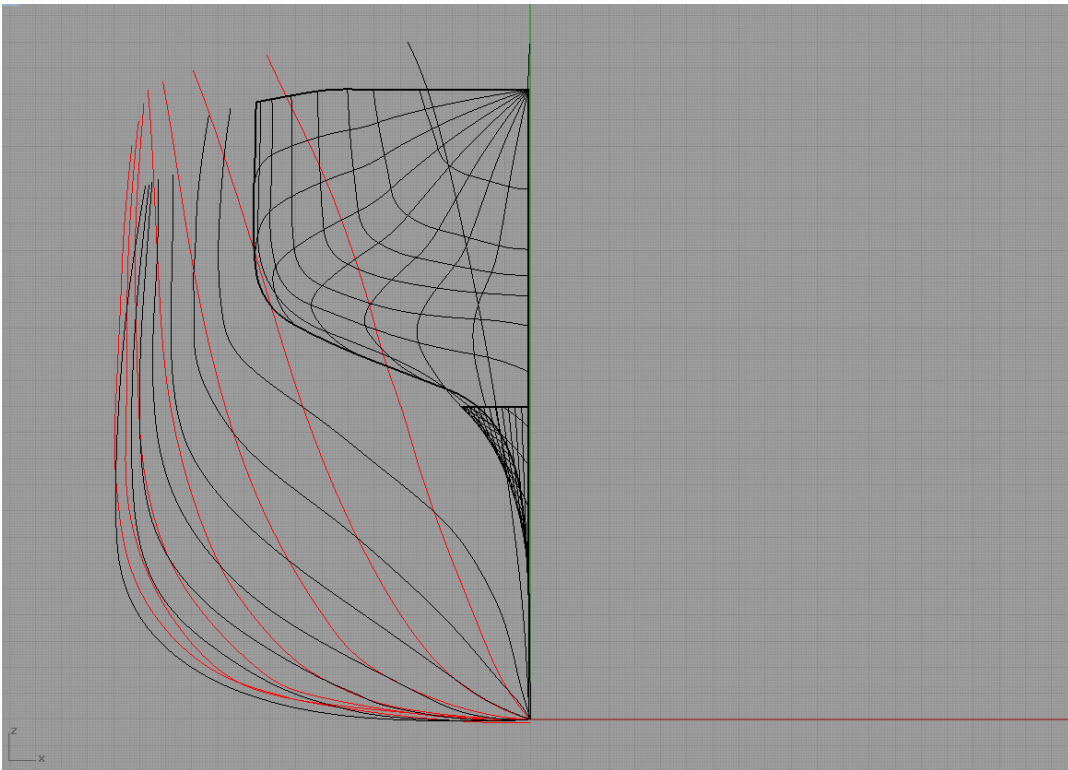


**Figure 20. Lines taken from the USS *Huron*'s builder's plans and then digitally traced in *Rhinoceros*. (Image by author, 2013.)**

Getting the hull shape and the resulting surface was the most difficult part of the modeling process. It was important to ensure all components of the model were securely joined and tight tolerances maintained. It is crucial to use the snap function in the software to ensure that different objects will snap into place at a predetermined tolerance.

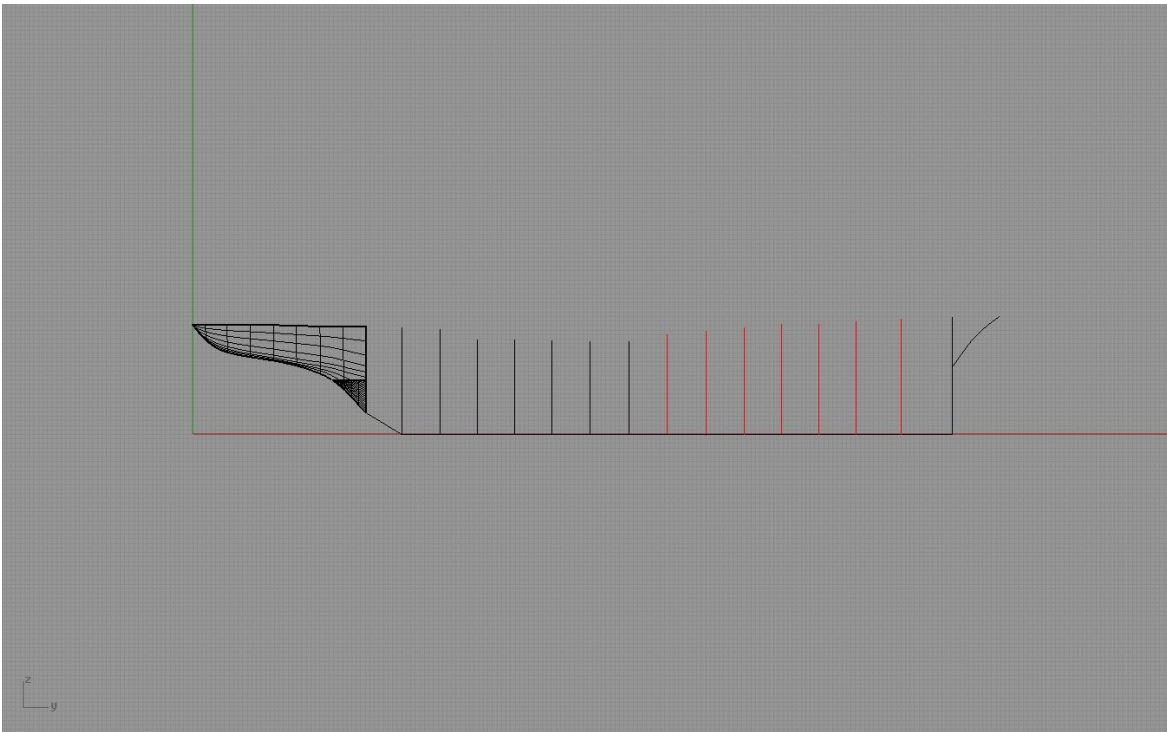


**Figure 21. Hull lines extrapolated onto the keel at the indicated stations. (Image by author, 2013.)**

The loose loft function in *Rhinoceros* created half the hull's surface. The first longitudinal half was then duplicated using the mirror function and the two sides joined together to complete the hull (Figure 22). The ship's mizzen, main, and fore mast were then modeled and attached in the correct places. Next, the smoke stack, mast stays, sail plan, main armament, propeller, and deck were rendered and snapped into place. Finally, the ship's textures and colors were added using *Rhinoceros* Material Editor (Figure 23). This is the extent of the USS *Huron* that could be reconstructed based on the original builder's plans.

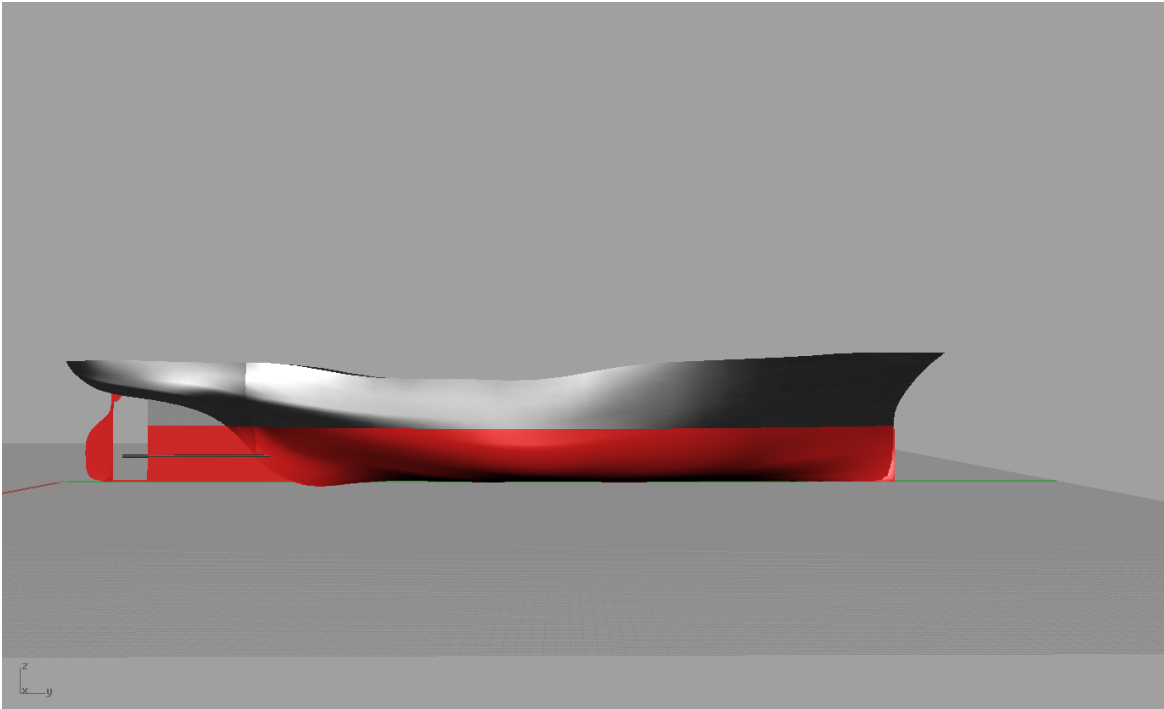


**Figure 22.** The loose loft function in *Rhinoceros* created the hull surface. (Image by author, 2013.)

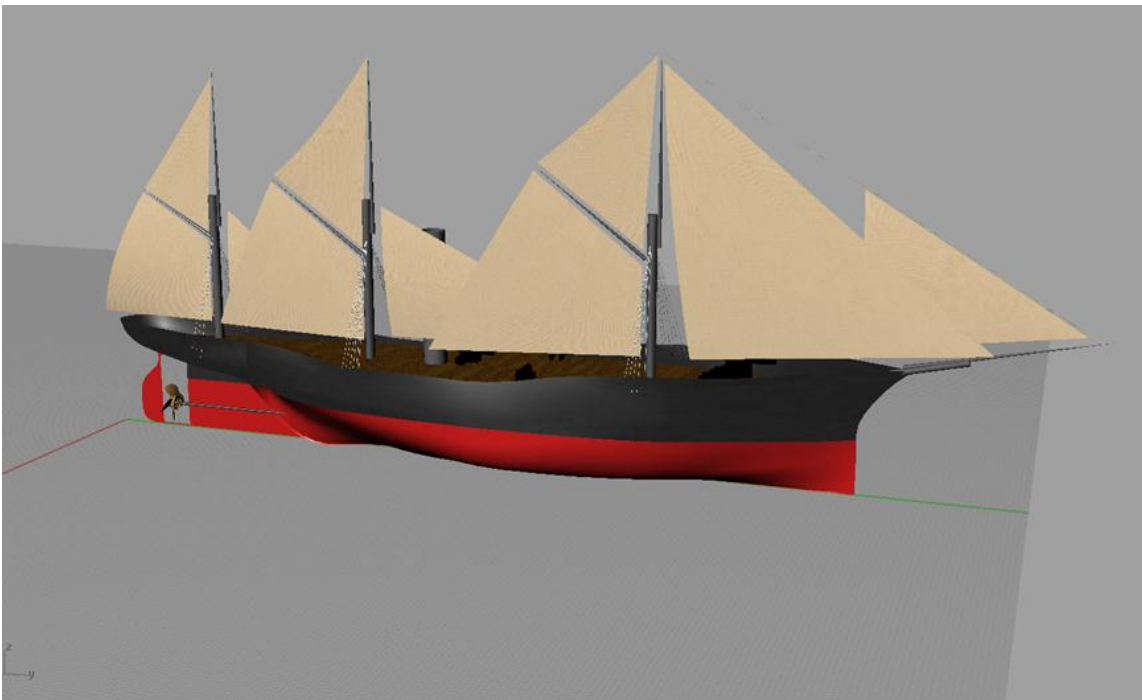


**Figure 23.** Complete three-dimensional model of the USS *Huron* as it was built and fitted in 1875. (Image by author, 2013.)

This three-dimensional model of *Huron* represents the baseline input of the site observed today. Comparing the ship before it wrecked and the wreck site as it lies today is crucial for site interpretation and understanding the archaeological site's formation. This information is important when making management decisions and predictions. To create the final three-dimensional model, the wreck site was mapped in plan and profile view; this process will be discussed in the next section.

### *Survey and Mapping*

The wreck of USS *Huron* is a popular dive site located 250 yards off Nags Head Public Beach (Figure 24), exactly east of the Bladen Street public access at 35° 58.670' north latitude, 75° 37.843' west longitude. The wreck lies at a depth of between 12 feet and 20 feet and sits in a 0.1m - 1.2m sand lens on top of a medium gravel substrate characteristic of the near shore morphology of the Outer Banks (McNinch 2004:132; Zorc 2010:3). There are several ways to find the wreck. The first, and most common when shore diving, is to swim out and use visual transits to estimate where the wreck is located. This requires lining up a particular house's window and the end of the Nags Head Fishing Pier (Figure 24). This method works, but is difficult if there is any current. GPS is a more reliable method to reliably find the wreck and locating the wreck with a waterproof GPS unit and a dive float made fieldwork more efficient.

During the summer months, the Town of Nags Head installs a marker buoy on the site. These marker buoys have a short life on this inshore wreck owing to the high swell energy and it is not uncommon to find the marker buoys submerged and wrapped around the stem post of the wreck. It is also possible to locate the wreck during periods of increased swell activity by observing the surge boiling off the wreck.

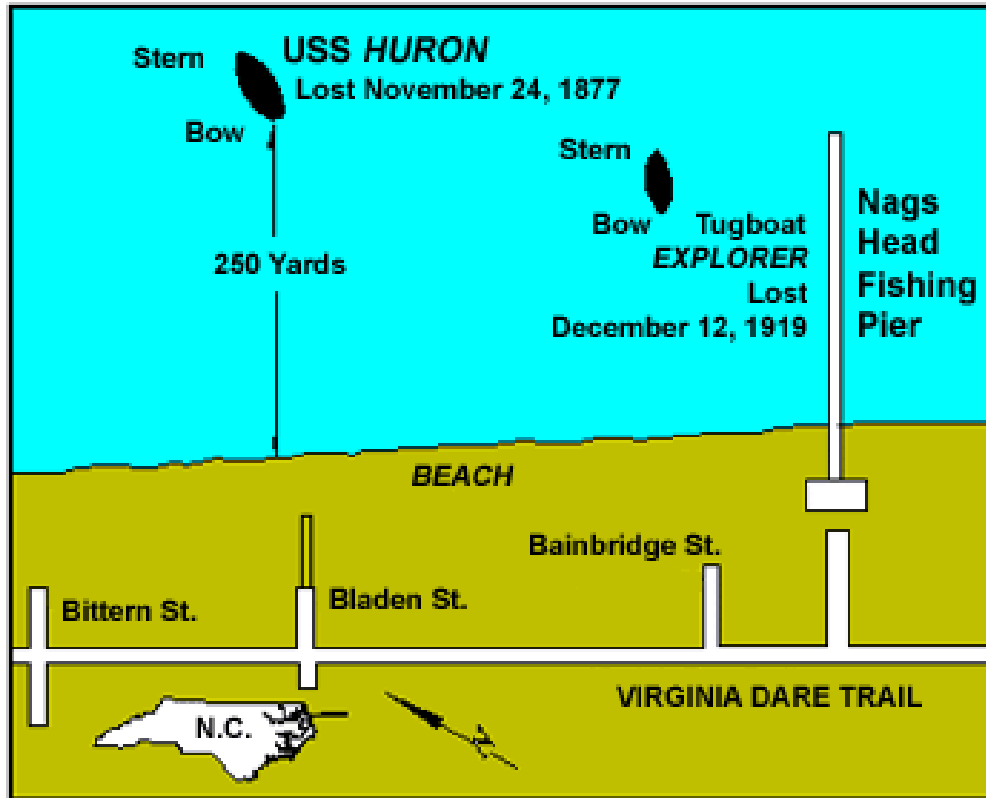


**Figure 24. Map showing the location of USS *Huron*. Accessed from North Carolina Department of Cultural Resources Underwater Archaeology Branch (<http://www.archaeology.ncdcr.gov/ncarch/underwater/huron.htm>). 1 April 2011.**

East Carolina University's (ECU) Maritime Studies Program fall field school students (course HIST 6850) in conjunction with University of North Carolina Coastal Studies Institute (CSI) and National Ocean and Atmospheric Administration (NOAA) researchers thoroughly mapped the wreck site during the month of September 2012. Dive operations were based off ECU's R/V *Cutting Edge* and CSI's *Miss Caroline* under the auspices of ECU's Diving and Water Safety Office.

The site was mapped in both plan and profile view. Conditions ranged from glassy seas topside coupled with 25 foot visibility underwater, to head high surf with 1 foot visibility. The surge is amplified in sections of the wreck site where gaps in the hull

plates create a venturi effect, and it was not uncommon for a diver to be sucked through these gaps while working during periods of heavy seas making field work difficult.

A semi-permanent baseline was installed on the site spanning from the stem post to the steering quadrant. The baseline consisted of a sturdy plastic coated steel line pulled taught with a come-a-long, and a calibrated fiberglass tape zip tied to the steel line. Offset and trilateration measurements were then taken from the baseline. Lateral movement of the baseline was a problem on the surge prone site. In response to this problem, buttressing lines were anchored at the midpoint of the baseline to minimize lateral movement. Using this type of baseline, researchers were able to clip the zero ends of their measuring tapes to the baseline and record the wreck in an efficient manner.

Profile drawings were made of both the port and starboard sides of the wreck site. The baseline was used as the X-axis and the hull relief was measured to complete the Y-axis. This profile mapping was vital to establishing the extent of sediment cover on the wreck site and in creating the digital three-dimensional model in *Rhinoceros*.

#### *Three-Dimensional Model of the Huron Wreck site*

To create the three-dimensional model of the *Huron* wreck site, the site plan inked in 2012 was used to digitally trace the starboard and port profiles of the wreck site. These two-dimensional drawings are called planar curves. The planar curves were then extruded into solids, giving them a third-dimension (Figure 25). After the port and starboard profiles were traced and made into solids, they were laid over the plan view map of the site and bent into place using the bend function in *Rhinoceros* (Figure 26).

The next step was to render and apply a texture layer using the *Rhinoceros* Material Editor function. This texture is based on digital photographs of the wreck site's concretion, but any JPEG image file can be used.

The final step in the modeling process is modeling the sediment cover of the wreck. This represents the percent sediment cover of the wreck in summer 2012 (Figure 27). This sediment cover data was important in understanding the correlation of sediment cover to the wreck site's corrosion potential. *Rhinoceros* has an area analysis function that can determine the area of the shipwreck that is exposed. This data can be used for each sampling season to calculate the area of the wreck that is exposed as the sediment cover changes.

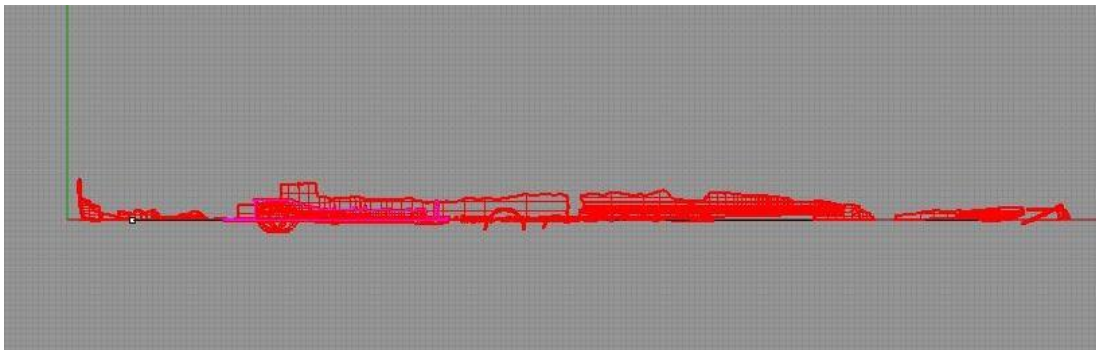


**Figure 25. Digitally traced port side profile view of the USS *Huron* wreck site with the planar curves extruded into solids. (Image by author, 2013.)**

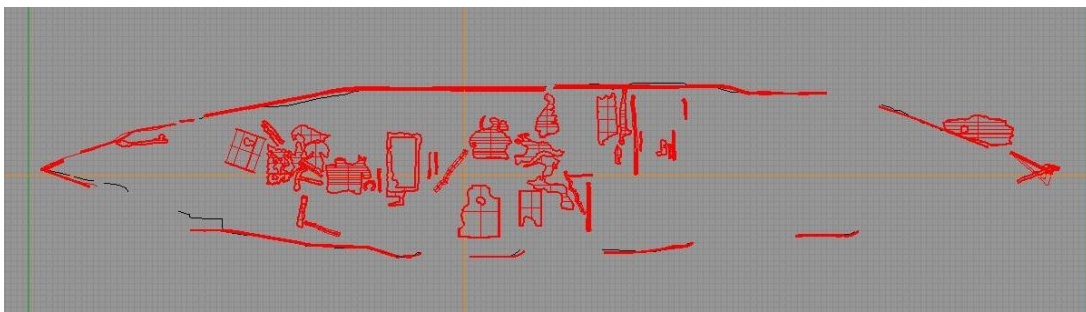


**Figure 26. Plan view of the USS *Huron* Site. The solids are then bent into shape using the bend function on *Rhinoceros*. (Image by author, 2013.)**



**Figure 27. Complete three-dimensional model of the wreck USS *Huron*. (Image courtesy of Nathan Richards and University of North Carolina Coastal Studies Institute, 2013.)**

#### *Side Scan Sonar Imaging of Huron*

22 July 2013, Dr. Nathan Richards in conjunction with CSI and ECU graduate students Danny Bera and Kara Fox, imaged the wreck site with a Klein 3000h dual frequency (445 and 900 kHz) digital side scan sonar. The crew made two passes on the wreck site, one with a stern deployment, and the second with a side-davit run. Both passes were successful and the sediment coverage of the wreck is readily visible.

These three-dimensional models and side scan image illustrate the wreck site formation and deterioration, and will aid in representing the relationship between corrosion rate and seasonal variables on the wreck site. Spatial control is further refined using the results of the side scan sonar and comparing the site plan from 2012 to the side scan sonar data taken in 2013. This shows, in part, the sedimentation behavior of the wreck site. This model also serves to expedite field mapping of USS *Huron* by acting as a base reference for the divers as they mapped the site and is crucial in locating the corrosion sampling sites.

## Corrosion Rate

A multimeter in a waterproof housing coupled with a silver/silver chloride reference electrode was used to determine the corrosion potential ( $E_{corr}$ ) of the sampling sites. These readings provide a snapshot of corrosion activity on the site during the different seasons. Eleven sampling sites were originally chosen, with four more sites added during the course of the study. The chosen sites represent the bow, amidships, and stern sections of the wreck including inboard and outboard sampling sites (Figure 28).

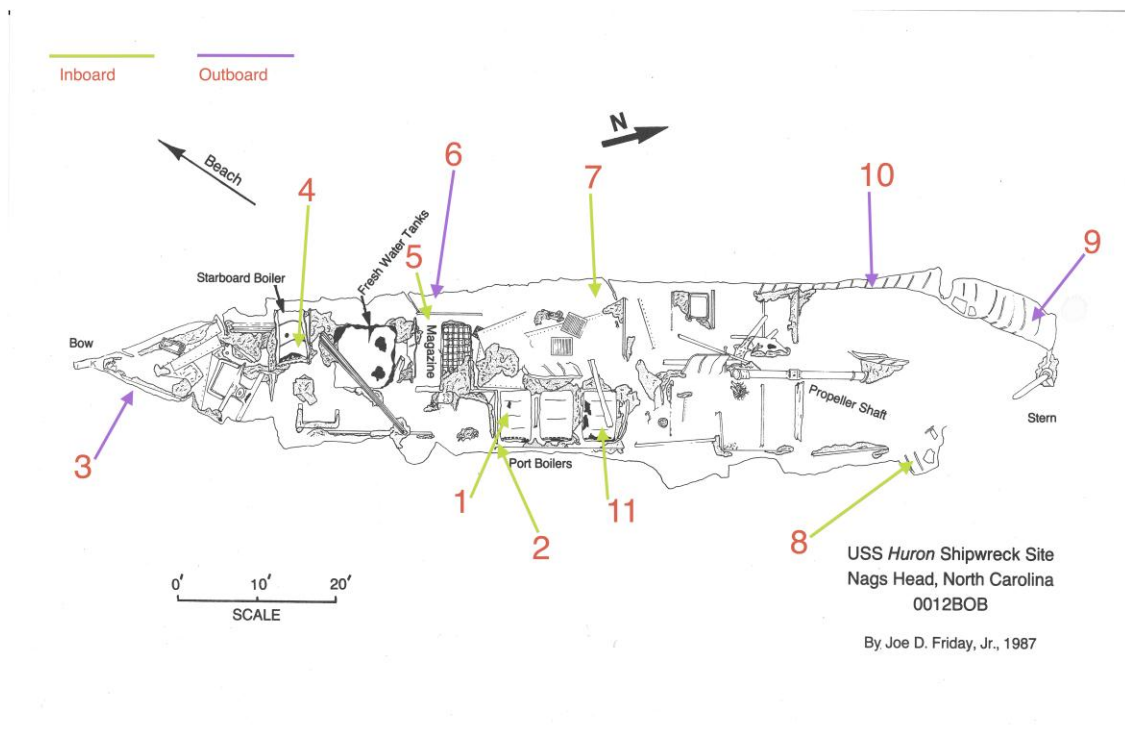


**Figure 28. Map of the original sampling sites on the USS *Huron* site (Friday 1988:114). (Amendments by author, 2013.)**

James Beringer-Pooley, in his 2005 thesis *Comparative Corrosion Analysis of J-Class Submarines*, outlines the materials and methods used to obtain corrosion potential measurements, which are similar to the methods MacLeod utilized in 1981. This method has been successful on multiple projects, including MacLeod's 1996 in-situ corrosion

study on the HMVS *Cerberus* (MacLeod 1996). This methodology is minimally invasive and efficient, making it a good fit for the USS *Huron* project.

The first step after determining an ideal testing location is to drill through the concretion into solid iron using a pneumatic drill with a low pressure quick disconnect fitting. The drill was tipped by a 15mm bit and powered by a SCUBA tank and first stage regulator with a submersible pressure gauge (Figure 29) (Beringer-Pooley 2005:76). A single 80 cubic foot SCUBA cylinder was adequate for obtaining eleven samples.



**Figure 29. The pneumatic drill powered by a SCUBA tank. (Photo by author, 2013.)**

The next step is to insert the platinum electrode from a multimeter (also housed in a waterproof housing) and record the E<sub>corr</sub> measurement (a measurement of corrosion potential). The housing is an Otterbox brand with aftermarket waterproof wire ports installed through the top (Figure 30). The wire ports are rated to a depth of 300 feet. The

multimeter probe was inserted until a stable negative millivolt (-mV) reading was obtained (about 2 minutes). One -mV is equivalent to -0.001 V. This process was then repeated for each sampling site.

For the 2012 summer data collection, concretion thickness was also measured using a millimeter ruler to measure how deep the drill bit had to go in order to reach sound iron. This was also useful for measuring the concretion thickness at the sampling site. Concretion thickness sampling was only done for summer 2012, as will be elaborated on in Chapter 5: Results of Data Collection.

It is important to note that all silver/silver chloride reference electrodes have an environmental baseline calibration of 25 °C and resulting values need to be temperature corrected (GMC Electrical 2014). All Ecorr results and analyses will use temperature-corrected values to ensure accuracy. The voltage was corrected by using the following equations (Equation 1 and Equation 2):

$$(t-25) \times 0.0006 = V_a \quad \text{Eq. 1}$$

To correct for the voltage, the temperature measured (t) was subtracted by 25, and then multiplied by 0.0006 V to obtain the voltage addition (Va). The voltage addition (Va) was then added to the actual voltage measured (V), which gives a temperature corrected Ecorr value.

$$V_a + V = \text{Temperature Corrected Ecorr Value} \quad \text{Eq. 2}$$



**Figure 30. Multimeter in waterproof housing with silver/silver chloride reference electrode (wrapped in plastic to protect it) and platinum tipped electrode. This instrument was replaced with a Polartrak CP bathyorrrometer. (Photo by author, 2013.)**

One critique of this method may be that the  $-mV$  reading is artificially inflated due to exposing the previously concreted metal to the direct effects of the seawater. In response to this critique, the area of the iron object relative to the drill hole needs to be considered. If the object is large, such as an iron hull plate or steam boiler, its surface area is immensely more than the diminutive drill hole, meaning that the subsequent exposure of the object to dissolved oxygen is insignificant (MacLeod 2013:467-468). As noted by MacLeod, “the minimal impact of such measurements on the integrity of an archaeological site is supported by the observation that repeated measurements on the boiler of the SS *Xantho* (1872) in coastal Western Australia have shown that there has not been any measurable impact on the overall corrosion process” (MacLeod 2006:206).

Further, if the drill hole is not plugged with epoxy, it will be rapidly filled with iron corrosion products (akaganeite and goethite) which seal the sampling site. Repeated measurements can be taken within a few centimeters of the original sampling site and accurate readings taken (Ian MacLeod 2011, pers. comm.). Additionally, experiments have shown that there is no difference between using a platinum tipped probe versus a stainless steel tipped probe (MacLeod 2013 467-468). It is important to note that Ecorr readings taken using a silver/silver chloride need to be adjusted by 0.250V if they are to be used on a traditional Pourbaix diagram or compared with a Standard Hydrogen reference electrode (Moore 2011:219).

There was a problem with the multimeter/reference electrode set-up when the system registered an Open Line warning during field use. Instead of risking another field day to unreliable equipment, the system was replaced by a Polatrak bathykorrometer style CP gun (CP gun). The Polatrak system is in wide use in the commercial dive industry, and similar systems have been used in a maritime archaeological setting (Moore 2011).

The CP gun is similar to the multimeter/reference electrode combination but in a more robust package that includes two separate voltmeters and silver/silver chloride reference electrode cells to ensure accurate results (Figure 31). The model has a 0.005 V accuracy that is easily checked with the two-element system (Deep Water Corrosion Services Inc. 2010:9). This model was rented from Ashtead Technology's Offshore Division for \$45 a day, and it comes with a spare element, batteries, contact tip, neutral buoyancy float, zinc coupon, and extra lens assembly screws. The CP gun was calibrated by an Ashtead Technology employee before shipment to ensure accuracy. This model can

also be calibrated in the field using the supplied zinc coupon, although this was not necessary on the “*Huron* project.”

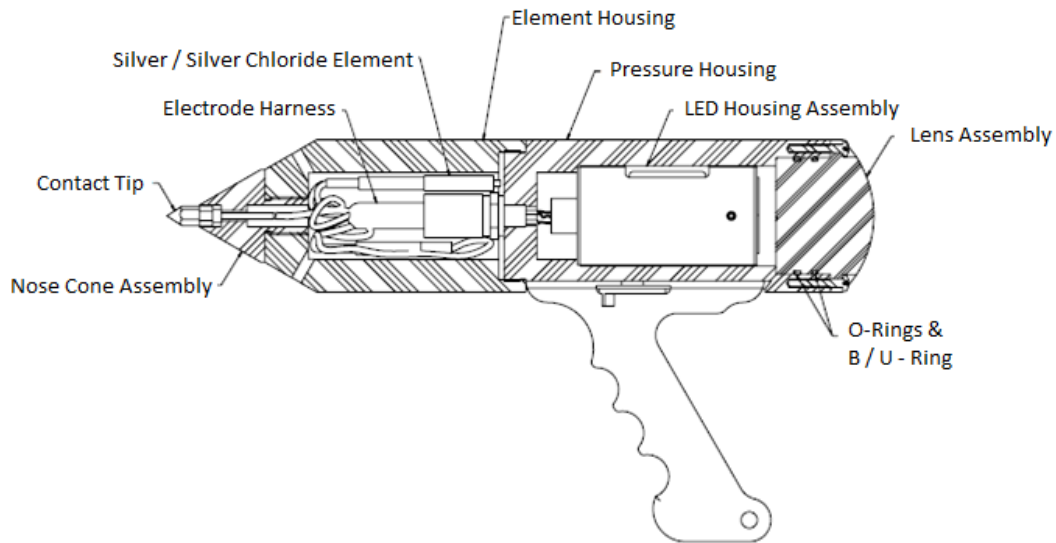


**Figure 31. Internals of the Polatrak CP Bathy Corrometer (Deep Water Corrosion Services, Inc 2010:6).**

The CP gun was used in two ways on the “*Huron* Project.” The first method required drilling through the concretion and sticking the CP gun tip into the drill hole, registering the results. The second method was to find portions of the wreck near the original drill sites where concretion had naturally been knocked off and using the sharp contact point of the CP gun to register the reading by stabbing the point into the metal. The CP gun was designed to be used in this manner; however, more reliable results can be obtained by using a drill in conjunction with the CP gun to ensure contact with the iron of the wreck (Deep Water Corrosion Services, Inc. 2010:9). This method was noninvasive and was used in a limited role on the summer 2013 sampling dive and used with imperfect results on the winter 2014 dive, where drill failure occurred. A simplified sampling regimen became a necessity and the methods evolved to maximize success in the harsh environment.

### *Water Parameters*

As discussed in the introduction, oxygen exposure and subsequent oxygen reduction is the primary driver of iron corrosion (microbes also contribute to iron corrosion). Variables like depth, concretion, water movement, and sediment cover influence exposure to oxygen and thus, corrosion rate (MacLeod 1981:292).

To obtain water parameter data for the 2012 summer sampling, a Conductivity, Temperature, and Depth device (CTD) was used and operated by Lauren Heesemann of NOAA. Dissolved oxygen content can be assumed to be 100% saturated owing to the wreck's shallow depth (MacLeod 1996:4). The CTD was tethered to a line and slowly lowered through the water column. The device recorded the water parameter data every ten seconds. This device was not left on the wreck site due to the risk of theft or equipment loss.

The CTD is a bulky, expensive device and to streamline shore-based dive operations for subsequent field sampling dives, temperature data was collected in real time by a Shearwater Petrel dive computer and salinity determined with water samples collected on site and then tested with an YSI meter. This put the risk of equipment loss to a minimum, as the site is prone to high levels of surge. Then, with temperature and salinity measured and 100% oxygen saturation assumed, the dissolved oxygen level was then calculated using online software, freely available from the United States Geologic Survey (U.S. Geologic Survey 2013).

### *Analysis*

The principal drivers of cathodic corrosion are dissolved oxygen and salinity; therefore, increased levels of exposure to dissolved oxygen and salinity will increase the rate of corrosion (Moore 2011:161-163). Temperature does have an effect on corrosion rate, but its influence on corrosion is difficult to isolate from its influence on the solubility of oxygen, which has a major effect on corrosion rate (Hackerman 1952:1752). Additionally, salinity variations should not be extreme in the temperate open ocean environment. Extreme variations in ocean salinity are observed both in Arctic waters, where freezing of the water causes salinity to increase, and near major sources of freshwater such as the Amazon delta (Talley 2002:631). Water temperature and salinity are, however, used to calculate dissolved oxygen content of the water. The water parameter and sedimentation data taken during the course of this study is compared to the corrosion potential data.

The primary unit of measurement for this study is  $E_{corr}$ , represented by Volts. As previously discussed in the Literature Review, the rate at which the cathodic reaction and the anodic reaction occur is the  $E_{corr}$  (Moore 2011:218). To interpret this data in a simplified manner is to view readings that have numerically higher negative values as being more cathodic, meaning less corrosion is taking place on the object (for example, a -0.612 V reading indicates less corrosion occurring relative to a reading of -0.532 V) (Beringer-Pooley 2005:95).

Since the “*Huron* project” does not have a graphitized iron component (this is only applicable to cast iron and not wrought, because wrought iron does not have enough carbon to graphitize), the actual site-specific Tafel Slope analysis and  $I_{corr}$  analysis can’t be done (converting  $E_{corr}$  to mm/year corrosion rate). Dr. Ian MacLeod’s study of

recurrent sampling of sites at the Isle of Mull (Scotland) indicates that a change in 3 mV (0.003 V) equaled a 2.5% change in corrosion rate. Similarly, his recurrent sampling of the shipwreck *Lively* (Western Australia) found that a change in 3 mV equaled a 1.6% change in corrosion rate (MacLeod 2002:701). If the percent change from Scotland and Western Australia are averaged, a theoretical 2.05% change in corrosion rate for every 3 mV is reasonable (i.e. a 1 mV difference = 0.683% in corrosion rate). This average is necessary because the *Huron* site is expected to have extremes in water temperature, and therefore, dissolved oxygen content across seasons. The U.S. Army Corp of Engineers Duck Research Pier, which is 13 miles north of the *Huron* wreck site, indicates a water temperature range of 3 °C to 28 °C (National Data Buoy Center 2014).

The average seasonal Ecorr for each successful sampling season is compared to the calculated dissolved oxygen content of the corresponding season. This analysis could show a relationship between the site's corrosion potential and a principal driver of corrosion dissolved oxygen. The average seasonal Ecorr is further compared to the sediment coverage of the site. As the sediment coverage changes, so does the wreck's exposure to dissolved oxygen, which could have an effect on corrosion potential. These two analyses are an attempt to represent the site's corrosion potential generally, to allow cross seasonal changes to be identified and perhaps identify the cause of these variations.

The next portion of analyses moves from the average seasonal Ecorr to site specific analyses. The site specific analysis begins with partitioning the wreck into different sections. The wreck is split into four areas of analysis: port versus starboard, bow versus midships versus stern, inboard versus outboard, and hull plates versus features. These analyses are then run for each successful corrosion sampling season. Site

specific analysis could potentially identify portions of the wreck that are electrically separate or are simply corroding at a higher rate.

It is hoped that through these analyses, both average seasonal Ecorr and site specific, differences in the wreck’s corrosion potential will become apparent and perhaps causative factors will be identified. These analyses are expressed numerically, as well as graphically, using the three-dimensional model of the wreck site.

*Sedimentation Survey From Yearly Site Reports*

The Town of Nags Head surveys the wreck of the *Huron* on a yearly basis. These reports are filed with the North Carolina Underwater Archaeology Branch (Zorc 2010). Sediment coverage can be estimated in two ways from these surveys. First is through a written checklist made by divers during the yearly survey (Figure 32).

<b>Artifact</b>	<b>Visible</b>	<b>Condition</b>
Bow Porthole Glass	No (covered by sand)	Unknown
Starboard Boiler	No (covered by sand)	Unknown
Anchor	No (covered by sand)	Unknown
Fresh Water Tanks	No (covered by sand)	Unknown
Magazine	No (covered by sand)	Unknown
Cannon Balls	No (covered by sand)	Unknown
Port Boiler #1	No (covered by sand)	Unknown
Port Boiler #2	No (covered by sand)	Unknown
Port Boiler #3	No (covered by sand)	Unknown
Propeller Shaft	No (covered by sand)	Unknown
Stuffing Box	No (covered by sand )	Unknown
Steering Post	No (covered by sand)	Unknown
Rudder	No (covered by sand)	Unknown
Propeller	No (covered by sand)	Unknown

**Figure 32. Town of Nags Head yearly *Huron* survey checklist showing sedimentation of specific features (Lawrence 2008:4).**

Second is through using Joe Friday’s 1988 site plan which represents, in two-dimensions, sedimentation of the wreck site. These site plan based surveys have only been made since

2004. Sediment coverage is represented by erasing portions of the wreck that are not visible (Figure 33). These surveys represent only a snap shot of the site as they are done on a single day during the year.

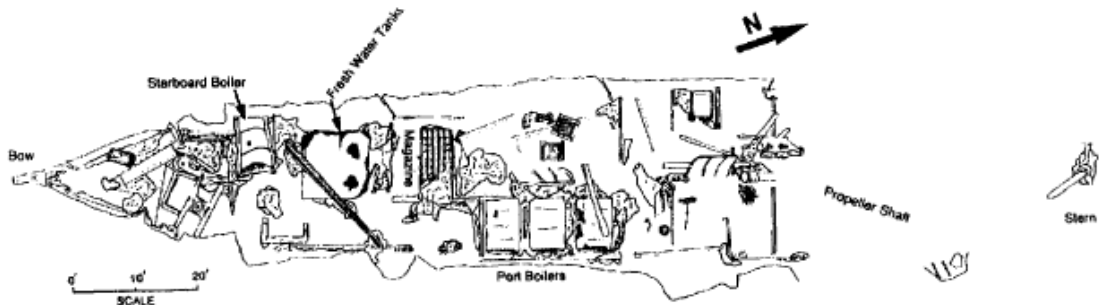


**Figure 33. Joe Friday's 1988 site plan used to aid the Town of Nags Head's yearly site surveys (Lawrence 2008:5). Note that the stern portion of the wreck has been erased.**

These reports, coupled with the three-dimensional model of the wreck, are used to create a time series of sedimentation of the highly dynamic site. They do not encompass the entirety of the wreck's sedimentation pattern, because as mentioned, surveys are limited to only being done once a year. Additionally, surface area of the wreck site exposed can be calculated using the three-dimensional wreck model and the *Rhinoceros* area analysis function.

### *Conclusion*

The digital model of *Huron* as built in 1875 represents the baseline input of the wreck site that is observed today. Surveying, mapping, and side scan survey of the USS *Huron* site allowed another digital model to be made, representing the site in 2012. This model represents the site formation output and allows percent sediment coverage to be calculated. Corrosion potential sampling evolved from a homemade sampling unit,

utilizing a commercially available silver/silver chloride reference electrode, to a completely commercial Polatrak CP gun equipped with two independent silver/silver chloride sampling units. Water sampling methodology evolved as well, going from a CTD sampling device that samples on site, to a method where temperature was recorded live on site, but samples were processed using an YSI meter in the lab to determine salinity. Dissolved oxygen was calculated from the temperature and salinity data. Sediment coverage data was further bolstered by using the Town of Nags Head yearly site surveys. The maps, models, corrosion potential, environmental sampling results, and sediment time series from the “*Huron* Project” are provided in the next chapter.

## CHAPTER 5: RESULTS OF DATA COLLECTION

### *Introduction*

This chapter is the culmination of the previously discussed methodology. The results of mapping the wreck site are displayed in several ways: a series of images highlight the evolution of the survey data into a digital reconstruction of the archaeological site. Next, field notes from data collection summarize successes and problems in obtaining the corrosion data; and the environmental parameters that were gathered are calculated. The cumulative results of both the corrosion potential sampling and environmental sampling are also displayed along with the sedimentation time series from the Town of Nags Head yearly site surveys.

### *Mapping*

The site plan from ECU's 2012 fall field school is the result of over 150 dives from the Maritime Studies graduate program and UNC- Coastal Studies Institute (East Carolina University Diving and Water Safety 2012) (Figure 34). This site plan is the basis of spatial control for the "*Huron* Project" and was essential in making the digital *Rhinoceros* three-dimensional model of the archaeological site (Figure 35). Additionally, the results of a side scan survey further tightened spatial control on the site and affirmed sediment coverage observed by divers (Figure 36).

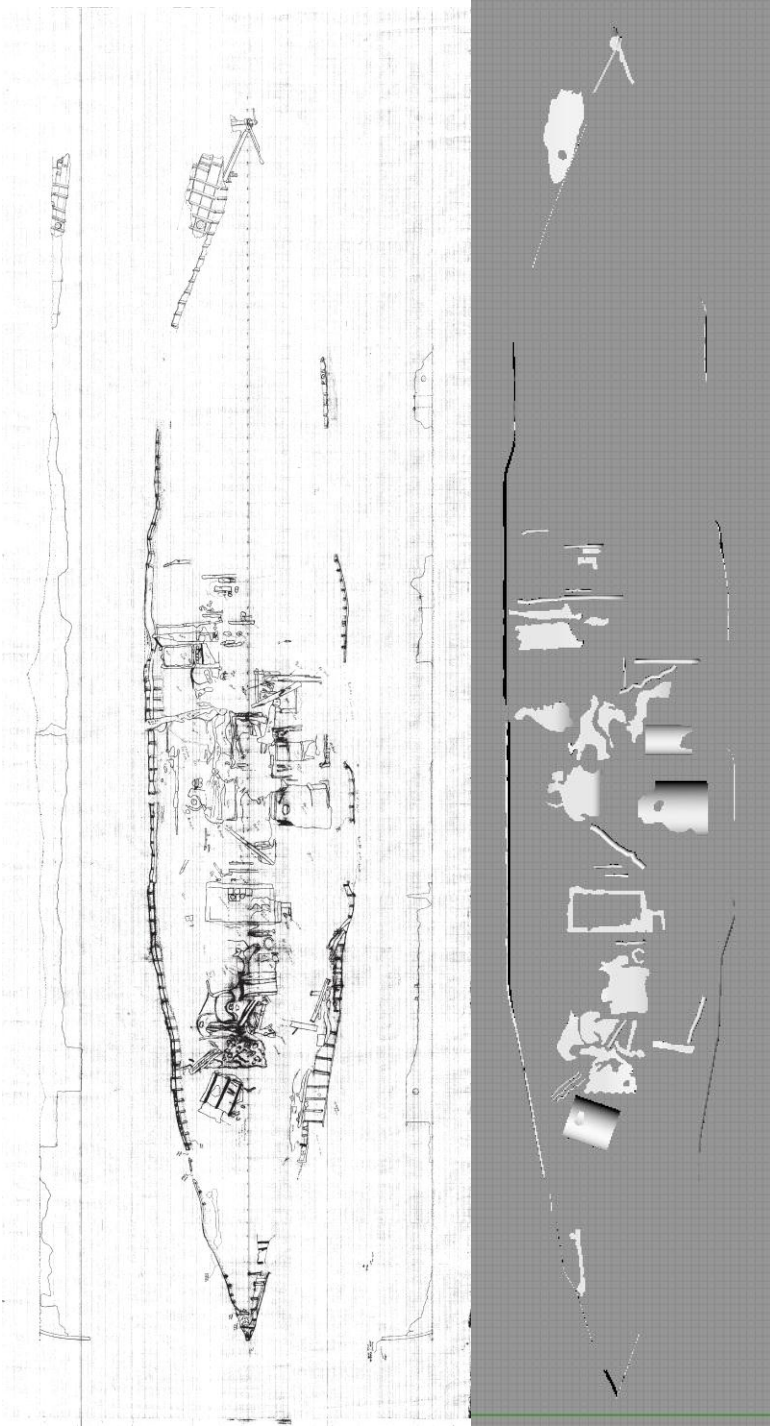


**Figure 34. *Huron* site plan (left) and three-dimensional rendering (right) from ECU's Program in Maritime Studies 2012 fall field school. (Right image by author, 2013.)**

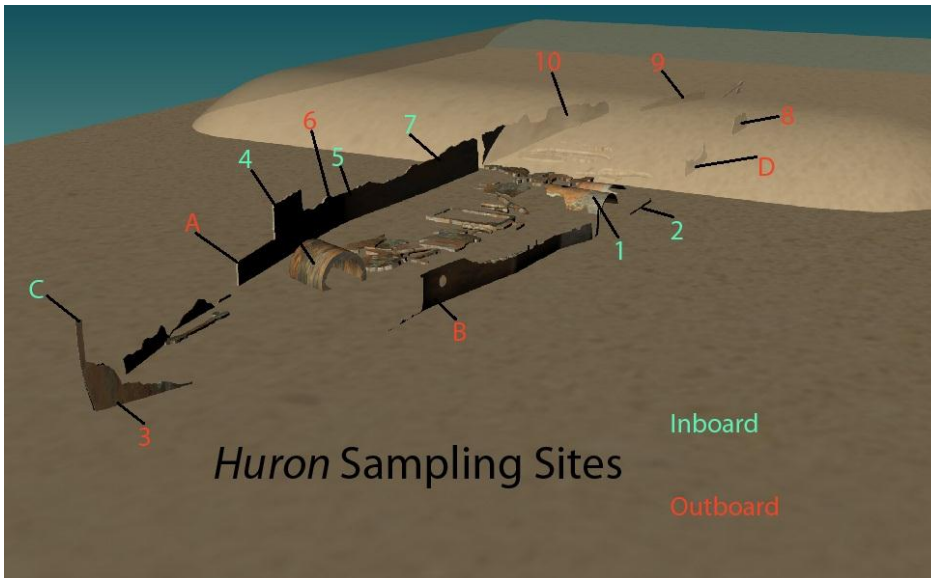


**Figure 35. Three-dimensional representation of the USS *Huron* showing the location of the study's sampling sites. (Image by author, 2014.)**

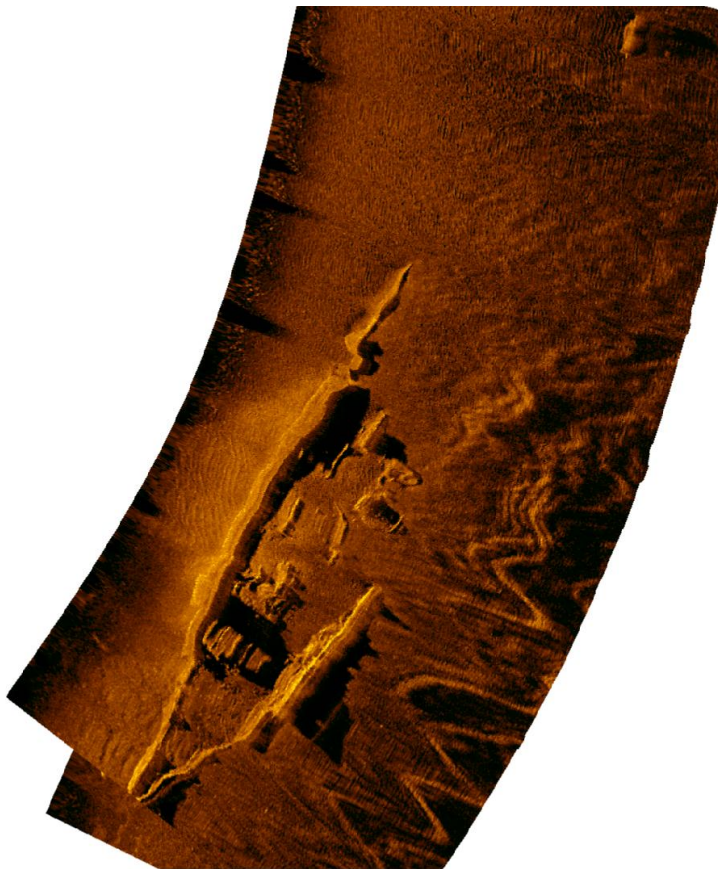


**Figure 36. Summer 2013 side scan sonar image of the *Huron* wreck site. (Image courtesy of Nathan Richards and University of North Carolina Coastal Studies Institute, 2013.)**

*Summer 2012*

After a series of setbacks, mainly concerning the wrong reference electrode model, data was collected 29 August 2012. The dive platform was a 25-foot Parker motorboat operated by Captain John McCord of UNC-Coastal Studies Institute. Underwater visibility went from approximately 3 meters over the course of the first dive, to nearly zero on the second data collection dive. Data collection was done using a multimeter and reference electrode attached to a computer that logged the readings in real time (Table 3 and Table 4). Concretion thickness sampling was only done during the summer 2012 season because further research indicated that total corrosion rate could not be identified with wrought iron from these measurements, unlike cast iron in which depth of graphitization is indicative of total corrosion rate of an object.

Depth (M)	Temperature (Celsius)	Salinity (parts per thousand)	Oxygen solubility (calculated)
4 M	25.79 °C	31.90 ppt	6.80 mg/L

**Table 3. Measurements of water parameters taken from the CTD sensor.**

Site Number	Ecorr(V) reading	Ecorr (V) corrected	Concretion Thickness (M)
1	-0.550	-0.5504	0.015
2	-0.550	-0.5504	0.021
3	-0.550	-0.5504	0.018
4	-0.550	-0.5504	0.023
5	-0.550	-0.5504	0.006
6	-0.550	-0.5504	0.021
7	-0.550	-0.5504	0.015
8	-0.550	-0.5504	0.011
9	-0.550	-0.5504	0.030
10	-0.550	-0.5504	0.017
11	-0.550	-0.5504	0.018

**Table 4. Measurements from the multimeter and concretion thickness. The Ecorr has been temperature corrected.**

The uniformity of Ecorr readings suggests a problem in data collection. This issue is possibly a result of the spacing of the silver/silver chloride reference electrode to the sampling site. The position of the reference electrode past a certain distance is remote earth placement (Ahmed 2012:312). When there is too much space between the two probes the Ecorr readings are representative of the feature as a whole and not the specific sampling site. It is not known if these corrosion potential readings indicate an electrically connected site or separate cathodic units with the same corrosion potential. This makes site specific analysis difficult. Further it is not conclusively proven that this is in fact a remote earth reading and as such, this data will not be used in the interest of scientific integrity.

*Winter 2012-2013*

On 1 April 2013, after weeks of foul weather, the sea state finally allowed a shore based dive operation. Two divers swam to the known shore transits, but they were unable to locate the wreck despite a series of circle searches with moderate visibility. Other divers reported that during the late winter and early spring, the USS *Huron* was covered with sediment and could not be located. No corrosion data could be collected, but environmental data collection was successful (Table 5).

Depth (Meters)	Temperature (Celsius)	Salinity (parts per thousand)	Dissolved Oxygen (calculated)
4 M	8.88 °C	29.56 ppt	9.58 mg/L

**Table 5. Winter 2012-2013 environmental data.**

*Spring 2013*

Conditions were conducive to a dive operation on 21 June 2013. The forward section of the USS *Huron* was uncovered, while the aft section was completely buried. The port side boilers were barely visible above the sediment, while the disarticulated

starboard boiler was exposed. Biofouling was minimal on the wreck site, and a complete absence of sea urchins was observed, indicative of the wreck being only recently uncovered.

Drill site 5 was located and the platinum probe inserted to the depth of sound iron. The multimeter, newly housed in its waterproof case, gave the Open Line warning indicating an equipment failure. Spring corrosion data collection could not be completed, although a site survey and environmental data collection was completed (Table 6).

Depth (Meters)	Temperature (Celsius)	Salinity (parts per thousand)	Dissolved Oxygen (calculated)
4 M	22.77 °C	30.99 ppt	7.20 mg/L

**Table 6. Spring 2013 environmental data**

*Summer 2013*

On 28 August 2013, a new instrument was introduced to gather the Ecorr data. The Polartrak CP gun bathycorrometer is fundamentally the same product as the previously used multimeter/reference electrode combination, with both using a silver/silver chloride reference electrode. The dive platform was East Carolina University’s R/V *Tom Cat* with support from the Coastal Studies Institute. A southwest wind had been blowing and created an upwelling with cold and murky water. A two-person dive team found poor visibility on the wreck site; however, familiarity with the wreck allowed the divers to locate the drill sites. Familiarity with the wreck allowed the divers to locate the drill sites using touch contact alone. With the aft section of the wreck buried in the sediment, four new test sites were sampled (labeled sites A-D).

The water parameters were successfully collected (Table 7). Two of the new test sites (the stem post and port midships) required no drilling, as damage to the wreck had exposed enough iron for the bathycorrometer to register a reading. The hull plate next to

the starboard boiler was purely concretion in the sampling zone near the break in the plate, and no reading was taken. Five of the original drill sites were located and the Ecorr recorded (Table 8 and Table 9). With the aft section of the wreck buried in sediment, four new test sites were sampled (Table 9). Summer 2013 Ecorr readings did not need to be temperature corrected because the water temperature was 25°C and this is the baseline temperature for silver/silver chloride reference electrodes.

Depth (Meters)	Temperature (Celsius)	Salinity (parts per thousand)	Dissolved Oxygen (calculated mg/L)
4 M	25 °C	30.5 ppt	6.95 mg/L

**Table 7. Summer 2013 water parameters.**

Site designation	Ecorr (V) reading	Ecorr (V) corrected
1	-0.601	-0.601
2	-0.612	-0.612
3	-0.603	-0.603
4	-0.610	-0.610
6	-0.603	-0.603

**Table 8. Repeat sampling sites (did not need to be temperature corrected).**

Site designation	Ecorr (V) reading	Ecorr (V) corrected
A (plate next to starboard boiler)	N/A No sound iron found on the drill site	N/A
B (portside porthole)	-0.604	-0.604
C (stem post, no drilling needed)	-0.610	-0.610
D (port side midships, no drilling needed)	-0.612	-0.612

**Table 9. New sampling sites (did not need to be temperature corrected).**

*Winter 2013-2014*

On 13 December 2013, calm seas allowed a two-person dive team to complete a shore dive on *Huron*. The wreck was located using a waterproof GPS unit mounted on a dive float with a tag line. A quick, line reel-based circle search located the wreck on the bottom. A strong offshore wind resulted in an ocean upwelling, resulting in cold and

murky conditions on the wreck site. Luckily, current was minimal, but dive safety concerns limited the team's bottom time (as requested by the Diving Safety Officer on site due to the cold water).

Locating the sampling sites was difficult in the low visibility conditions, but familiarity with the wreck site and locating the disarticulated starboard boiler aided navigation. To further complicate data collection, the pneumatic drill was lost in the murky conditions as the divers descended onto the wreck site. As a contingency, the stab method was utilized as per the manufacturer's directions, and samples were taken within feet of the drill sites on areas where the calcium carbonate concretion had naturally been removed and the hull plate exposed. The CP gun's extremely sharp tip was adequate to create an electrical connection through the corrosion products, allowing retrieval of two samples, one each from starboard and portside of the wreck (Table 10).

Although the samples taken were not taken precisely on the original drill holes, the Ecorr value is still representative of the feature as a whole. (Ian MacLeod. elec. comm. 2011). It needs to be emphasized that two other samples were in error as evidenced by extremely low readings in the  $-0.200$  V range evidence of incomplete connection between the sampling probe and sound iron. These erroneous readings were discovered only upon data analysis topside, as the task-loaded divers worked to orient themselves on the wreck (Deepwater Corrosion Services 2010:10-11). For winter 2013-14, only two sites (B and 5) will be used for analysis because of the poor readings from sites 4 and 6.

As discussed, this method was also used successfully to collect two extra samples for summer 2013 (Table 9). The water parameter samples were successfully taken (Table

10). These Ecorr readings have been temperature corrected 0.008 V, to account for the 13.9 °C difference from the reference electrode’s 25 °C baseline (Table 11). These samples required the highest temperature correction in the study due to the low water temperature.

Site designation	Ecorr (V) reading	Ecorr (V) corrected
B	-0.539	-0.531
5	-0.532	-0.524
4	-0.273	-0.265
6	-0.295	-0.287

**Table 10. Winter 2013-2014 temperature corrected Ecorr readings (0.008 V).**

Depth (Meters)	Temperature (Celsius)	Salinity (parts per thousand)	Dissolved Oxygen (calculated in mg/L)
4M	11.1°C	30.9 ppt	9.05 mg/L

**Table 11. Winter 2013-2014 water parameters.**

*Cumulative Water Parameter Data and Corrosion Potential Data*

The following are the cumulative results from the “*Huron Project*.” Listed are the results from each season’s water parameter collection (Table 12). The cumulative corrosion potential from each season is listed, with temperature corrected readings (Table 13). Site number with a site description is also included (Table 14). These results will be analyzed and discussed in Chapter 6: Analysis and Discussion of Seasonal Water Parameters and Corrosion Variables at the USS *Huron*. All listed Ecorr values have been temperature corrected, with the exception of summer 2013, which did not need to be corrected due to the 25°C water temperature.

Year	Season	Depth (m)	Temp (Celsius)	Salinity (ppt)	DO (mg/L)
2012	Summer	4	25.79	31.9	6.8
2013	Winter	4	8.88	29.56	9.58
2013	Spring	4	22.77	30.99	7.2
2013	Summer	4	25	30.5	6.95
2013	Winter	4	11.1	30.9	9.05

**Table 12. Cumulative water parameter data from all the seasons.**

Site Number	Summer 2012 (V)	Spring 2013	Summer 2013 (V)	Winter 2013-2014 (V)
1	-0.550	No data	-.601	No data
2	-0.550	No data	-0.612	No data
3	-0.550	No data	-0.603	No data
4	-0.550	No data	-0.61	-0.273
5	-0.550	No data	No data	-0.524
6	-0.550	No data	-0.603	-0.295
7	-0.550	No data	No data	No data
8	-0.550	No data	No data	No data
9	-0.550	No data	No data	No data
10	-0.550	No data	No data	No data
11	-0.550	No data	No data	No data
A	No data	No data	No data	No data
B	No data	No data	-0.604	-0.531
C	No data	No data	-0.61	No data
D	No data	No data	-0.612	No data

**Table 13. Cumulative seasonal temperature corrected Ecorr readings from the “Huron Project.”**

Site Number	Side	Location	Inboard (I) or Outboard (O)
1	Port	Midships	I
2	Port	Midships	I
3	Port	Bow	O
4	Starboard	Bow	I
5	Starboard	Midships	I
6	Starboard	Midships	O
7	Starboard	Midships	I
8	Port	Stern	I
9	Starboard	Stern	O
10	Starboard	Stern	O
11	Port	Midships	I
A	Starboard	Midships	O
B	Port	Midships	O
C		Bow	N/A
D	Port	Midships	O

**Table 14. Ecorr sampling sites with location descriptions.**

### *Collection of Sediment Data*

The sand lens atop the medium gravel substrate, typical of the Outer Banks, is in a semi-suspended state, and heavy objects will gradually settle through this top layer (Dolan 1966; Muckelroy 1978:284). The ship settled into the sediment just below its waterline. Sedimentation of the site is a dominant seasonal transform. On the Outer Banks, northeast swells power a north to south long shore current (Mallinson 2008:2). This long shore current is the primary mover of sediment, and increased northerly swell activity during the winter results in increased sedimentation of the site, as *Huron* acts as a sediment trap creating a sandbar. This is a reasonable explanation as to why the wreck could not be located during the winter 2012 sampling attempt. Several months later in mid-spring, divers reported that the wreck's bow was barely exposed and the aft end of the wreck site was still buried. The wreck was further uncovered during the 2013 summer field work, with the port boilers and the hull plate fore of these boilers exposed.

The North Carolina Outer Banks, and the Carolina Coastal system as a whole, are a highly dynamic environment, with subtle changes due to sea level rise and riverine influences. The shoreline's steady evolution is punctuated with changes from nor'easters and hurricanes that dramatically shape the coastline. However, shoreline migration on the *Huron* site in North Nags Head was found to be minimal in 58 years (Figure 37) compared to South Nags Head where the shoreline has receded 1,000 feet in the last 149 years (Riggs 2008:11).

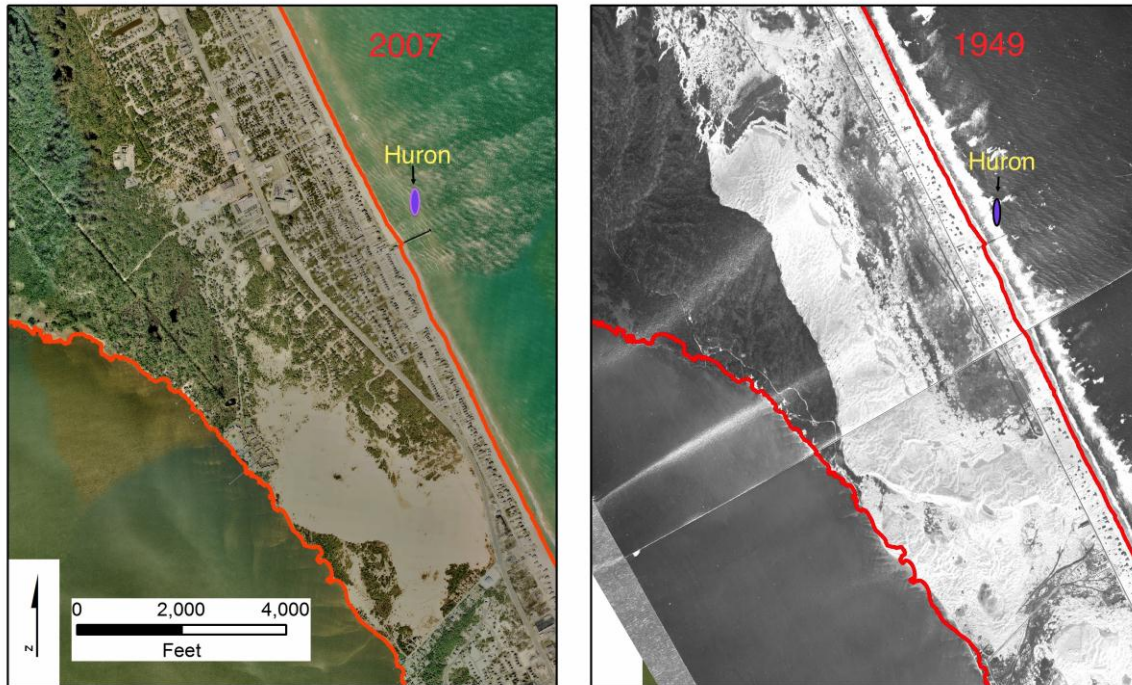
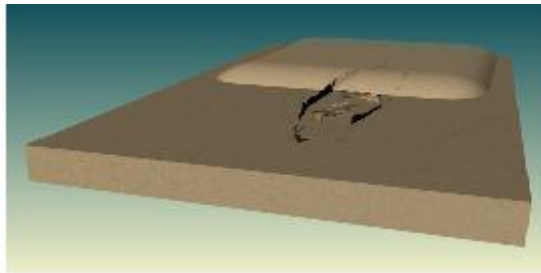
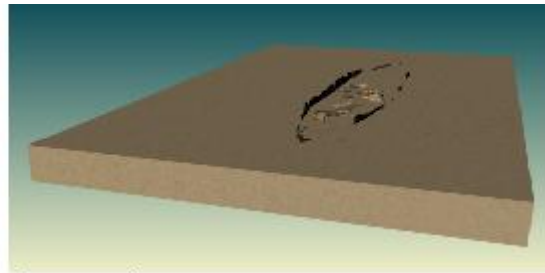


**Figure 37. An aerial photo from 2007 and 1949 of Nags Head, NC. The *Huron* site is represented and the two shorelines are transposed atop each other showing a stable shoreline (red border). (Time series by Ian Conery of East Carolina University Department of Geological Sciences, 2013.)**

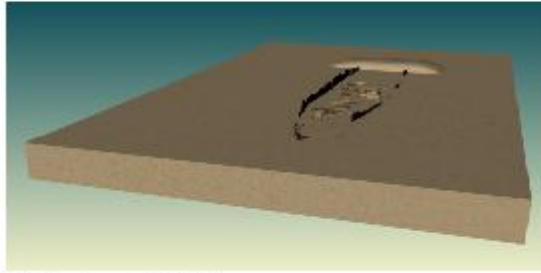
The Town of Nags Head and Nags Head Fire and Rescue oversee the site and also do yearly surveys. The results of these surveys are filed with the North Carolina Underwater Archaeology Branch. As mentioned in Chapter 5, these yearly site surveys were used to create a three-dimensional time series of the *Huron* site that shows the dynamic sedimentation of this site since 2003 (Figure 38), with the exception of 2006 and 2007 for which no sedimentation data was found. This data is limited in that the time series only represents a snap shot of the sedimentation of the site because the surveys were done only once a year. This data will be analyzed in Chapter 6: Analysis and Discussion of Seasonal Water Parameters and Corrosion Variables at the USS *Huron*.



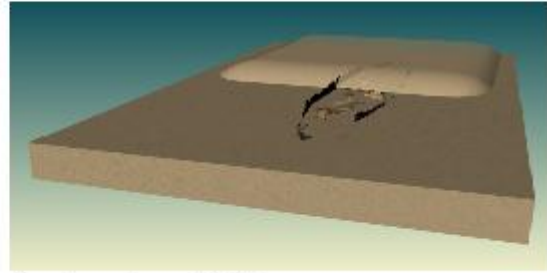
August 2013



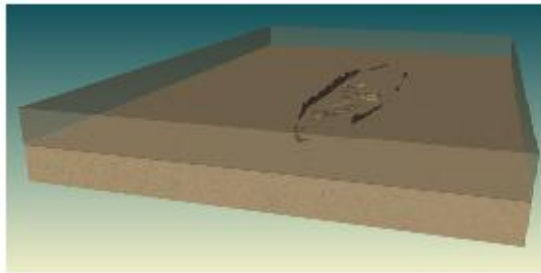
September 2012



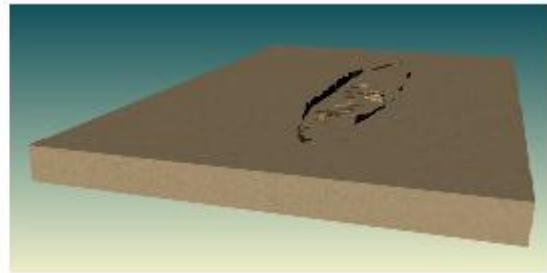
October 2010



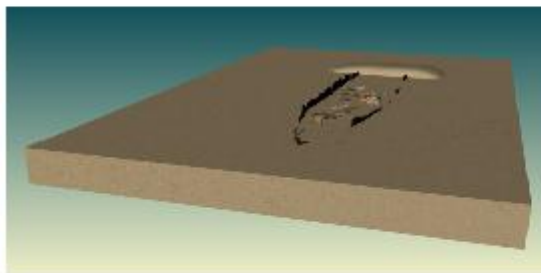
September 2009



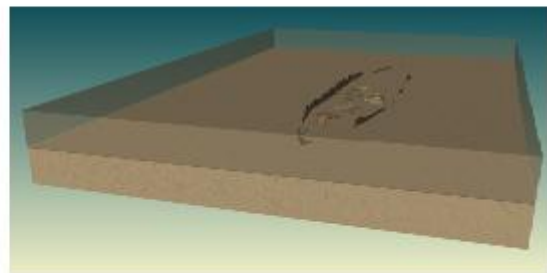
September 2008



September 2005



September 2004



October 2003

**Figure 38. Sedimentation time series taken from the *Huron* wreck preserve yearly reports (Lawrence 2004, 2005, 2006, 2007, 2008, 2009; Zorc 2010). (Image by author, 2013.)**

## *Conclusion*

Mapping the wreck in 2012, in both plan and profile view, is the basis of the creation of a *Rhinoceros* three-dimensional digital model of the wreck site. This digital model coupled with the results from the side scan survey further tightened spatial control on the site. Field sampling was difficult owing to the harsh conditions of the *Huron* wreck site, with failures to collect corrosion potential data for multiple seasons. Equipment issues plagued the study with problems such as spacing with the reference electrode for summer 2012, open line warnings for spring 2013, and a drill failure that meant only two samples could be taken for winter 2013-2014. Summer 2013 provides the best data set collection with a total of 8 successful corrosion potential readings. The sedimentation surveys from the Town of Nags Head were used to create a three-dimensional time series. The “*Huron* Project’s” data set including corrosion potential, seasonal water parameters, and sedimentation of the site will be analyzed in the following chapter.

## **CHAPTER 6: ANALYSIS AND DISCUSSION OF SEASONAL WATER PARAMETERS AND CORROSION RATES AT THE USS *HURON***

### *Introduction*

The primary goal of the “*Huron Project*” was to investigate whether seasonal environmental parameters affect corrosion on the USS *Huron* archaeological site. As mentioned in Chapter 2, iron in an underwater archaeological setting is usually actively corroding (in a strongly reducing state) with the microenvironment having a pH of 4.8 on average. Hence, the wreck of the USS *Huron* is assumed to be in a state of active corrosion (MacLeod 2002:700). This assumption is further supported by the range of corrosion potentials sampled on the site (-0.524 to -0.612 V) (Deep Water Corrosion Services, Inc. 2010:7).

The role of this chapter is to analyze the results outlined in Chapter 5 with the goal of identifying seasonal variables affecting the corrosion rate of USS *Huron*. The first set of analyses focuses on the examination of average  $E_{corr}$  readings across seasons. Concluding this section, a discussion explores the relationship of dissolved oxygen and sediment coverage to average seasonal  $E_{corr}$  at USS *Huron*. However, because these analyses treat the shipwreck as a contiguous cathodic unit, more specific analyses are attempted.

From this foundation, analysis of the data goes further with site element-specific analyses that attempt to identify areas of the wreck that are either subject to differing environmental variables such as exposure to ocean currents, or that may be separate cathodic units (i.e. undergoing their own corrosion process). For the site element-specific analyses, USS *Huron* is split into four separate areas for study that consist of port versus

starboard; bow versus midships versus stern; inboard versus outboard; and hull plates versus features. These specific analyses are explored by each season, before each season is compared. All Ecorr values have been temperature corrected.

#### *Analysis of Average Ecorr Across Seasons*

Two analyses compare the average Ecorr from each successful sampling season to two different seasonal variables. The first analysis compares dissolved oxygen readings in the water to the average Ecorr of each season. This variable was chosen because a metal's exposure to dissolved oxygen is the principal cause of cathodic corrosion. Any change in corrosion potential could be linked to changes in the dissolved oxygen content of the water column.

#### Average Seasonal Ecorr Compared to Dissolved Oxygen

This analysis compares the average Ecorr from each successful sampling season and compares this data to the dissolved oxygen present in the water during that specific season (Figure 39). The water parameter variables measured were temperature and salinity and from these, dissolved oxygen was calculated (Table 15). Exposure to dissolved oxygen will be the principal driver of corrosion, in which an increased corrosion rate occurs when a metal is subjected to increased ambient dissolved oxygen in the water column. The percentage change in corrosion potential can be calculated as

0.003 V equals a 2.05% change in corrosion rate as discussed in Chapter 4 (Table 15).

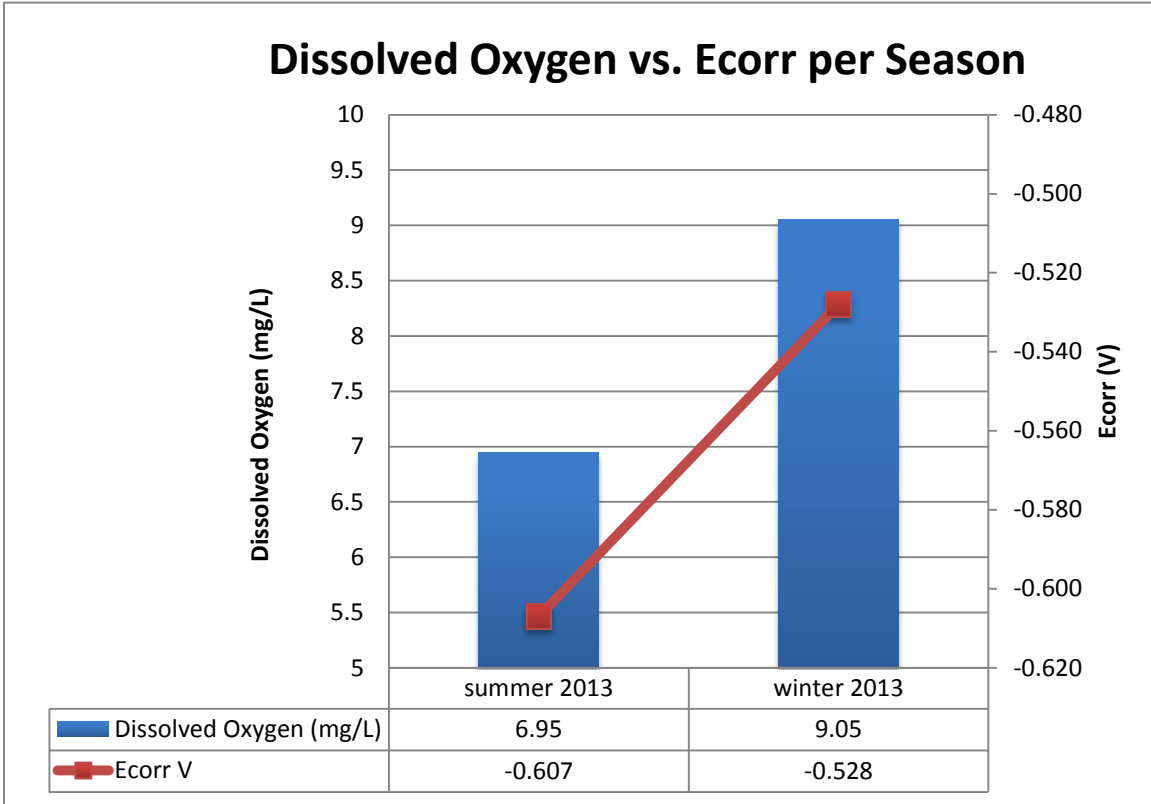


**Figure 39. Relative amounts of dissolved oxygen to average corrosion potential. Lower Ecorr readings (red) indicate higher corrosion environments. (Image by author, 2014).**

Season	Dissolved Oxygen (mg/L)	Ecorr (V)	% change in corrosion rate
Summer 2013	6.95	-0.607	Baseline
Winter 2013-2014	9.05	-0.528	+54.0%

**Table 15. Average seasonal Ecorr and dissolved oxygen (mg/L) for each season.**

The result of this analysis shows that winter 2013-2014 had the highest average corrosion potential (-0.528 V) and the highest dissolved oxygen content (9.05 mg/L). Summer 2013 had the lowest corrosion potential (-0.607 V) and the lowest dissolved

oxygen content (6.95 mg/L). Corrosion rate increased 54% from summer 2013 to winter 2013-2014 (Table 15).

#### Average Ecorr in Relation to Sedimentation of the Wreck Site

This analysis tests the relationship of the average seasonal Ecorr to the degree that sediments covered the USS *Huron*. Sedimentation of the wreck site was significantly different between the 2012 and 2013 summer seasons. No change in sedimentation of the site was observed between summer 2013 and winter 2013-2014. In 2012, the wreck was mapped in plan and profile view, forming the basis of the three-dimensional model. The major features exposed in 2012, such as the stem post, hull plates, boilers, and steering quadrant were subjected to a surface area analysis in *Rhinoceros* (Figure 40). The resulting area of these features is 1,372.7 square feet. Running this analysis on the wreck as observed in the 2013 summer season with the main features being the stem post, hull plates, and the boilers, gives a resulting area of 933.3 square feet.

The result of this analysis shows a 32.1% change in exposed surface area lying proud of the seabed and increased exposure to the dissolved oxygen which drives cathodic corrosion on the site. The surface area analysis was not run on the winter 2013-2014 data, as diving conditions were not conducive to a visual survey of the wreck site. A 17-foot max depth from the winter 2013-2014 dive was recorded versus a 22-foot max depth reading from the summer 2012 fieldwork.

The sediment time series shown in Chapter 5 (Figure 38) clearly shows an irregular pattern of reoccurring burial of the site from stern to stem, often leaving the bow exposed. This time series illustrates the highly dynamic state of sedimentation of the wreck site that also potentially has a major effect on the corrosion rate of the site.

Additionally, the sediment time series shows that there is no clear seasonal pattern to sediment coverage of the site.

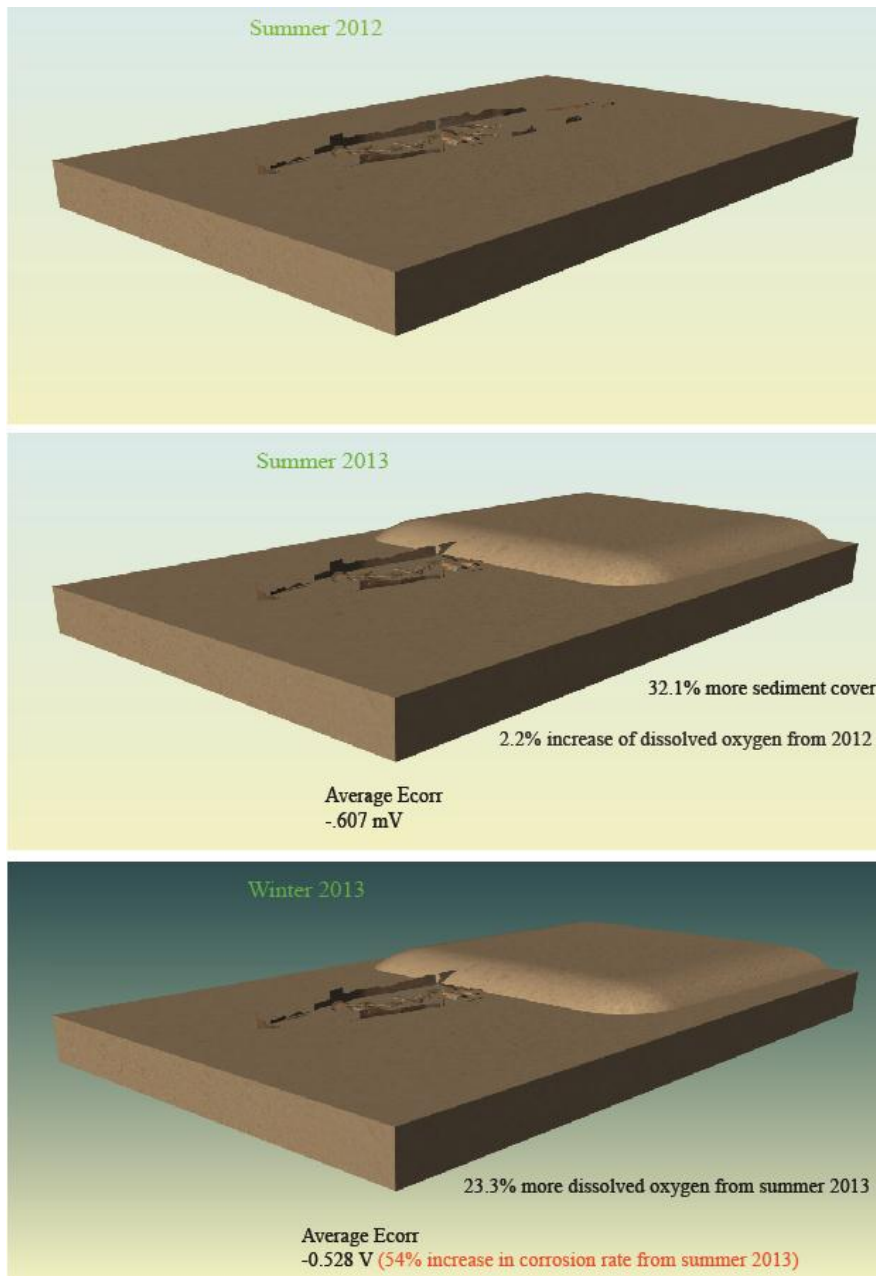


**Figure 40. Seasonal sediment model of the wreck site and resulting *Rhinoceros* area analysis. (Image by author, 2014.)**

#### Discussion

The result of the dissolved oxygen and corrosion potential analysis of the wreck site suggests that the site is highly susceptible to changes in dissolved oxygen content of

the water column. Increases in dissolved oxygen appears to increase the wreck's corrosion rate, as changes in dissolved oxygen control the overall cathodic corrosion of an object (Moore 2011:165). This is shown by the 54% increase in corrosion rate from summer 2013 to winter 2013. One problem resides in our assumption that the average  $E_{corr}$  in each season is a reflection of the overall corrosion rate of a single cathodic unit, when in fact USS *Huron* may actually be a series of distinct cathodic units. Additionally, because the pattern of covering and uncovering seen at the USS *Huron* site is irregular, but cannot currently be proved to be *seasonal* (i.e. *Huron* is not covered to the same extent during summers and winters), any further examination of the comparison of the relationship between sediment coverage and  $E_{corr}$  would have to include detailed periodic bathymetric recording coupled with extensive recording of corrosion data. These problems are explored further in the following section by comparing  $E_{corr}$  readings of the elements of the *Huron* wreck, to see if distinct cathodic units exist, and if they are differentially affected by dissolved oxygen and sediment coverage.

#### *Site Specific Analyses of the Wreck*

These analyses require that the wreck of the USS *Huron* be split into different element-specific areas for comparison (Figure 41). Each of these areas have within them sample locations which can be categorized by their starboard or port, bow, midships or stern, and inboard (inside) or outboard (outside) location on the wreck. They can also be categorized as a piece of structure (e.g. frame or plate) or a feature (e.g. boiler) of USS *Huron*. What follows is a comparison of temperature-corrected  $E_{corr}$  readings according to these differentiations. Due to a problem with the  $E_{corr}$  readings from summer 2012, it has been excluded from each analyses, leaving for comparison readings from summer

2013 and winter 2013-2014. These analyses could show areas of the wreck subject to increased corrosion rates due to their proximity to other environmental variables (such as currents) and potentially identify areas of the wreck that are electrically separate cathodic units.

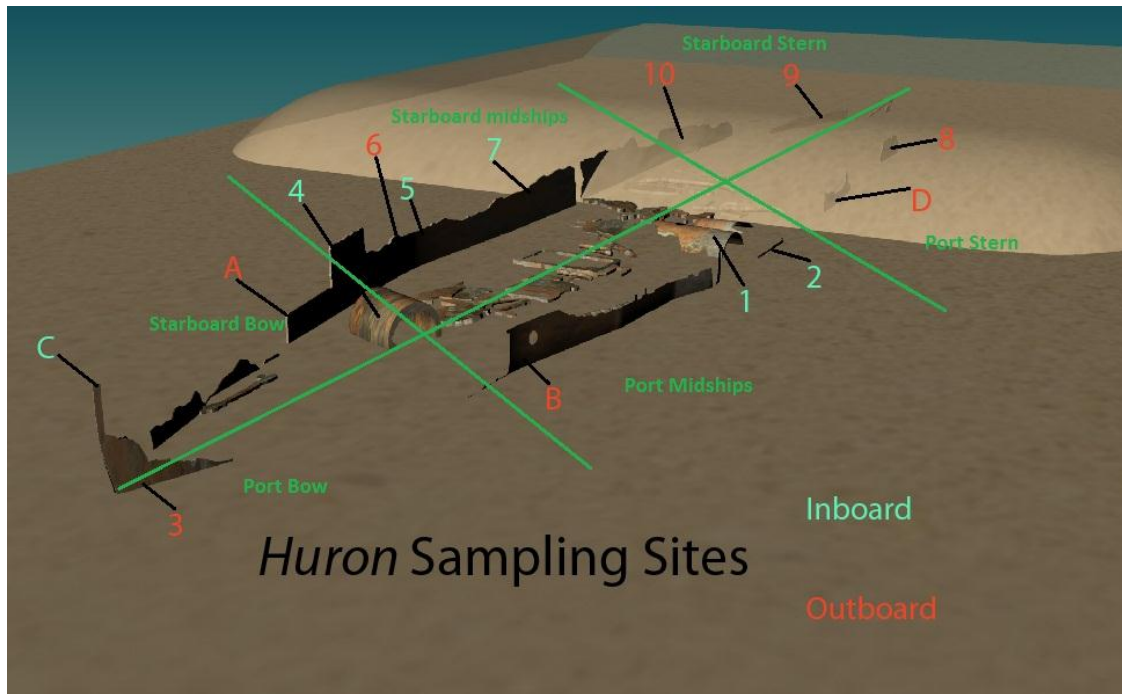


**Figure 41. *Huron* sampling sites with areas of site specific analysis indicated. (Image by author, 2014.)**

#### Port versus Starboard Corrosion Potential Comparison

This analysis compares the corrosion potential between the port and starboard sides of the wreck during the summer 2013 season followed by the winter 2013-2014 season, and finally a comparison of sites across these seasons. The port versus starboard comparisons are inclusive of both features and hull plates.

The purpose of the analysis is to explore the potential for statistically significant differences between the corrosion potential on the opposite sides of the wreck site. This difference could be suggestive of changes in the corrosion environment. For example, on the *Xantho* Project, objects in the lee of the prevailing current experienced a lower rate of

corrosion to those that were not, as they are exposed to less damaging currents and dissolved oxygen (McCarthy 2000:77).

All data is displayed in graphical form to better show the corrosion potential variations between locations, and to depict the 0.005 V tolerance of the sampling equipment. A comparison of Ecorr data from summer 2013 is displayed in Figures 42 and 43.

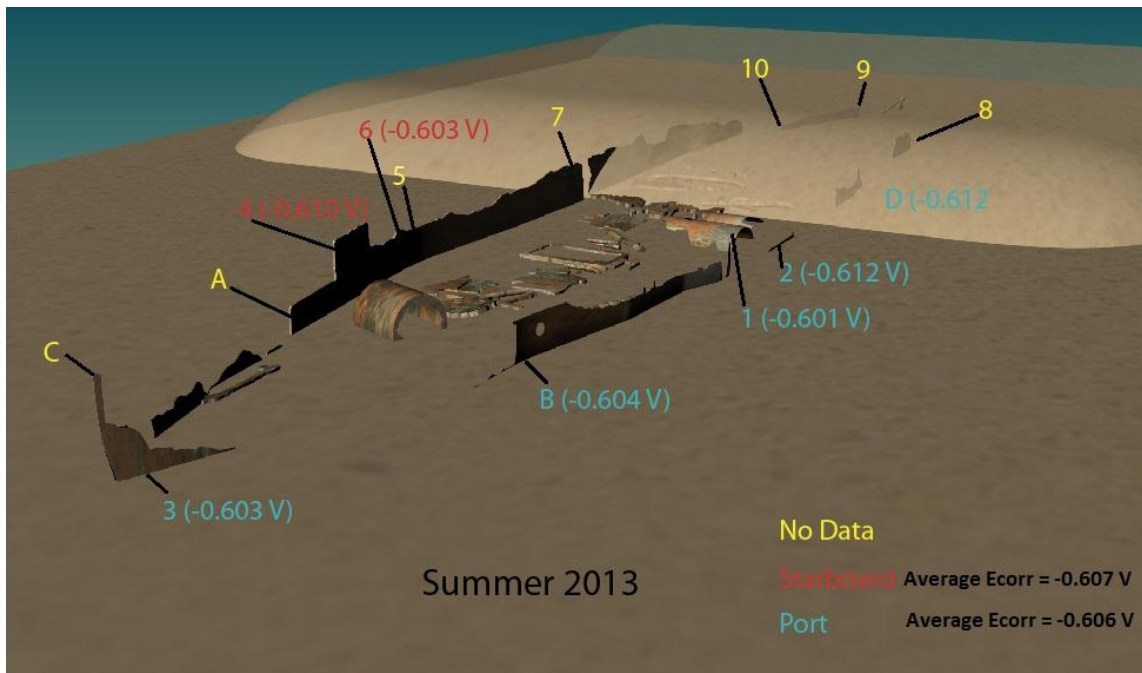


**Figure 42. Corrosion potential readings partitioned into port and starboard sides of the wreck. (Image by author, 2014.)**

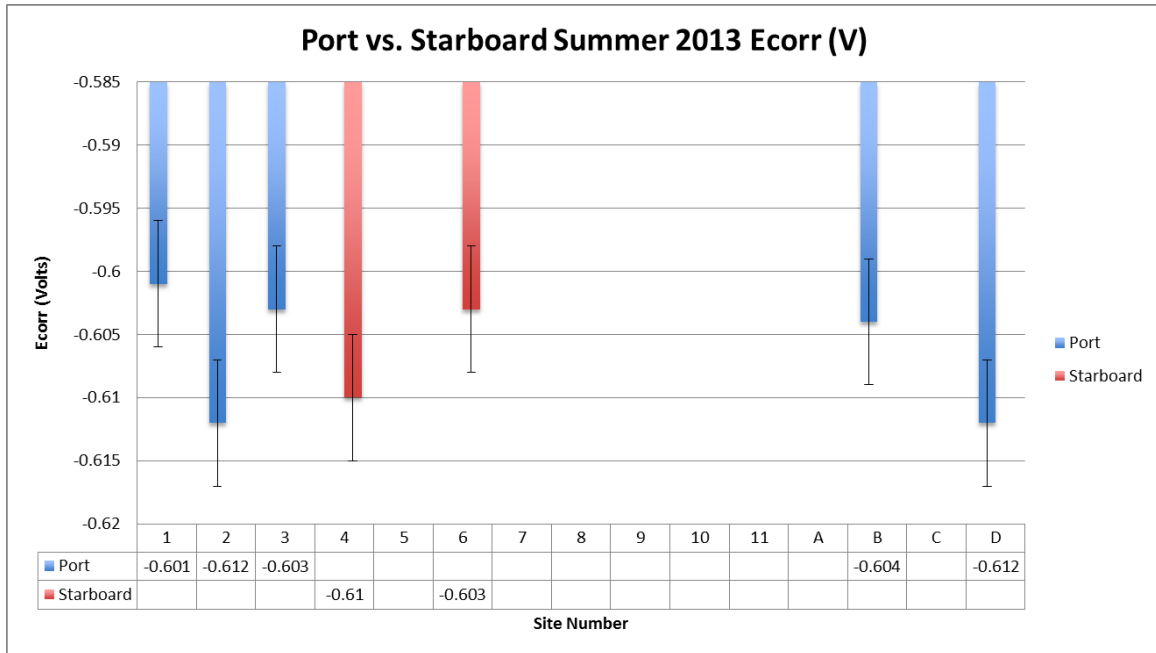


**Figure 43. Graph of port and starboard corrosion potentials (Ecorr) for summer 2013. (Image by author, 2014.)**

The result of this analysis shows no significant difference between port and starboard Ecorr averages from the summer 2013 data set (Figure 42). The 0.001 V (0.68%) change observed falls within the .005 V error range of the sampling device (Figure 43). One critique of the data set is the overall weighting of five starboard sampling sites to the port side's two sampling sites. However, the similarity between the sites suggests either both the sides are electrically connected and thus, these portions of the wreck are corroding in the same cathodic cell, or these sides are electrically separate but are of similar metallurgical composition and corroding in the same environment. The latter explanation would indicate that no significant difference was observed in the corrosion environment between the sides, unlike the results from the *Xantho* Project.

The same analysis between the port and starboard sides of the wreck can be applied to the winter 2013-2014 data (Figure 44). The data set is not nearly as sizeable as the summer 2013, with only two successful samples taken (Figure 45), one from each

side of the wreck (the sites where poor readings were taken are highlighted in green, on Figure 44).

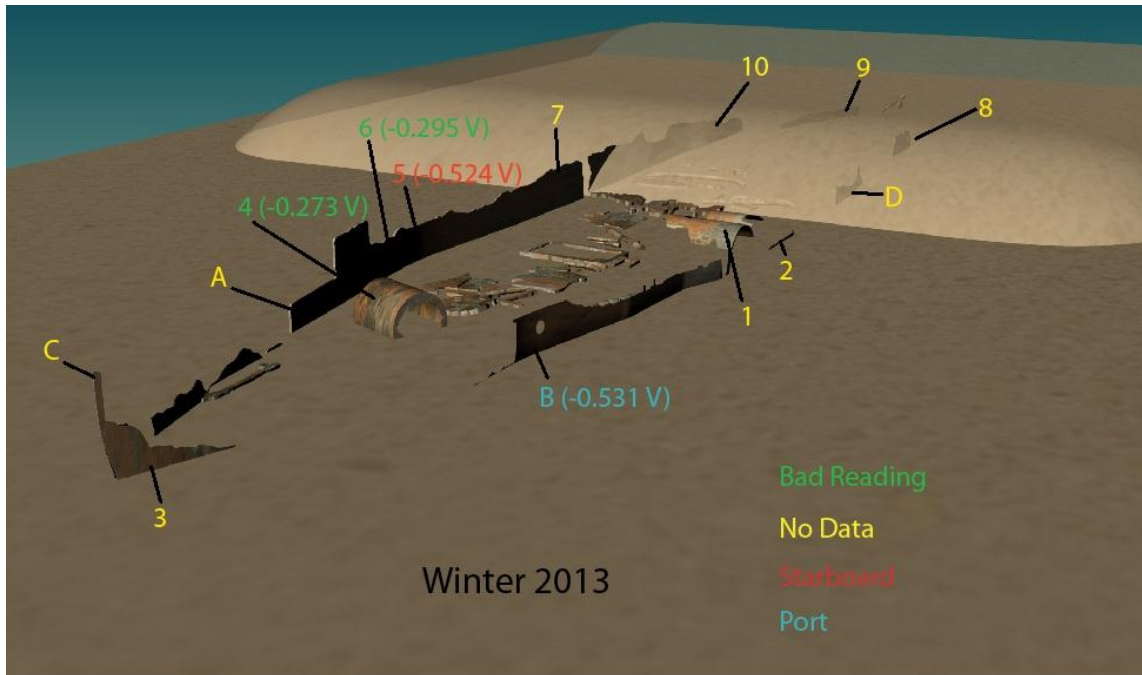


Figure 44. Corrosion potential readings partitioned into port and starboard sides of the wreck for winter 2013-2014. (Image by author, 2014.)

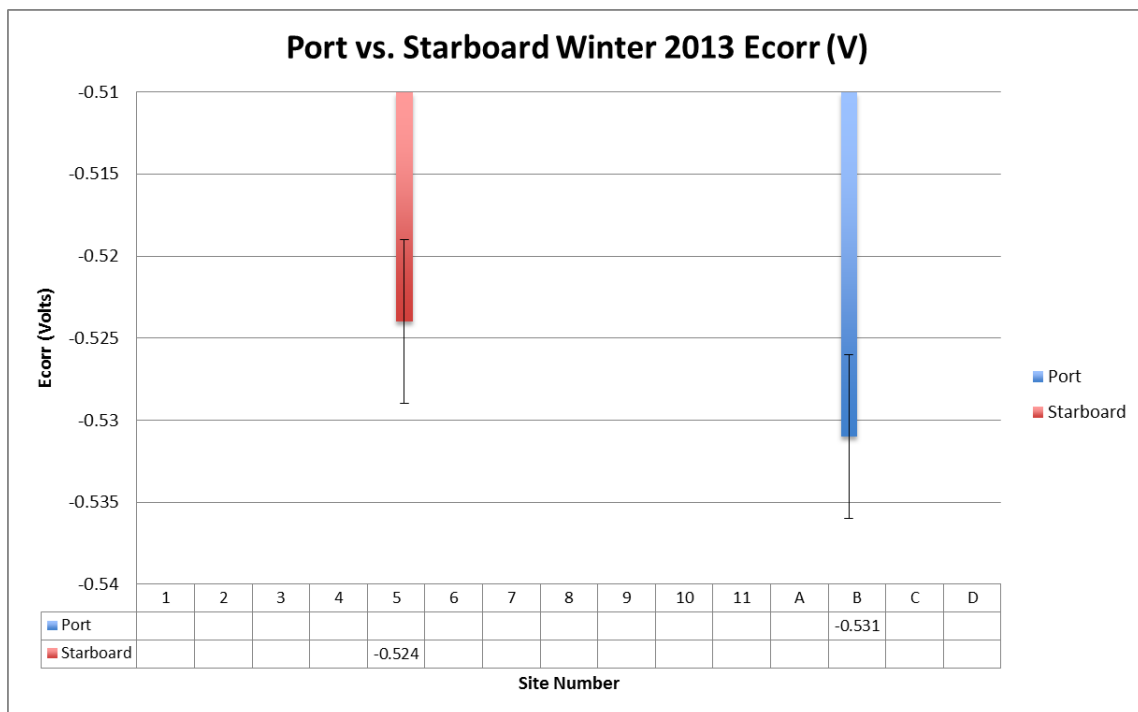
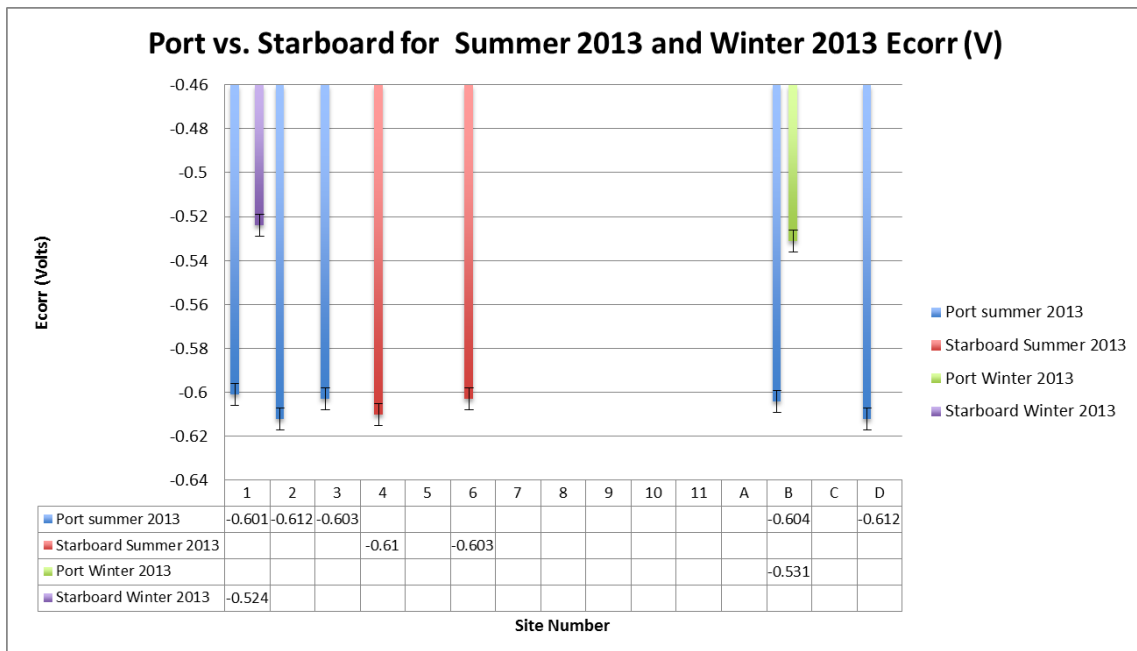


Figure 45. Graph of port and starboard side corrosion potentials ( $E_{corr}$ ) for winter 2013-2014. Invalid readings are not included. (Image by author, 2014.)

The winter 2013-2014 data set shows the poor readings in the  $-0.200$  V range, evidence of a missed connection with the wreck and the Polatrak CP gun. The two good readings between sample locations 5 and B are  $0.007$  V apart, which is just outside the equipment's  $0.005$  V tolerance, indicating a potential 4.8% difference in corrosion rate. However, this small difference, coupled with the paucity of samples taken, means this site specific analysis is inconclusive.

One final examination of port versus starboard corrosion can be undertaken by comparing the summer 2013 and winter 2013-2014 datasets (Figure 46). This may further highlight differences in corrosion potential between the port and starboard sides not found in the individual season analysis, such as elements of the wreck site that are electrically separate or that are subject to differences in the ocean's current. This data set also highlights the seasonal difference in corrosion potential observed (Table 16).



**Figure 46. Port versus starboard Ecorr for Summer 2013 and Winter 2013-2014. (Image by author, 2014.)**

Side	Season	Average Ecorr	Difference Summer-Winter
Port	Summer 2013	-0.604	49.88%
	Winter 2013-2014	-0.531	
Starboard	Summer 2013	-0.607	56.72%
	Winter 2013-2014	-0.524	

**Table 16. Average Ecorr from summer 2013 compared to the Ecorr of Winter 2013-2014 with percent change in corrosion rate.**

There was a 49.9% increase in corrosion rate observed from the port side of summer 2013 to winter 2013-2014 and a 56.7% increase on the starboard side. This 6.8% difference in corrosion potential suggests that there is a site specific variable affecting the corrosion rate between the seasons. This variable could be the difference in area covered by sediment between port and starboard. Using the *Rhinoceros* area analysis function it was calculated that the exposed area for the starboard side is 607.8 square feet and the port side is 359.0 square feet. The starboard side has 41% more surface area exposed which may account for the higher corrosion rate observed on the starboard side. This comparison, however, is limited by the winter data set comprising only two sites and therefore, an average Ecorr for the specific sides cannot be calculated.

#### Bow, Midships, Stern Corrosion Comparison

This analysis compares the corrosion potential across bow, midships and stern sections of the USS *Huron* wreck during the summer 2013 season followed by the winter 2013-2014 season, and finally a comparison of sites across these seasons. Similar to the port and starboard analysis, this inquiry could show areas of the wreck subject to increased corrosion rates or identify areas of the wreck that are electrically separate. Comparisons do not differentiate by structure or feature. The summer 2013 season data is depicted in Figure 47 and 48. During this season the majority of the stern section was covered by sand, however, some sampling locations (such as site D) were barely exposed

and a reading could be obtained.

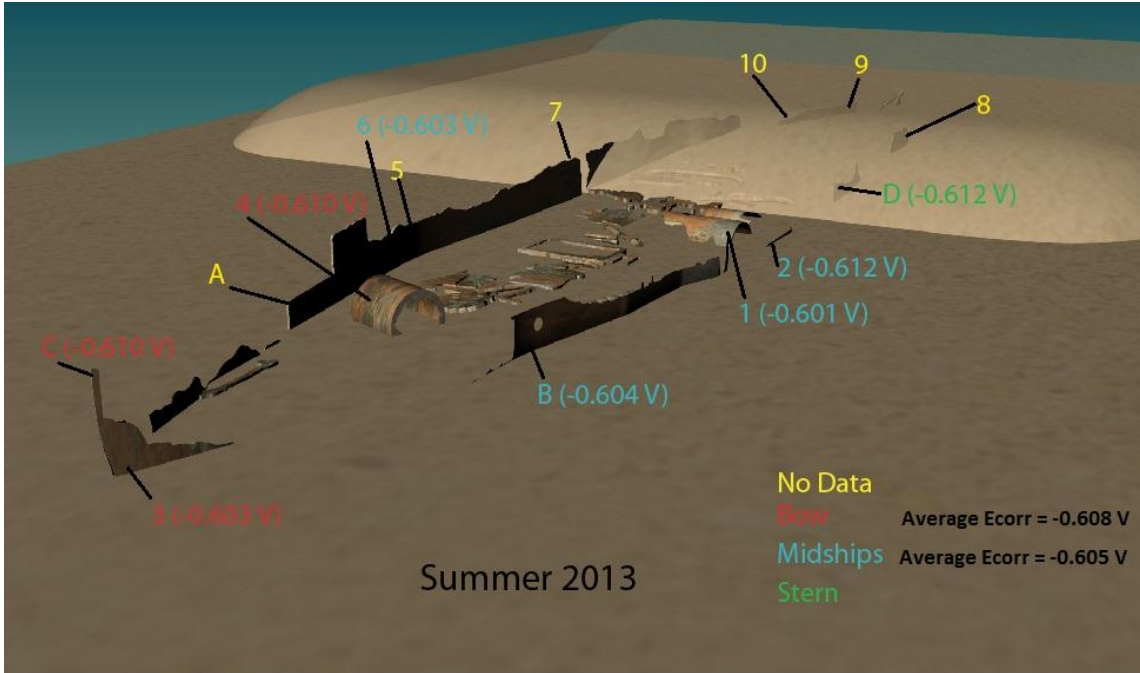


**Figure 47. Summer 2013 bow, midships, and stern section corrosion potential results. (Image by author, 2014.)**

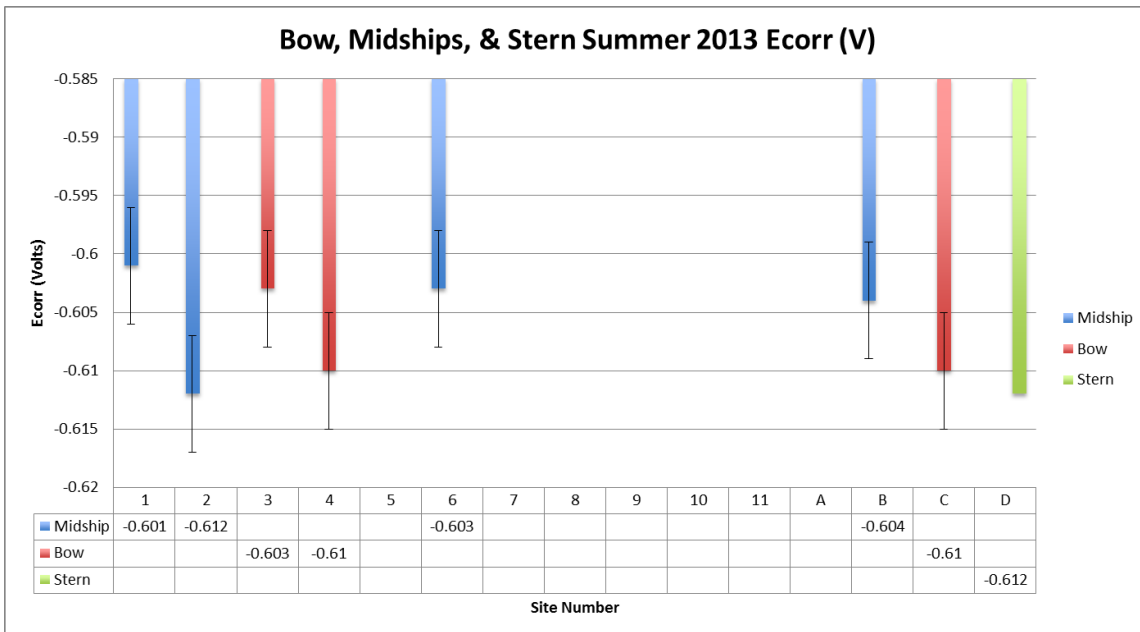


**Figure 48. Graph of the bow, midships, and stern corrosion potentials (Ecorr) from the summer 2013 sampling season. (Image by author, 2014.)**

The average Ecorr of the bow was -0.608 V compared to the midships average Ecorr of -0.605 V. This 0.003 V difference equates to 2.05%, however, it is also within

the margin of error for the testing equipment (0.005 V). The result of this analysis is that there is arguably no significant difference between the bow and midships section of the wreck site for this season. The stern sampling comprised of one sample (D). Sample site D had the lowest corrosion potential (-0.612 V) which equals a 4.4% reduction in corrosion rate from the stern when compared to the midships samples. Sampling site 2 is adjacent to sampling site D with an identical reading of -0.612 V. This may suggest that the stern is corroding at a slower rate than the bow and midships portions. Alternatively, this could suggest that the stern might be electrically separate.

The same analysis between the bow, midships, and stern aspects of the wreck can be applied to the winter 2013-2014 data (see Figure 49 and 50).

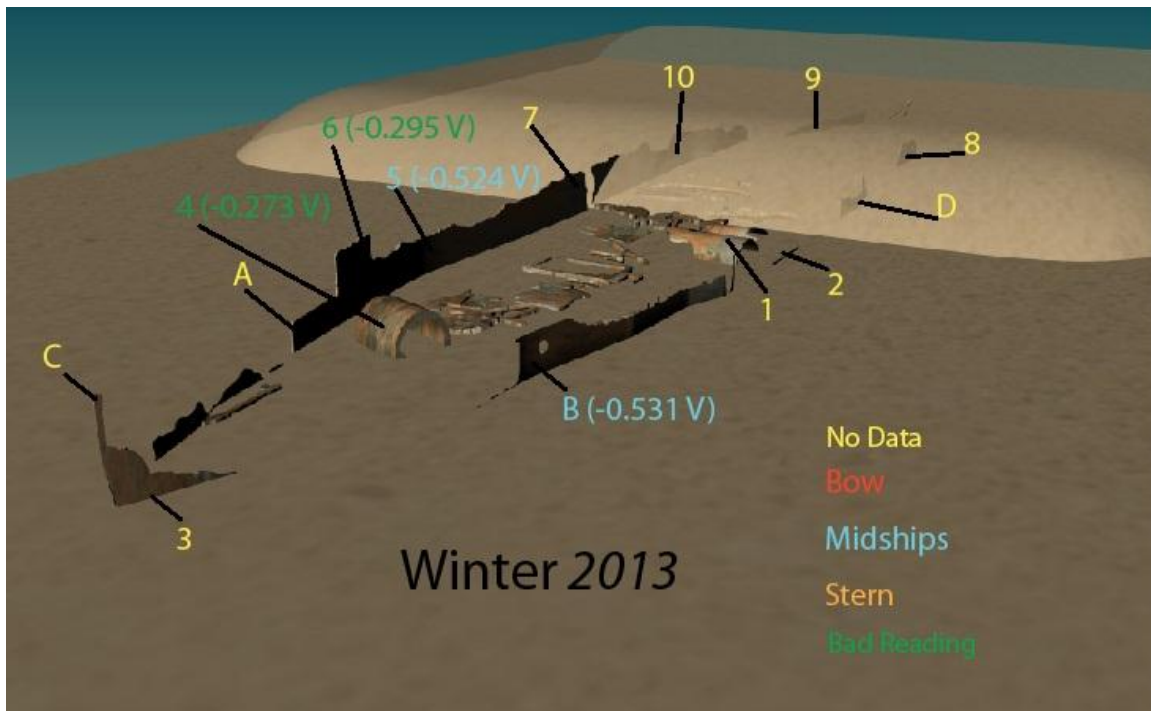


**Figure 49. Winter 2013-2014 bow, midships, and stern section corrosion potential results. (Image by author, 2014.)**

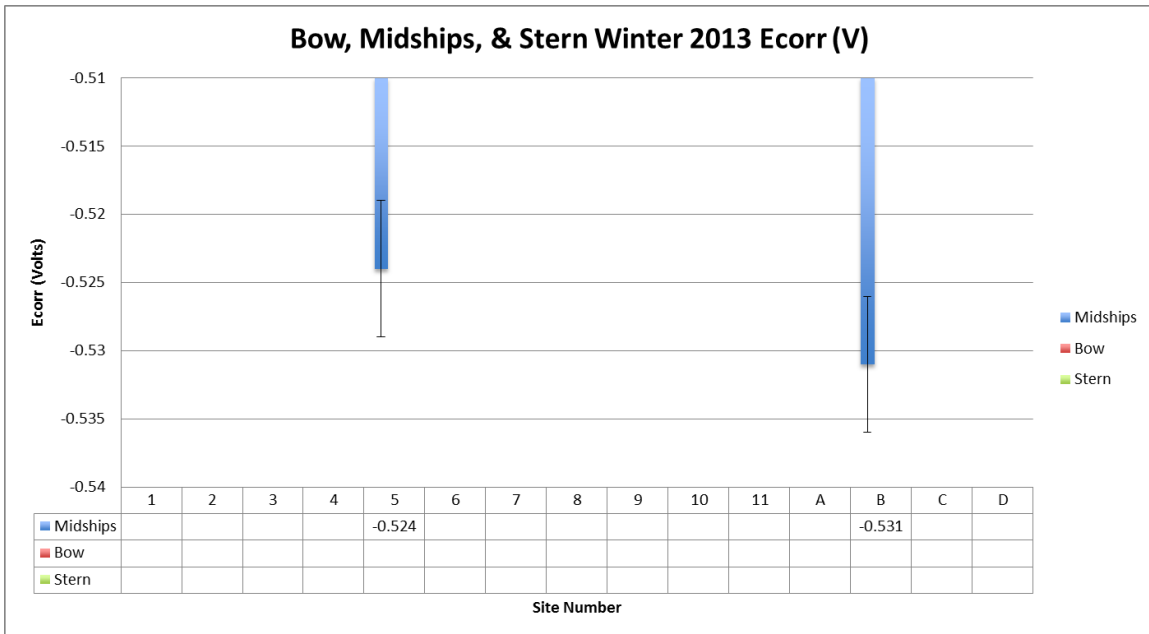


**Figure 50. Graph of the bow, midships, and stern corrosion potentials (E<sub>corr</sub>) from the summer 2013 sampling season. Invalid readings are not included. (Image by author, 2014.)**

The analysis shows an average corrosion potential of -0.528 V for the midships portion of the wreck. As an average of the midships is the only reading that can be obtained for this period of data collection, no comparison can be attempted and an analysis is not possible.

One final comparison of bow, midships, and stern corrosion can be undertaken by comparing the summer 2013 and winter 2013-2014 datasets (see Figure 51). This analysis could show differences in corrosion potential caused by changes in the corrosion environment or identify areas of the wreck that are electrically separate cathodic units not readily apparent in each season’s individual analysis (Table 17). This analysis can only compare the seasonal change in corrosion potential from sample sites within the midships portion of the wreck because of the limited data from winter 2013-2014.

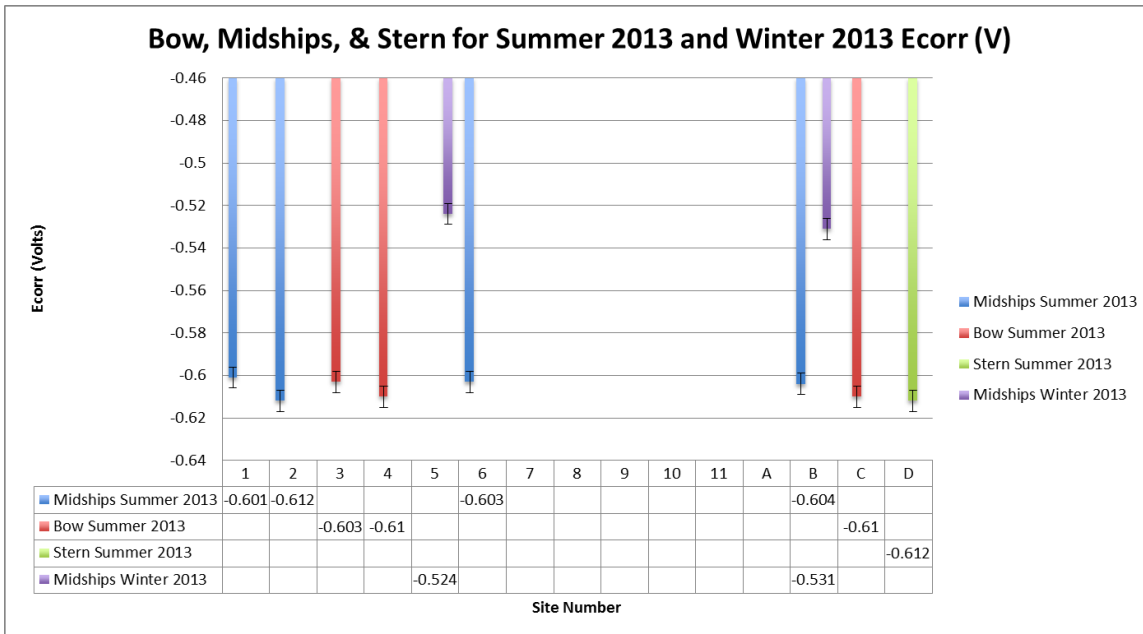


**Figure 51. Bow, midships, and stern Ecorr for summer 2013 and winter 2013-2014. (Image by author, 2014.)**

Element	Season	Average Ecorr	Difference Bow-Midships-Stern
Bow	Summer 2013	-0.608	N/A
	Winter 2013-2014	No data	
Midships	Summer 2013	-0.605	N/A (52.6% change at midships across season)
	Winter 2013-2014	-0.528	
Stern	Summer 2013	-0.612	N/A
	Winter 2013-2014	No data	

**Table 17. Average Ecorr of summer 2013 and winter 2013-2014 with percent change in corrosion rate.**

The result of this analysis shows that there was a 52.6% increase in corrosion rate from summer 2013 to winter 2013-2014, which as mentioned in previous analyses may be attributable to changes in sediment cover. A comparison of different corrosion rates *between* the bow, midships, and stern is not possible due to a lack of locations in each area across the two sampling periods.

## Inboard versus Outboard Ecorr

This analysis compares the corrosion potential between inboard and outboard sections of the USS *Huron* wreck during the summer 2013 season followed by the winter 2013-2014 season, and finally a comparison of sites across these seasons. Similar to previous analyses, this inquiry could show areas of the wreck subject to increased corrosion rates or identify areas of the wreck that are electrically separate. Comparisons do not differentiate by structure or feature. The summer 2013 season data is depicted in Figures 52 and 53. This analysis is inclusive of both hull plates and features. Summer 2013 has the most extensive data set, and is the best candidate to illustrate any changes observed in corrosion potential between the inboard and outboard portions of the wreck site.

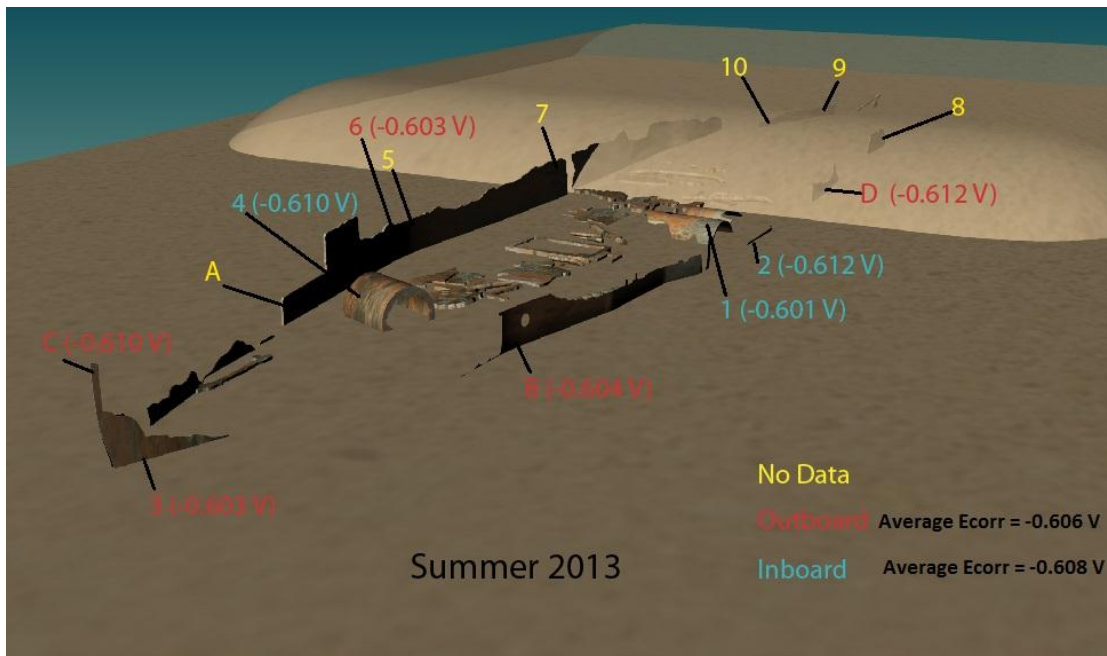


**Figure 52. Summer 2013 inboard versus outboard Ecorr comparison. (Image by author, 2014.)**

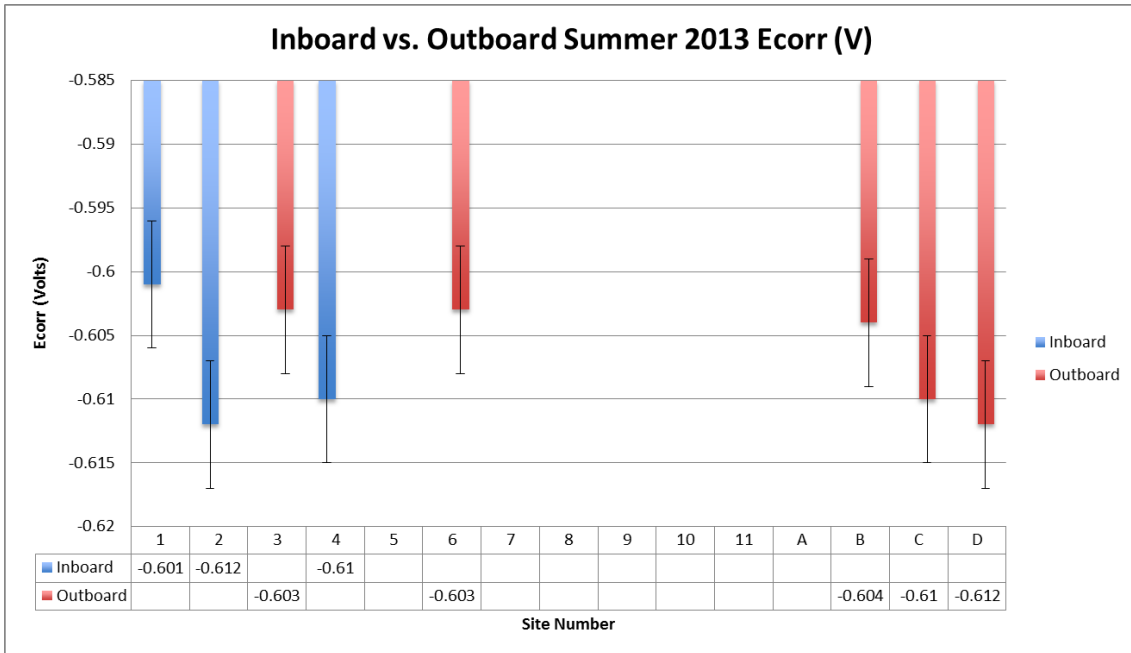


**Figure 53. Graph of the summer 2013 inboard versus outboard Ecorr. (Image by author, 2014.)**

The result of this analysis shows an average corrosion potential of -0.608 V for the inboard sampling sites and an average corrosion potential of -0.606 V for the outboard sites. This 0.002 V (1.37%) difference between inboard and outboard corrosion potential falls within the margin of error for the sampling equipment (0.005 V) and indicates a negligible difference.

The winter 2013-2014 samples similarly attempted to partition the wreck site into both inboard and outboard sampling sites to determine if there were environmental factors affecting the corrosion rate of the different portions of the wreck site (Figure 54 and 55). The winter 2013-2014 sampling season only had two successful samples, one each from the inboard and outboard portions of the wreck, however, the small sample size means conclusions from the site specific analysis is limited.

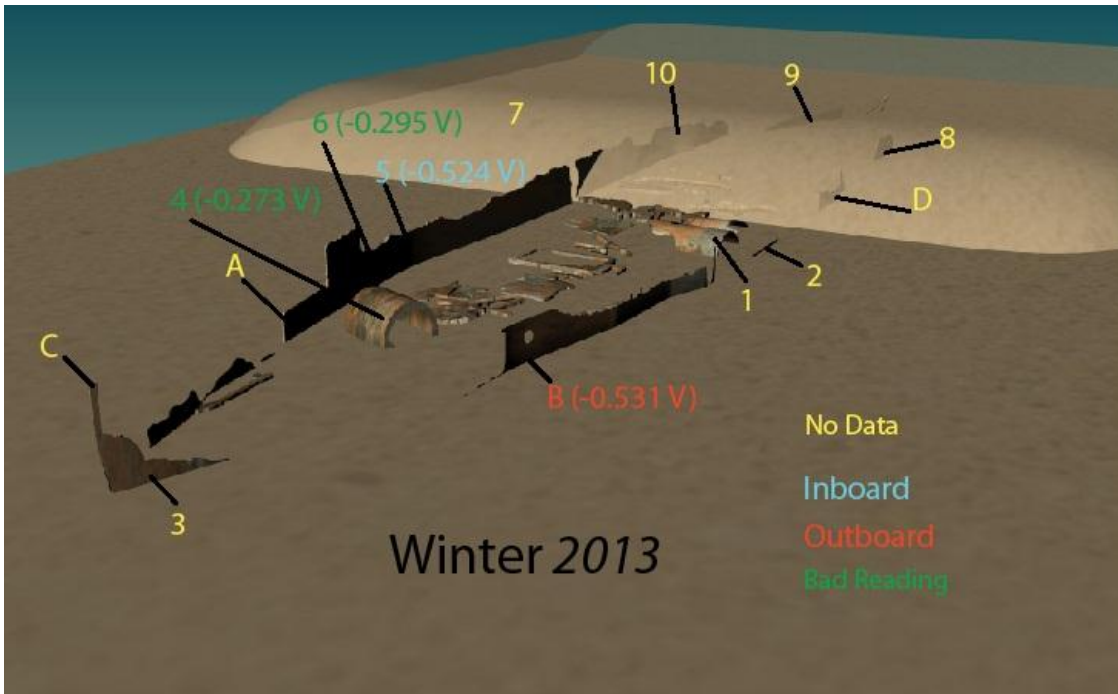


Figure 54. Winter 2013-2014 inboard versus outboard Ecorr comparison. (Image by author, 2014.)

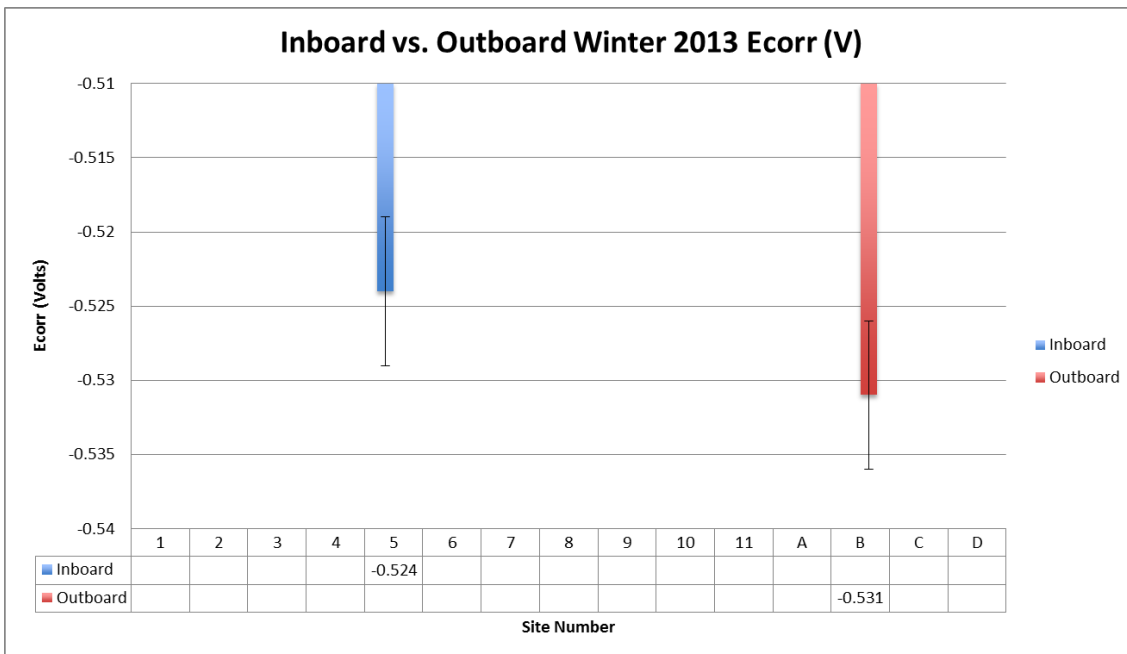
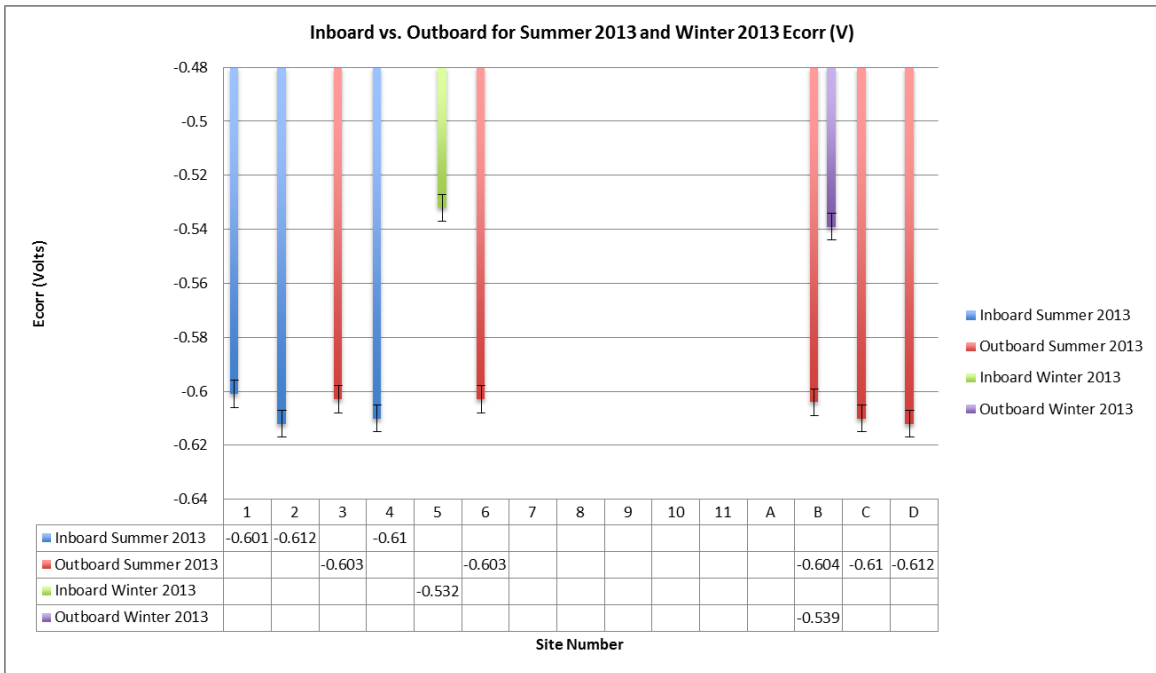


Figure 55. Graph of the winter 2013-2014 inboard versus outboard Ecorr. Invalid readings are not included. (Image by author, 2014.)

The result of the inboard versus outboard analysis for winter 2013-2014 shows a single outboard reading of -0.531 V and a single inboard reading of -0.524 V. The 0.007

V difference lies outside of the 0.005V equipment tolerance, and suggests a 4.6% difference in corrosion rate between inboard and outboard portions of the wreck for winter 2013-2014. However, the lack of sampling sites lessens confidence in any site specific conclusion.

One final comparison of inboard and outboard corrosion can be undertaken by comparing the summer 2013 and winter 2013-2014 datasets (Figure 56 and Table 18).



**Figure 56. Inboard versus outboard Ecorr for summer 2013 and winter 2013-2014. (Image by author, 2014.)**

Orientation	Season	Average Ecorr	Difference Summer-Winter
Inboard	Summer 2013	-0.608	52.50%
	Winter 2013-2014	-0.531	
Outboard	Summer 2013	-0.606	56.00%
	Winter 2013-2014	-0.524	

**Table 18. Comparison between the Ecorr of inboard and outboard portions of the wreck for summer 2013 and winter 2013-2014.**

This analysis shows a 52.5% increase in corrosion rate on the inboard side and a 56% increase in corrosion rate on the outboard side from summer 2013 to winter 2013-2014 (Table 18). This 3.5% difference is within the error of the corrosion sampling equipment and suggests that the corrosion rates between the inboard and outboard sides are similar and not affected by site specific variables such as ocean currents or cathodic separation. The data, however, is limited by the winter 2013-2014 data having only two sampling sites.

#### Features versus Hull Plates Ecorr

This analysis compares the corrosion potential between the structure and features of the USS *Huron* wreck during the summer 2013 season followed by the winter 2013-2014 season, and finally a comparison of sites across these seasons. Such a comparison could show differences in not only the corrosion environment, but also differences in metallurgy between separate features and hull plates. This analysis could potentially identify features that have become electrically separate from the rest of the wreck site and this can inform on the wreck site's post-depositional site formation processes.

The features chosen for this analysis are major features on the wreck site such as the stem post, disarticulated starboard boiler, and port boiler. These features corrosion potentials are then compared to the corrosion potentials of the wreck's hull plates. The result of this analysis for the summer 2013 sampling season is depicted in Figure 57. The summer 2013 data set has the most site specific readings and is the best candidate for this analysis (Figure 58).

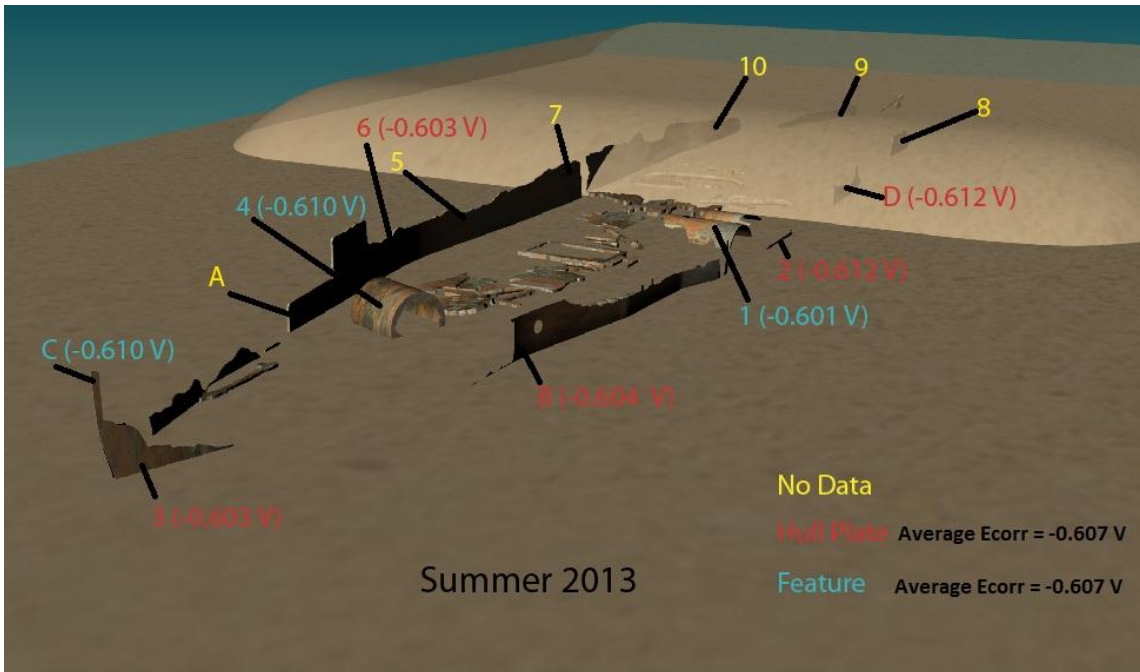


**Figure 57. Summer 2013 hull plate versus feature Ecorr comparison. (Image by author, 2014.)**

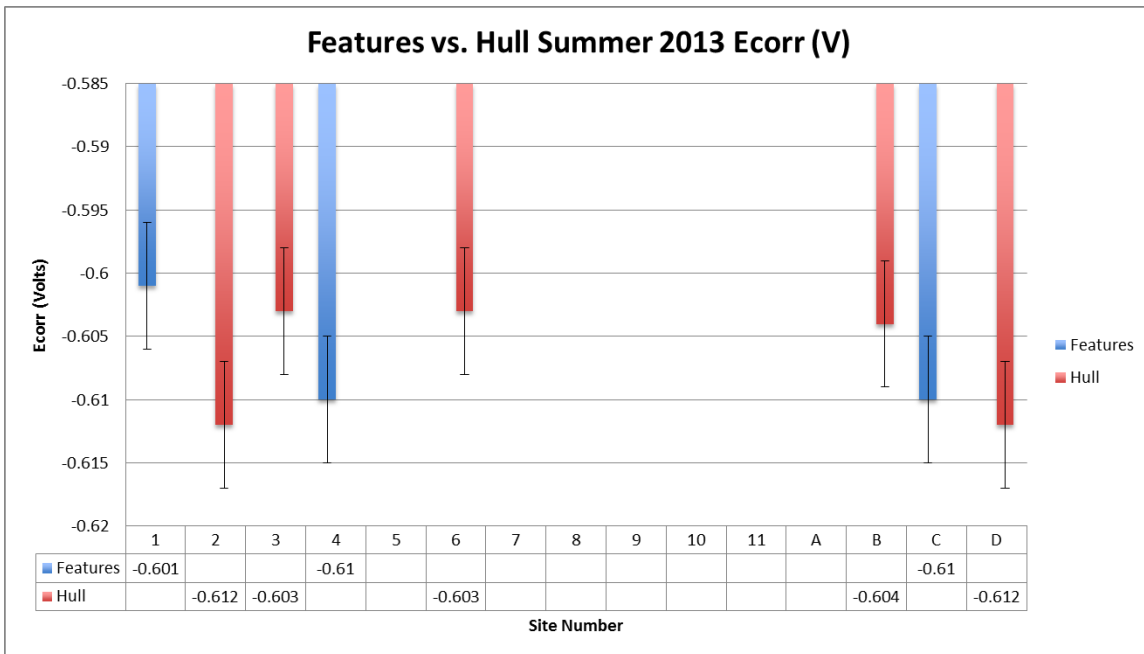


**Figure 58. Graph of the summer 2013 hull plates versus features Ecorr. (Image by author, 2014.)**

The average corrosion potential readings from hull plates versus the same readings from the aforementioned features show that both have an average Ecorr of -0.607 V, meaning that both have the same corrosion potential. This suggests that the hull

plates and features are still electrically connected, or are of similar enough wrought iron, that under the same corrosion environment, these different parts of the wreck corrode at the same rate.

Site specific analysis comparing the Ecorr of the wreck's features versus the hull plates could not be done on the winter 2013-2014 dataset. The two successful samples consist only of hull plate sites. This makes comparison between the hull plates and features impossible. This deficiency also limits the ability of a cross seasonal analysis to be performed.

The element specific Ecorr analysis did not conclusively find that the features are electrically separate from the hull. However, there is a chance that the disarticulated starboard boiler may be a separate cathodic unit. This is supported by Joe Friday (1988:91), who theorizes that this boiler was moved to its present day position as the result of post wrecking salvage attempts, which used dynamite to access the hull of the ship. From this post depositional transform it is possible that this particular feature is not in electrical contact with the rest of the ship and may be corroding similarly owing to its wrought iron construction and a similar corrosion environment.

## Discussion

The data collected during the course of the "*Huron Project*" was subjected to analyses that attempted to dissect the data from the general to the specific. The first series of analyses took the data sets from summer 2013 and winter 2013-2014 and compared corrosion potential to dissolved oxygen content of the water column. There was marked increase of 53.9% between summer 2013 and winter 2013-2014, commiserate with the dissolved oxygen increase found in winter 2013-2014. This discrepancy between

dissolved oxygen levels of the water column and corrosion rate suggested that another seasonal variable was affecting the site. The analysis comparing average seasonal Ecorr to sedimentation of the site may account this discrepancy; however corrosion potential data from summer 2012 was omitted from this study because of a field sampling error. From summer 2012 to summer 2013 there was a 32.1% increase of sedimentation of the site calculated using the *Rhinoceros* area analysis function. Further study of the relationship between corrosion rate and sedimentation for the site needs to be done. Sedimentation was similar between summer 2013 and winter 2013-2014, and the analysis suggests that corrosion rate was primarily affected by the change in dissolved oxygen for these seasons. Thus, the results show that the site is sensitive to changes in dissolved oxygen. The sediment time series taken from the annual Town of Nags Head surveys shows a pattern of reoccurring burial and also that the site covers from stern to stem.

The series of analyses went from comparing the average Ecorr of the wreck to seasonal variables and moved to site specific analyses. These site specific analyses were designed to test if there were site specific variables affecting the corrosion potential of different areas of the wreck specifically, whether there were differential exposure to the ocean's current, or if portions of the wreck are separate cathodic units. The wreck was split into four different areas of analysis, port versus starboard; bow versus midships, versus stern, inboard versus outboard, and hull plates versus features. These site specific analyses were applied to summer 2013 and winter 2013-2014 where applicable. The summer 2012 data set could not be used for site specific analysis.

The site specific analysis comparing the Ecorr of port versus starboard for summer 2013 showed no significant variation between the two sides. This same analysis

was run on winter 2013-2014 and indicated a potential 4.8% increase in corrosion rate for the starboard side; however, this analysis is limited by the small sample size. Further analysis comparing the port versus starboard sides between summer 2013 and winter 2013-2014 showed a 6.8% increase for the starboard side. Confidence in this result is again limited by the paucity of data for winter 2013-2014.

The site specific analyses continued with an analysis comparing the Ecorr of the bow versus midships versus stern. The summer 2013 analysis found the average Ecorr of the bow being -0.608 V compared to the midships average Ecorr of -0.605 V. This 0.003 V difference is within the margin of error for the testing equipment (0.005V). The stern data consisted of only sampling site D, but this site had a 4.4% lower corrosion rate than the bow. This, coupled with sampling site 2, directly adjacent to site D (but included in the midships portion of analysis) with an identical reading of -0.612 V further supports that the stern of the wreck corrodes at a slower rate than the bow and midships portions of the wreck. This could be indicative of the stern being electrically separate from the wreck, and that the lower corrosion potential observed might be due to the stern being buried.

The analysis continued with a comparison of the winter 2013-2014 Ecorr data to the bow, midships, and stern sections of the wreck. This analysis was limited because there is only data for the midships portion; however, data was used to compare the midships sections between summer 2013 and winter 2013-2014. The result of this analysis showed a 52.6% increase in corrosion rate for winter 2013-2014, further evidence of the seasonality of corrosion on the wreck site.

The next site specific analysis compared the inboard versus outboard Ecorr from summer 2013. The result was a 0.002 V difference between inboard and starboard suggesting that there is no variation in site specific variables acting on the inboard and starboard sides for summer 2013. The inboard versus starboard analysis was also applied to the winter 2013-2014 data set. The result was a 4.6% increase in corrosion rate on the inboard side of the wreck. This analysis was, however, limited by the sample size. The inboard versus outboard analysis continued with a comparison of the Ecorr from summer 2013 to winter 2013-2014. This analysis showed 3.5% increase in corrosion rate on the outboard portion of the wreck. This 3.5% increase translates to a .005 V difference, which falls within the error range of the sampling equipment. This means that there is no significant change in corrosion rate between the inboard and outboard portions of the wreck between summer 2013 and winter 2013-2014.

The site specific analysis finished with a comparison of Ecorr between the hull versus features. The features sampled included the port boiler, starboard disarticulated boiler, and the stem post. This analysis was only run on summer 2013, because winter 2013-2014 only had hull sampling sites. The results of the summer 2013 analysis showed a 0% change between the hull and the wreck sites features indicating that both the hull and the features corrode at the same rate.

### *Conclusion*

The overall result of analyses is that the corrosion rate of USS *Huron* is dictated by dissolved oxygen in the water. When the site is exposed to water with higher dissolved oxygen content, it will experience a higher corrosion rate as a result. Further study needs

to be done to identify the relationship between sedimentation of the site and corrosion potential.

There is a correlation between the seasonality of dissolved oxygen in the water determined by the seasonal changes in water temperature. However, this study cannot determine definitively the seasonality of sediment cover on the wreck of the *Huron* or the relationship between corrosion potential and sediment cover. The sediment time series created from the town of Nags Head yearly site surveys does not show a clear pattern of seasonality of sediment cover. The data from these surveys is biased towards the summer and fall diving seasons. It is suggested from the literature, that the site may experience increased sediment cover in the winter from increased northerly swells powering a north to south long shore current (Mallinson 2008:2). This is also suggested by the winter 2013 sampling season where the site could not be located, and may have been completely covered. Further sediment and corrosion data needs to be collected to determine the seasonality of sediment cover on the site which will be discussed in the next chapter.

The site specific analyses results were not as apparent compared to the average seasonal corrosion analysis; however, these analyses, despite the explicit limitations imposed from sampling errors, showed that the wreck of the *Huron* is corroding relatively uniformly from sampling site to site in regards to the inboard versus outboard and hull plates versus features analyses.

The analysis, however, comparing starboard and port sides of the wreck between summer 2013 and winter 2013-2014 resulted in a 6.8% shown increase on the starboard side. This 6.8% increase in corrosion rate was accompanied by 41% more surface area exposed for the starboard side. This suggests that the starboard and port sides might be

electrically separate, however, a difference in corrosion rate between port and starboard was not observed for summer 2013, casting doubt on this conclusion. The bow versus midships versus stern analysis for summer 2013 suggests a 4.4% lower corrosion rate on the stern of the wreck compared to the bow and midships portions of the wreck. This might be accounted for by the majority of the stern being covered with sediment and suggests that the stern is electrically separate.

## CHAPTER 7: CONCLUSION

The USS *Huron* began its service as a well-built ship from an outmoded era in ship construction. It and the two other *Alert*-class ships, *Ranger* and *Alert*, launched in 1875 were not only the last iron-hulled ships built for the U.S. Navy, but also the last to have auxiliary sails and smooth bore ordnance. *Huron* served admirably in its role as an extension of the United States' influence in the Western Hemisphere, and as a research vessel. Unfortunately, the ship's legacy is not one of a long, prosperous career, but one of disaster.

The loss of the USS *Huron* on that night in November 1877 was a tragedy with repercussions such as renewed support for the U.S. Lifesaving Service found growth in the wake of the disaster. Today, the wreck persists as a concreted hulk just past the surf line and is a popular shore dive on North Carolina's Outer Banks. While this wreck is one of countless many that dots the rugged North Carolina coastline, the sacrifice of those 98 men is not forgotten, and while this ship's past is one marked by agony, the current state of this ship is more positive. It is reflective of the maritime heritage of the United States and North Carolina's Outer Banks, and serves an economic role in supporting local dive shops with recreational dive operations on the site. Understanding how this important resource interacts with its environment is essential for creating an adequate management plan and perhaps taking steps to remediate destructive processes on the site.

The overall primary research question outlined in the present study asks: *Is there a relationship between seasonal water parameters (temperature, salinity, dissolved oxygen, and sedimentation cover), and the corrosion rates of ferrous metal shipwrecks in*

*a near shore environment?* In order to adequately assess this question, a series of multiple-working hypotheses were offered:

*Null hypothesis:* There is no relationship between seasonal water parameters and sedimentation to corrosion rates of ferrous metal in a near shore environment.

*1a:* There is an increase in corrosion rate observed during periods of less sedimentation cover and increased exposure to cold water with high dissolved oxygen content.

*1b:* There is a decrease in corrosion rate observed during periods of less sedimentation cover and increased exposure to cold water with high dissolved oxygen content.

*1c:* There is no observed corrosion during the study period, indicating the wreck is in a state of equilibrium.

*1d.* Mixed corrosion rates are observed with no correlation to the studies variables.

Iron in an underwater archaeological setting is usually actively corroding (strongly reducing state) with the microenvironment having a pH of 4.8 on average and the wreck of the USS *Huron* is assumed to be in a state of active corrosion (MacLeod 2002:700). This assumption is further supported by the range of corrosion potentials sampled on the site (-0.524 V to -0.612 V) (Deep Water Corrosion Services, Inc. 2010:7).

The results of analysis suggest that hypothesis 1a is correct with one big limitation: There is an increase in corrosion rate observed during periods of less sedimentation cover and increased exposure to cold water with high dissolved oxygen content. Dissolved oxygen content was 23.3% percent higher from summer 2013 to

winter 2013-2014. This resulted in a 53.9% higher corrosion rate. These combined analyses, show that the site's corrosion rate is sensitive to changes in dissolved oxygen content of the water. However, a seasonal pattern could only be linked to dissolved oxygen content in the water. The seasonality of sediment cover on the site is not definitive and further data needs to be collected. With this in mind, the hypothesis could be rewritten as: There is an increase in corrosion rate observed during periods of increased exposure to cold water with high dissolved oxygen content, but sediment coverage is not defined seasonally.

Finer grained examination came from the site specific analyses. The goal of these experiments was to identify areas of the wreck that are subject to site specific variables such as exposure to the ocean's currents or sites that are cathodically separate. These analyses found that there was no discernible difference in corrosion rate between the inboard and outboard sides, or the hull plates and features. There was, however, a marked increase of 6.8% increase in corrosion rate on the starboard side observed on the site specific port versus starboard between summer 2013 and winter 2013-2014 analysis, although, this difference in corrosion rate was not observed during the summer 2013 season. Further, there was a 4.4% decrease in corrosion rate observed on the site specific analysis of the stern versus the bow and midships portion of the wreck.

#### *Future Work*

This thesis leaves room for further research. The basic research model, methods, data, and spatial control are available for use and expansion. Future research lies in continuing the seasonal monitoring of the wreck site and building upon the analyses

presented here. Additionally, there were problems with the “*Huron Project’s*” methodology that should be corrected for future research.

The first problem was troubleshooting the corrosion monitoring equipment. Issues with the homemade multimeter with the silver/silver chloride reference electrode plagued the study with problems and limited the useable data obtained. Summer 2012 suffered from the reference electrode being much too far spatially from the sample sites and resulted in remote earth reference readings, limiting any site specific analysis. When this system was eschewed in favor of the Polatrak CP gun, the quality of data improved for the summer 2013 season. Drill failure on the winter 2013-2014 data required the “stab method” be employed resulting in a 50% failure in corrosion sampling. Ideally, the CP gun and drill would be used to ensure quality results. This project would have benefited from a much larger data set to make more concrete conclusions, especially concerning the site specific analyses.

The second problem was outside any control. Accessing the site required there to be limited surf and ideally, clear water. This requires a gentle northeast wind to blow clearer water in from offshore. The timing of the project usually had divers sampling during periods of light offshore winds, which meant minimal surf but murky water as the result of ocean upwelling. Diving in limited visibility conditions is difficult and results in severely task-loaded divers, further limiting the quality of data. The project evolved as lessons were learned the hard way such as the need for redundant drill bits while diving and securing the pneumatic drill to the low pressure hose using a lanyard to avoid loss of the equipment. This resulted in the methodology evolving concurrently to streamline the sampling process and maximize success in the harsh conditions.

The third problem is much of this data is only a snapshot of the site at the time of sampling. This problem is obvious when looking at the sediment time series from the Town of Nags Head yearly surveys where the site is only representative of each respective survey. The sediment time series could be improved with increased diver surveys, or absent this, using side scan surveys to supplement the yearly survey. Future corrosion studies would also benefit from using a HOBO Conductivity Data Logger. This device is capable of recording water temperature, conductivity, and salinity every minute for up to one year. This results in a vastly higher resolution of seasonal water parameters. This data can then be downloaded and profiles stored on a PC/Mac. This device would be installed semi-permanently on the wreck and serve as the primary recorder of water parameters and associated seasonal change. These devices are diminutive and rugged, but need to be placed inconspicuously to minimize risk of theft.

Future work primarily requires that the sampling equipment be user friendly to maximize success. The results of the seasonal Ecorr analyses show a wreck site that is actively corroding with a corrosion rate that is heavily influenced by dissolved oxygen content of the water and sedimentation of the site. The seasonality of dissolved oxygen is shown; however, definite seasonal changes in sediment cover need further investigation. Monthly or quartile site surveys, either diver based or remote sensing based (e.g. side scan or multibeam survey) could identify the seasonality of sediment cover on the wreck site. Future work on the USS *Huron* site need to focus on determining the seasonality of sediment cover, site specific analyses, and corrosion remediation.

### *Corrosion Remediation*

The wreck of the USS *Huron* would be an ideal case study for the implementation of cathodic protection on North Carolina's near-shore wrecks. The wreck is a good fit for installation of a sacrificial anode, despite the wreck's dynamic sedimentation. Sacrificial anodes have been proven to be effective. Installation of an aluminum anode on the drive train of *Xantho* showed a 37% reduction in corrosion rate (MacLeod 2002:707). Anodes (less noble metals, usually aluminum or zinc) are ineffective when buried and need to lie proud of the seabed to provide cathodic protection to metal structures. It appears from the sedimentation time series that the bow of the wreck is exposed except when the entire wreck is buried (Figure 38). This means that sacrificial anodes could be placed near the bow (and inboard) of the ship and would provide cathodic protection until the majority of the wreck was buried. When the wreck and the anode are buried, cathodic corrosion slows and the anode's protective role is diminished. Any anodes installed on the wreck would have to be periodically inspected and scrubbed of biofouling and corrosion. This process could be added to the yearly inspection checklist. In addition to continuing the basic Ecorr recording on the wreck site, concretion equivalent corrosion rate analysis could be performed and a long-term corrosion rate determined.

Testing the feasibility of cathodic protection and in-situ conservation on near-shore North Carolina wrecks could help safeguard these valuable heritage resources for future generations. Future management plans could also include routine corrosion potential monitoring of the site. This data could be used to further refine understanding of the wreck's interaction with the environment and identify periods of increased corrosion rates and the efficacy of in-situ conservation efforts.

### *Conclusion*

The “*Huron* Project” spanned from 2012 to 2013 and investigated how this important shipwreck interacts with the highly dynamic North Carolina Outer Banks environment. The project had explicit trouble at times, but it was successful in quantifying the effect of dissolved oxygen on the corrosion rate of the ferrous wreck, however, future work on the seasonality of sediment cover on the site needs to be done. The project could not have been done without help from the students, staff, and equipment from East Carolina University and UNC-Coastal Studies Institute. It is hoped that the foundation of data taken during the course of studying the wreck of USS *Huron* will be used to further refine management, not only of this specific site, but submerged archaeological sites the world over.

## REFERENCES CITED

Ahmed, Zaki

2006 Principles of Corrosion Engineering and Corrosion Control. Elsevier, Oxford, United Kingdom.

Barnard, Charles

1878 The American Clyde. *Harper's New Monthly Magazine* 56 (335): 641-653.

Beringer-Pooley, James

2005 Comparative Corrosion Analysis of J-Class Submarines. Master's thesis, Department of Archaeology, Flinders University, Adelaide, Australia.

Buck, R.P., Rondinini, S., Covington, A.K., Baucke, F.G.K., Brett, C.M.A., Camoes, M.F., Milton M.J.T., Mussini T., Naumann, R., Pratt, K.W., Spitzer, P., Wilson, G.S.

2002 Measurement of pH. Definition, Standards, and Procedures. *Pure Applied Chemistry* 74(11): 2169-2200.

Deep Water Corrosion Services, Inc.

2010 Deepwater Polatrak: Polatrak CP Gun Product Manual. Document Number 352-MN01-ENG, Rev. C.

Dolan, Robert

1966 Beach Changes on the Outer Banks of North Carolina. *Annals of the Association of American Geographers* 56(4): 699-711.

East Carolina Diving and Water Safety

2012 Dive logs from the 2012 Fall Field School, East Carolina University, Greenville <<http://www.research2.ecu.edu/InetPub/wwwroot/aausfiles/ecudivingsafety/ecudsolog1.cfm>>, Accessed 18 March 2014.

Foecke, Tim., Li Ma, Matthew A. Russell, David L. Conlin, and Larry E. Murphy

2010 Investigating Archaeological Site Formation Processes on the Battleship USS Arizona Using Finite Element Analysis. *Journal of Archaeological Science* 37: 1090-1101.

Friday, Joe D. Jr.

1988 A History of the Wreck of the USS *Huron*. Master's thesis, Department of History, East Carolina University, Greenville, NC.

Gamry Instruments

2010 Getting Started with Electrochemical Corrosion Measurement: Quantitative Corrosion Theory. <[http://www.gamry.com/App\\_Notes/DC\\_Corrosion/GettingStartedWithEchemCorrMeasurements.htm](http://www.gamry.com/App_Notes/DC_Corrosion/GettingStartedWithEchemCorrMeasurements.htm)>, Accessed 29 September 2011.

Gibbs, Martin

- 2006 Cultural Site Formation Processes in Maritime Archaeology: Disaster Response, Salvage and Muckelroy 30 Years On. *The International Journal of Nautical Archaeology*.35.1: 4-19.

GMC Electrical, Inc.

- 2014 Temperature Correction Information for Cu-CuSO<sub>4</sub>, Zn-ZnSO<sub>4</sub> and Ag-AgCl Reference Electrodes.  
<[http://www.gmcelectrical.net/Pages/GMC\\_STAPERM\\_REFERENCE\\_ELECTRODES.aspx](http://www.gmcelectrical.net/Pages/GMC_STAPERM_REFERENCE_ELECTRODES.aspx)>, Accessed 28 February 2014.

Gregory, David

- 1999 Monitoring the effect of sacrificial anodes on the large iron artefacts on the Duart Point wreck, 1997. *The International Journal of Nautical Archaeology*. 28.2:164-173.

Gu, J.D., T.E. Ford, R. Mitchell

- 2000 Microbiological Corrosion of Metals. In *Uhlig's Corrosion Handbook*, second edition, R. Winston, editor, pp. 915-927. Wiley and Sons, New York, NY.

Hackerman, Norman

- 1952 Effect of Temperature on Corrosion of Metals by Water. *Industrial and Engineering Chemistry* 44 (8): 1752-1755

Hamilton, Donnie L

- 1999 Basic Methods of Conserving Underwater Archaeological Material Culture. Conservation Research Laboratory, Center for Maritime Archaeology and Conservation. Texas A&M University.

Johnson, Matthew

- 2010 *Archaeology Theory: An Introduction*. Wiley-Blackwell, West Sussex, United Kingdom.

Lawrence, Richard

- 2004 USS *Huron* Historic Shipwreck Preserve Status Report January 1, 2003 to December 31, 2003. *Letter to Underwater Archaeology Branch Department of Cultural Resources*.
- 2005 USS *Huron* Historic Shipwreck Preserve Status Report January 1, 2004 to December 31, 2004. *Letter to Underwater Archaeology Branch Department of Cultural Resources*.
- 2006 USS *Huron* Historic Shipwreck Preserve Status Report January 1, 2005 to December 31, 2005. *Letter to Underwater Archaeology Branch Department of Cultural Resources*.

- 2007 USS *Huron* Historic Shipwreck Preserve Status Report January 1, 2006 to December 31, 2006. *Letter to Underwater Archaeology Branch Department of Cultural Resources.*
- 2008 USS *Huron* Historic Shipwreck Preserve Status Report January 1, 2007 to December 31, 2007. *Letter to Underwater Archaeology Branch Department of Cultural Resources.*
- 2009 USS *Huron* Historic Shipwreck Preserve Status Report January 1, 2008 to December 31, 2008. *Letter to Underwater Archaeology Branch Department of Cultural Resources.*

MacLeod, Ian D.

- 1981 Shipwrecks and Applied Electrochemistry. *Journal of Electroanalytical Chemistry.* 118: 291-303.
- 1989 The Application of Corrosion Science to the Management of Maritime Archaeological Sites. *Bulletin of the Australian Institute for Maritime Archaeology.* 13(2): 7-16.
- 1996 An In-Situ Study of the Corroded Hull of HMVS Cerberus (1926). 13<sup>th</sup> *International Corrosion Congress proceedings* paper 125:1-10.
- 2002 In-situ Corrosion Measurements and Managing Shipwreck Sites. In *International Handbook of Underwater Archaeology*, Carol V. Ruppé and Janet F. Barstad, editors, pp. 697-714. Springer, New York, NY.
- 2011 Chapter 5. Assessment of the impact of scallop dredging, site clearance and cathodic protection on the City of Launceston (1865) through in-situ corrosion monitoring. In *Final Report on SS City of Launceston (1863-1865) Excavation and Conservation 1997-2009*, Ross Anderson, Editor, pp. 94-103.
- 2013 Chapter 21. Monitoring, Modelling, and Predication of Corrosion Rates of Historical Iron Shipwrecks. In *Corrosion and Conservation of Cultural Heritage of Metallic Artefacts*. Dillman, P., Watkinson D., Angelini E., Adriaens A, Editors, pp. 466-477.

Mallinson, David J., Stephen J. Culver, Stanley R. Riggs, J.P. Walsh, Dorothea Ames, and Curtis W. Smith.

- 2008 Past, Present, and Future Inlets of the Outer Banks Barrier Islands, North Carolina. North Carolina Coastal Geology Cooperative Research Program.

McCarthy, Mike

2000 Iron and Steamship Archaeology: Success and Failure on the SS *Xantho*. Plenum Publishers, New York, NY.

McNinch, Jesse E.

2004 Geologic control in the nearshore: shore-oblique sandbars and shoreline erosional hotspots, Mid-Atlantic Bight, USA. *International Journal of Marine Geology, Geochemistry and Geophysics*. 211: 121-141.

Moore, James D.

2011 Corrosion analyses of Iron and Steel Archaeological Shipwreck sites. Dissertation, Oceanography, University of Rhode Island, Kingston, RI.

Muckelroy, Keith

1976 The Integration of Historical and Archaeological Data Concerning an Historic Wreck Site: The *Kennemerland*. *World Archaeology*. 7.3:280-289.

National Data Buoy Center

2014 DUKN7 Sea Temperature (Degrees C) 7/2008- 12/2012.  
<[http://www.ndbc.noaa.gov/view\\_climplot.php?station=dukn7&meas=st.](http://www.ndbc.noaa.gov/view_climplot.php?station=dukn7&meas=st.)>,  
Accessed 25 March 2014.

North, Neil A

1976 Formation of Coral Concretions on Marine Iron. *The International Journal of Nautical Archaeology and Underwater Exploration*. 5(3): 252-258.

1982 Corrosion Products on Marine Iron. *International Institute for Conservation of Historic and Artistic Works*. 27(2): 75-83.

Past Foundation

2004 Project Objective 1: Ultrasonic Thickness Measurements. Past Foundation in partnership with the National Park Service, Columbus OH  
<<http://pastfoundation.org/previous-programs/Arizona/HullThickness.htm>>,  
Accessed 3 January 2014.

Piero, Jaqueline

2004 Deterioration of Ferrous Hulled Shipwrecks. Master's Thesis. East Carolina University

Overfield, Michael L.

2004 Resources and UnderSea Threats (RUST) Database: An Assesment Tool for Identifying and Evaluating Submerged Hazards within the National Marine Sanctuaries. *Marine Technology Society Journal* 38(3): 72-77.

- Riggs, Stanley R., Stephen J. Culver, Dorothea V. Ames, David J. Mallinson, D. Reide Corbett, and J.P. Walsh  
2008 North Carolina's Coasts In Crisis: A Vision for the Future. North Carolina Coastal Geology Cooperative Research Program.
- Roach, John  
1875 Deck plans of USS *Huron*. Record Group 19. National Archives and Records Administration, Washington.
- Rodgers, Bradley A.  
1989 The case for biologically induced corrosion at the Yorktown shipwreck archaeological site. *The International Journal of Nautical Archaeology*. 18.4: 335-340  
  
2004 *The Archaeologist's Manual for Conservation: A Guide to Non-Toxic, Minimal Intervention Artifact Stabilization*. Kluwer Academic/Plenum Publishers, New York, NY.
- Rogers, Dennis  
1987 U.S.S. *Huron* Salvagers Bring Up Bits of Nautical History. *Raleigh News and Observer*. 2 September 1987.
- Russell, Matthew A., David L. Conlin, Larry E. Murphy, Donald L. Johnson, Brent M. Wilson, James D. Carr.  
2006 A Minimum-Impact Method for Measuring Corrosion Rate of Steel-Hulled Shipwrecks in Seawater. *The International Journal of Nautical Archaeology*. 35(2): 310-318.
- Talley, Lynne  
2002 *Salinity Patterns in the Ocean. In The Earth System: Physical and Chemical Dimensions of Global Environmental Change, Volume 1*. M. MacCracken and J. Perry, editors, pp. 629-640. Chichester, New York: John Wiley and Sons.
- Thiesen, William H.  
2006 *Industrializing American Shipbuilding: The Transformation of Ship Design and Construction, 1820-1920*. University Press of Florida, Gainesville, FL.
- U.S. Geologic Survey  
2013 Dissolved Oxygen Solubility Tables  
<<http://water.usgs.gov/software/DOTABLES/>>, Accessed 3 October 2013.
- U.S. Naval Inquiry  
1877 Proceedings of Court of Inquiry on the Loss of the *Huron*. Senate Executive Document Number 26. 45<sup>th</sup> Congress, second session. U.S. Serial set No. 1780, fiche 9-10.

Welsh, Wendy M.

2010 A Case Study of In Situ Monitoring on an Anchor From the Queen Anne's Revenge (1718). *Metal 2010. International Conference on Metal Conservation: 52-58.*

Wilson, Brent M., Donald L. Johnson, Hans Van Tilburg, Matthew A. Russell, Larry E. Murphy, James D. Carr, Robert J. De Angelis, and David L. Conlin

2007 Corrosion Studies on the *USS Arizona* with application to a Japanese Midget Submarine. *Journal of Metallurgy*. 10 (October): 14-18.

Zorc, Kevin

2010 *USS Huron* Historic Shipwreck Preserve Status Report for the period 1 January 2010 through 11 October 2010. *Letter to Underwater Archaeology Branch Department of Cultural Resources.*